(12) INTERNATIONAL APPLICATION PUBLISHED UNDER THE PATENT COOPERATION TREATY (PCT)

(19) World Intellectual Property Organization
International Bureau

(43) International Publication Date
26 January 2023 (26.01.2023)

WIPO | PCT

(10) International Publication Number
WO 2023/004060 A2

(51) International Patent Classification:
Not classified

(21) International Application Number:
PCT/US2022/037905

(22) International Filing Date:
21 July 2022 (21.07.2022)

(25) Filing Language: English

(26) Publication Language: English

(30) Priority Data:

| | | |
|---|---|---|
| 17/383,735 | 23 July 2021 (23.07.2021) | US |
| 17/383,744 | 23 July 2021 (23.07.2021) | US |
| 17/383,756 | 23 July 2021 (23.07.2021) | US |
| 17/383,769 | 23 July 2021 (23.07.2021) | US |
| 17/383,793 | 23 July 2021 (23.07.2021) | US |
| 17/383,803 | 23 July 2021 (23.07.2021) | US |
| 17/563,183 | 28 December 2021 (28.12.2021) | US |

(71) Applicant: **LYTEN, INC.** [US/US]; 145 Baytech Drive, San Jose, California 95134-2303 (US).

(72) Inventors: **LANNING, Bruce**; 145 Baytech Drive, San Jose, California 95134-2303 (US). **STOWELL, Michael, W.**; 145 Baytech Drive, San Jose, California 95134-2303 (US). **KUMAR, Anurag**; 145 Baytech Drive, San Jose, California 95134-2303 (US). **BELL, Jeffrey**; 145 Baytech Drive, San Jose, California 95134-2303 (US). **HUANG, Qianwen**; 145 Baytech Drive, San Jose, California 95134-2303 (US). **BAUCOM, Jesse**; 145 Baytech Drive, San Jose, California 95134-2303 (US). **LI, You**; 145 Baytech Drive, San Jose, California 95134-2303 (US). **THORNE, John**; 145 Baytech Drive, San Jose, California 95134-2303 (US). **VANHEUSDEN, Karel**; 145 Baytech Drive, San Jose, California 95134-2303 (US). **ROGOJINA, Elena**; 145 Baytech Drive, San Jose, California 95134-2303 (US). **GAZDA, Jerzy**; 145 Baytech Drive, San Jose, California 95134-2303 (US). **SHAN, Jingning**; 145 Baytech Drive, San Jose, California 95134-2303 (US).

(74) Agent: **PARADICE, William, L., III**; Paradice & Li LLP, 1999 S. Bascom Ave., Suite 300, Campbell, California 95008 (US).

(81) Designated States *(unless otherwise indicated, for every kind of national protection available)*: AE, AG, AL, AM, AO, AT, AU, AZ, BA, BB, BG, BH, BN, BR, BW, BY, BZ, CA, CH, CL, CN, CO, CR, CU, CV, CZ, DE, DJ, DK, DM, DO, DZ, EC, EE, EG, ES, FI, GB, GD, GE, GH, GM, GT, HN, HR, HU, ID, IL, IN, IQ, IR, IS, IT, JM, JO, JP, KE, KG, KH, KN, KP, KR, KW, KZ, LA, LC, LK, LR, LS, LU, LY, MA, MD, ME, MG, MK, MN, MW, MX, MY, MZ, NA, NG, NI, NO, NZ, OM, PA, PE, PG, PH, PL, PT, QA, RO,

(54) Title: LITHIUM-SULFUR BATTERY CATHODE FORMED FROM MULTIPLE CARBONACEOUS REGIONS

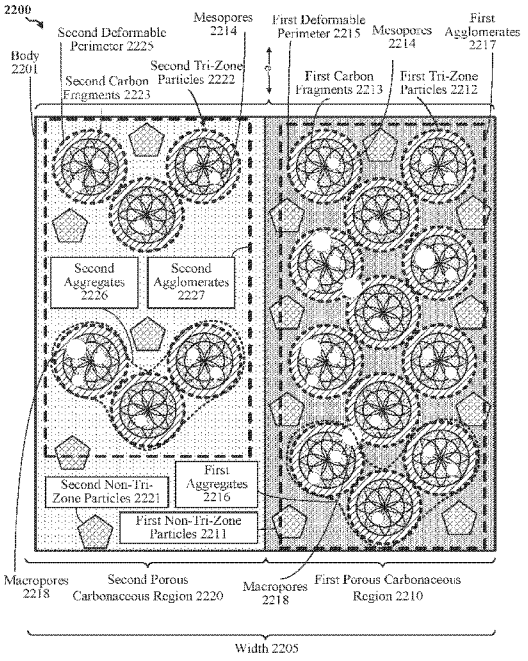


*Figure 22*

(57) Abstract: A composition of matter suitable for incorporation into a battery electrode is disclosed. In some implementations, the composition of matter may include pores that may be defined in size or shape by several carbonaceous particles. Each of the particles may have multiple regions such that adjacent regions are separated from each other by some of the pores. Deformable regions may be distributed throughout a perimeter of each of the particles, for example, to accommodate coalescence of multiple adjacent particles. The composition of matter may also include a plurality of aggregates and a plurality of agglomerates, where each aggregate includes a multitude of the particles joined together, and each agglomerate includes a multitude of the aggregates joined together.

WO 2023/004060 A2

[Continued on next page]

RS, RU, RW, SA, SC, SD, SE, SG, SK, SL, ST, SV, SY, TH, TJ, TM, TN, TR, TT, TZ, UA, UG, US, UZ, VC, VN, WS, ZA, ZM, ZW.

(84) **Designated States** *(unless otherwise indicated, for every kind of regional protection available)*: ARIPO (BW, GH, GM, KE, LR, LS, MW, MZ, NA, RW, SD, SL, ST, SZ, TZ, UG, ZM, ZW), Eurasian (AM, AZ, BY, KG, KZ, RU, TJ, TM), European (AL, AT, BE, BG, CH, CY, CZ, DE, DK, EE, ES, FI, FR, GB, GR, HR, HU, IE, IS, IT, LT, LU, LV, MC, MK, MT, NL, NO, PL, PT, RO, RS, SE, SI, SK, SM, TR), OAPI (BF, BJ, CF, CG, CI, CM, GA, GN, GQ, GW, KM, ML, MR, NE, SN, TD, TG).

**Declarations under Rule 4.17:**

— *as to applicant's entitlement to apply for and be granted a patent (Rule 4.17(ii))*

— *as to the applicant's entitlement to claim the priority of the earlier application (Rule 4.17(iii))*

**Published:**

— *without international search report and to be republished upon receipt of that report (Rule 48.2(g))*

# LITHIUM-SULFUR BATTERY CATHODE FORMED FROM MULTIPLE CARBONACEOUS REGIONS

## CROSS-REFERENCE TO RELATED APPLICATIONS

**[0001]** This Patent Application claims priority to U.S. Patent Application No. 17/563,183 entitled "LITHIUM-SULFUR BATTERY CATHODE FORMED FROM MULTIPLE CARBONACEOUS REGIONS" filed on December 28, 2021, which is a continuation-in-part application claiming priority to U.S. Patent Application No. 17/383,803 entitled "CARBONACEOUS MATERIALS FOR LITHIUM-SULFUR BATTERIES" filed on July 23, 2021, all of which are assigned to the assignee hereof. This Patent Application also claims priority to U.S. Patent Application No. 17/383,735 entitled "POWDERED MATERIALS INCLUDING CARBONACEOUS STRUCTURES FOR LITHIUM-SULFUR BATTERY CATHODES" filed on July 23, 2021, to U.S. Patent Application No. 17/383,744 entitled "PROTECTIVE POLYMERIC LATTICES FOR LITHIUM ANODES IN LITHIUM-SULFUR BATTERIES" filed on July 23, 2021, to U.S. Patent Application No. 17/383,756 entitled "BATTERY INCLUDING MULTIPLE PROTECTIVE LAYERS" filed on July 23, 2021, to U.S. Patent Application No. 17/383,769 entitled "CARBON-SCAFFOLDED LITHIUM-SULFUR BATTERY CATHODES FEATURING A POLYMERIC PROTECTIVE LAYER" filed on July 23, 2021, and to U.S. Patent Application No. 17/383,793 entitled "PROTECTIVE LAYER INCLUDING TIN FLUORIDE DISPOSED ON A LITHIUM ANODE IN A LITHIUM-SULFUR BATTERY" filed on July 23, 2021, all of which are assigned to the assignee hereof. The disclosure of the prior Applications are considered part of and is incorporated by reference in this Patent Application in their respective entireties.

## TECHNICAL FIELD

**[0002]** This disclosure relates generally to batteries, and, more particularly, to lithium-ion batteries that can compensate for operational cycle losses.

## DESCRIPTION OF RELATED ART

**[0003]** Recent developments in batteries allow consumers to use electronic devices in many new applications. However, further improvements in battery technology are desirable.

## SUMMARY

**[0004]** This Summary is provided to introduce in a simplified form a selection of concepts that are further described below in the Detailed Description. This Summary is not intended to identify key features or essential features of the claimed subject matter, nor is it intended to limit the scope of the claimed subject matter.

**[0005]** One innovative aspect of the subject matter described in this disclosure can be implemented as a composition of matter including a plurality of pores. The composition of matter, which may be suitable for incorporation into a battery electrode, includes a plurality of particles, each of the particles containing a first zone including a plurality of first pores having a uniform pore size and a second zone including a plurality of second pores. The second zone may be concentrically positioned relative to the first zone and separated from the first zone by at least some of the plurality of first pores, where the plurality of second pores has a pore size that gradually decreases along a radial direction from the center of the particle to a boundary of the particle. The composition of matter may also include a plurality of aggregates, each including a multitude of the particles joined together, and a plurality of agglomerates, each including a multitude of the aggregates joined together.

**[0006]** In some implementations, each of the particles may have a principal dimension in between 20 nanometers (nm) and 150 nm. Each of the aggregates may have a principal dimension in between 10 nanometers (nm) and 10 micrometers (μm). Each of the agglomerates may have a principal dimension in between 0.1 μm and 1,000 μm. At least some of the pores may be dispersed throughout one or more of the particles or the aggregates, where each of the pores may have a principal dimension in between 0 nm and 100 nm.

**[0007]** In one implementation, each of the particles may include a first porosity region and a second porosity region that is positioned adjacent to the first porosity region. The first porosity region may have a first type of pores and the second porosity region may have a second type of pores, such that the first porosity region has a different porosity than the second porosity region. As such, the first type of pores may have a first pore density, and the second type of pores have a second pore density. For example, the first porosity region may have a first pore density between 0.0 cubic centimeters (cc)/g and 2.0 cc/g, and the second porosity region may have a second pore density between 1.5 and 5.0 cc/g. In some aspects, the second porosity region may be at least partially encapsulated by the first porosity region.

**[0008]** In some implementations, some of the pores may be interspersed throughout the agglomerates, where at least some of the pores have a principal dimension in between 1.3 nm

and 32.3 nm. Electrically conductive additives may be dispersed within at least some of the pores. In some aspects, the composition of matter may have exposed carbon surfaces with a surface area in between 10 $m^2/g$ to 3,000 $m^2/g$ and/or a composite surface area (e.g., with sulfur micro-confined within the pores) in between 10 $m^2/g$ to 3,000 $m^2/g$. In one implementation, the composition of matter may have an electrical conductivity in between 100 S/m to 20,000 S/m at a pressure of 12,000 pounds per square in (psi). In one implementation, the particles, aggregates, and/or agglomerates may include exposed carbon surfaces that may assist in the nucleation of sulfur, such that the composition of matter has a sulfur to carbon weight ratio between approximately 1:5 to 10:1. In some aspects, some of the agglomerates are connected to each other with one or more polymer-based binders.

**[0009]** Another innovative aspect of the subject matter described in this disclosure may be implemented as a battery. In some implementations, the battery may include an anode, a polymeric network disposed over one or more exposed surfaces of the anode, a cathode positioned opposite to the anode, an electrolyte at least partially dispersed throughout the cathode and in contact with the anode, the electrolyte configured to transport the plurality of alkali ions between the cathode and the anode, and a separator. In some implementations, the anode may include an alkali metal that can release alkali ions during operational discharge-charge cycling of the battery. The polymeric network may include carbonaceous materials grafted with fluorinated polymer chains cross-linked with each other. The fluorinated polymer chains may produce an alkali-metal containing fluoride in response to operational cycling of the battery. In one implementation, formation of the alkali-metal containing fluoride may suppress alkali metal dendrite formation from the anode, for example, such that lithium is consumed to form lithium fluoride rather than forming lithium-containing dendritic structures. The electrolyte may be at least partially dispersed throughout the cathode and in contact with the anode and may assist in the transport of the alkali ions between the cathode and the anode. The separator may be positioned between the anode and the cathode.

**[0010]** In one implementation, the carbonaceous materials may include flat graphene, wrinkled graphene, carbon nano-tubes (CNTs), and/or carbon nano-onions (CNOs). The fluorinated polymer chains may include monomers including 2,2,3,3,4,4,5,5,6,6,7,7-Dodecafluoroheptyl acrylate (DFHA), 3,3,4,4,5,5,6,6,7,7,8,8,9,9,10,10,10-Heptadecafluorodecyl methacrylate (HDFDMA), 2,2,3,3,4,4,5,5-Octafluoropentyl methacrylate (OFPMA), Tetrafluoropropyl methacrylate (TFPM), 3-[3,3,3-Trifluoro-2-hydroxy-2-(trifluoromethyl)propyl]bicyclo[2.2.1]hept-2-yl methacrylate (HFA monomer),

and/or vinyl-based monomers including 2,3,4,5,6-Pentafluorostyrene (PFSt). The polymeric network may have a thickness approximately of between 0.001 μm and 5 μm.

**[0011]** In some aspects, the fluorinated polymer chains may be grafted to a surface of the carbonaceous materials, such that the grafting may be based on radical initiators including at least one of benzoyl peroxide (BPO) or azobisisobutyronitrile (AIBN). The fluorinated polymer chains may chemically react with alkali metal ions via a Wurtz reaction, which may be associated with production of the alkali metal fluoride. Graphene nanoplatelets may be dispersed throughout the polymeric network, where the graphene nanoplatelets are isolated from each other within the polymeric network. The dispersion of the graphene nanoplatelets may include different concentration levels (of the graphene nanoplatelets). In some aspects, the dispersion of the graphene nanoplatelets may include carbonaceous materials functionalized with at least some fluorinated polymer chains.

**[0012]** In one implementation, the polymeric network includes between approximately 0.001 wt.% to 2 wt.% of the fluorinated polymer chains. In some aspects, the polymeric network includes an interphase layer in contact with the anode and a protective layer disposed on top of the interphase layer. The interphase layer may be based on a Wurtz reaction at an interface between the anode and the polymeric network. In some aspects, the cross-linked polymeric network may include between approximately 5 wt.% to 100 wt.% of carbonaceous materials grafted with fluorinated polymer chains with a remaining balance of fluorinated polymers, non-fluorinated polymers, or cross-linkable monomers, or combinations thereof. In one implementation, the carbonaceous materials grafted with fluorinated polymer chains may include 5 wt.% to 50 wt.% of fluorinated polymer chains and a balance of carbonaceous material.

**[0013]** In some aspects, the polymeric network may further define a density gradient associated with self-healing properties of the interphase layer and/or the protective layer and may strengthen the polymeric network, which may suppress dendritic growth from the anode. In one implementation, the anode may be an alkali metal layer and/or include surfaces exposed to the electrolyte, where each exposed surface may include alkali metal-containing nanostructures or microstructures. In some aspects, the alkali metal-containing nanostructures or microstructures may include carbonaceous particles, a number of aggregates each including carbonaceous particles, or a number of agglomerates each including several aggregates.

**[0014]** In one implementation, each of the carbonaceous particles has a first porosity region with a first pore density and a second porosity region with a second pore density. The second porosity region may be at least partially encapsulated by the first porosity region, and the second density may be less than the first density. In some aspects, the second porosity region may at least temporarily micro-confine an elemental sulfur as may be associated with operational discharge-charge cycling of the batter.

**[0015]** In some implementations, the anode may be structurally defined by a three-dimensional (3D) scaffold and/or structure, which may include adjacent graphene sheets that may at least intercalate alkali metal. For example, the anode may be formed as a lattice with adjacent graphene sheets that have exposed surfaces for alkali metal electrodeposition and/or intercalation. In one implementation, a film may be disposed on the cathode and include a lattice with a tri-functional epoxy compound and a di-amine oligomer compound chemically bonded to each other. The film may bond with alkali metal containing polysulfide intermediates generated during operational discharge-charge cycling of the battery and complement the polymeric sheath disposed on the anode.

**[0016]** Another innovative aspect of the subject matter described in this disclosure may be implemented as a battery including an anode, a cathode positioned opposite to the anode, a protective sheath disposed on the cathode, an electrolyte, and a separator. A polymeric network may be disposed on the anode and may include carbonaceous materials grafted with a plurality of fluorinated polymer chains cross-linked into a lattice. In some aspects, the lattice may produce an alkali metal fluoride in response to operational cycling of the battery. The alkali metal fluoride may be configured to suppress alkali metal dendrite formation from the anode. In addition, the anode may output alkali ions during operational cycling of the battery. The protective sheath disposed on the cathode may include a tri-functional epoxy compound and a di-amine oligomer-based compound, both of which may chemically react with each other. The electrolyte may disperse throughout the cathode and contact with the anode. The separator may be positioned between the anode and the cathode.

**[0017]** In some implementations, the polymeric network may be deposited over one or more exposed surfaces of the anode. The carbonaceous materials may include one or more of flat graphene, wrinkled graphene, a plurality of carbon nano-tubes (CNTs), or a plurality of carbon nano-onions (CNOs). The fluorinated polymer chains may include a plurality of monomers, one or more monomers including 2,2,3,3,4,4,5,5,6,6,7,7-Dodecafluoroheptyl acrylate (DFHA), 3,3,4,4,5,5,6,6,7,7,8,8,9,9,10,10,10-Heptadecafluorodecyl methacrylate

(HDFDMA), 2,2,3,3,4,4,5,5-Octafluoropentyl methacrylate (OFPMA), Tetrafluoropropyl methacrylate (TFPM), 3-[3,3,3-Trifluoro-2-hydroxy-2-(trifluoromethyl)propyl]bicyclo[2.2.1]hept-2-yl methacrylate (HFA monomer), or vinyl-based monomers including 2,3,4,5,6-Pentafluorostyrene (PFSt). The polymeric network may have a thickness approximately between 0.001 μm and 5 μm. Fluorinated polymer chains may be grafted to a surface of a respective one of the carbonaceous materials.

**[0018]** In various implementations, the fluorinated polymer chains may chemically interact with the one or more surfaces of the alkali metal of the anode via a Wurtz reaction. In some aspects, the carbonaceous materials may include graphene nanoplatelets dispersed throughout the polymeric network. The graphene nanoplatelets may be isolated from each other within the polymeric network. The dispersion of the plurality of graphene nanoplatelets throughout the polymeric network may have different concentration levels. The graphene nanoplatelets may be functionalized with the fluorinated polymer chains.

**[0019]** In some implementations, the polymeric network includes between approximately 0.001 wt.% to 2 wt.% of the fluorinated polymer chains. In one implementation, the polymeric network may include an interphase region in contact with the anode and a protective region disposed on top of the interphase region. The interphase region may be based on a Wurtz reaction at an interface between the anode and the polymeric network. The interphase region may include one or more of a plurality of cross-linkable monomers including methacrylate (MA), acrylate, vinyl functional groups, or a combination of epoxy and amine functional groups. The protective region may be characterized by a density gradient, which may be associated with self-healing properties of the protective region. The density gradient may strengthen the polymeric network. In this way, the polymeric network may suppress dendritic growth from the anode.

**[0020]** In various implementations, the anode may include exposed surfaces, where each exposed surface has alkali metal-containing nanostructures and/or microstructures, each of which may include the carbonaceous materials. In one implementation, the anode may have three-dimensional (3D) structure, where some adjacent graphene sheets may intercalate alkali metal ions.

**[0021]** Another innovative aspect of the subject matter described in this disclosure may be implemented as a battery include an anode, a cathode, a protective sheath disposed on the cathode, a separator, and an electrolyte. The anode may be arranged in a lattice configuration and include carbonaceous materials. The cathode may be positioned opposite to the anode.

The separator may be disposed between the anode and cathode. The protective sheath disposed on the cathode may include a tri-functional epoxy compound and a di-amine oligomer-based compound, both of which may chemically react with each other. In this way, the protective sheath may prevent polysulfide migration within the battery based on chemical binding between the protective sheath and one or more lithium-containing polysulfide intermediates. The electrolyte may disperse within the cathode and contact the anode.

**[0022]** In one implementation, a polymeric network may be deposited over one or more exposed surfaces of the anode. The polymeric network may have fluorinated polymer chains grafted with carbonaceous materials and be cross-linked with each another. In this way, the polymeric network may retain an alkali-metal containing fluoride, which in turn may suppress alkali metal dendrite formation associated with the anode.

**[0023]** In various implementations, cracks may extend into the cathode, where protective sheath may disperse throughout the one or more cracks. In this way, the protective sheath may be arranged to reduce a susceptibility of the cathode to rupturing. In one implementation, the protective sheath has a cross-linked, three-dimensional structure based on the tri-functional epoxy compound and the di-amine oligomer-based compound. In some examples, the tri-functional epoxy compound is one or more of trimethylolpropane triglycidyl ether (TMPTE), tris(4-hydroxyphenyl)methane triglycidyl ether, or tris(2,3-epoxypropyl) isocyanurate, and the di-amine oligomer-based compound is one or more of dihydrazide sulfoxide (DHSO) or JEFFAMINE ® D-230 polyetheramine. In addition, or the alternative, the protective sheath may include trimethylolpropane tris[poly(propylene glycol) and amine terminated ether.

**[0024]** In some implementations, the carbonaceous materials may include flat graphene, wrinkled graphene, a plurality of carbon nano-tubes (CNTs), and/or a plurality of carbon nano-onions (CNOs). In one implementation, the cathode may include a host structure with one or more of flat graphene, wrinkled graphene, carbon nanotubes (CNTs), or carbon nano-onions (CNOs), where the anode includes a solid lithium metal layer.

**[0025]** In one implementation, a tin fluoride layer may be disposed on the anode, and a lithium fluoride layer may be formed between the tin fluoride layer and the anode. The lithium fluoride layer may be associated with chemical reactions between fluorine ions and lithium ions. In this way, the lithium fluoride layer may inhibit lithium-containing dendritic growth from the anode. In some aspects, a solid-electrolyte interphase may be disposed on the anode. The solid-electrolyte interphase may include tin, manganese, molybdenum,

fluorine compounds, tin fluoride, manganese fluoride, silicon nitride, lithium nitride, lithium nitrate, lithium phosphate, manganese oxide, and/or lithium lanthanum zirconium oxide (LLZO).

**[0026]** Another innovative aspect of the subject matter described in this disclosure may be implemented as a battery. In various implementations, the battery may include an anode configured to output a plurality of lithium ions during cycling of the battery, a graded layer disposed on the anode, a cathode positioned opposite to the anode, an electrolyte dispersed throughout the cathode and the anode, and a separator positioned between the anode and cathode. In some implementations, the graded layer may include a polymeric network including a density gradient formed of wrinkled graphene associated with graphene nanoplatelets dispersed throughout and isolated from one other within the polymeric network, at least some wrinkled graphene configured to expand in volume along one or more flexure points and retain polysulfides generated during cycling of the battery. In some instances, the polymeric network may include a plurality of fluorinated poly(meth)acrylates grafted onto one of more flexure points of at least some wrinkled graphene, a plurality of carbon-fluorine (C-F) bonds within the polymeric network, at least some of the plurality of carbon-fluorine (C-F) bonds configured to chemically react, by a Wurtz reaction, with at least some of the plurality of lithium ions and convert into carbon-lithium (C-Li) bonds by displacing fluorine ions ($F^-$), a plurality of carbon-carbon (C-C) bonds formed during displacement of fluorine ions ($F^-$) during the Wurtz reaction, formation of carbon-carbon (C-C) bonds associated with cross-linking of the polymeric network, and lithium fluoride (LiF) formed responsive to displacement of fluorine ions ($F^-$), lithium fluoride (LiF) associated with consumption of at least some of the plurality of lithium ions.

**[0027]** In some instances, the battery may also include a solid-electrolyte interphase formed at a surface of the anode exposed to the electrolyte during cycling of the battery. In other instances, the graded layer may be configured to grow the solid-electrolyte interphase during cycling of the battery. In some aspects, the graded layer may be deposited on the anode by one or more of atomic layer deposition (ALD), chemical vapor deposition (CVD), or physical vapor deposition (PVD).

**[0028]** Another innovative aspect of the subject matter described in this disclosure may be implemented as a battery. In various implementations, the battery may include an anode configured to output a plurality of lithium ions during cycling of the battery, a graded layer disposed on the anode, a cathode positioned opposite to the anode, an electrolyte dispersed

throughout the cathode and the anode, and a separator positioned between the anode and cathode. In some implementations, the graded layer may include a polymeric network including a density gradient formed of wrinkled graphene associated with graphene nanoplatelets dispersed throughout and isolated from one other within the polymeric network, at least some wrinkled graphene configured to expand in volume along one or more flexure points and retain polysulfides generated during cycling of the battery. In some instances, the polymeric network may include a plurality of fluorinated poly(meth)acrylates grafted onto one of more flexure points of at least some wrinkled graphene, a plurality of carbon-fluorine (C-F) bonds within the polymeric network, at least some of the plurality of carbon-fluorine (C-F) bonds configured to chemically react with at least some of the plurality of lithium ions and convert into carbon-lithium (C-Li) bonds by displacing fluorine ions ($F^-$), a plurality of carbon-carbon (C-C) bonds formed during displacement of fluorine ions (F-) during a Wurtz reaction, and lithium fluoride (LiF) formed responsive to formation of at least some of the plurality of carbon-carbon (C-C) bonds, where the lithium fluoride (LiF) may be associated with consumption of at least some of the plurality of lithium ions.

**[0029]** In some aspects, the first plurality of mesopores has a first mesopore density, and the second plurality of mesopores has a second mesopore density different than the first mesopore density. In other aspects, the first plurality of macropores has a first pore density, and the second plurality of macropores has a second pore density different than the first pore density. In some other aspects, one or more of the first porous carbonaceous region or the second porous carbonaceous region may be configured to nucleate sulfur.

**[0030]** In some implementations, the cathode contains a plurality of pores, and may include a plurality of non-tri-zone particles, a plurality of tri-zone particles, a plurality of aggregates each including a multitude of the tri-zone particles joined together, a plurality of mesopores interspersed throughout the plurality of aggregates, a plurality of agglomerates each including a multitude of the aggregates joined to each other, and a plurality of macropores interspersed throughout the plurality of aggregates. In some instances, each tri-zone particle may include a plurality of carbon fragments intertwined with each other and separated from one another by mesopores, and a deformable perimeter configured to coalesce with one or more adjacent non-tri-zone particles or tri-zone particles. In some aspects, each aggregate may have a principal dimension in a range between 10 nanometers (nm) and 10 micrometers (μm), each mesopore may have a principal dimension between 3.3 nanometers (nm) and 19.3 nm, each agglomerate may have a principal dimension in an approximate

range between 0.1 μm and 1,000 μm, and each macropore may have a principal dimension between 0.1 μm and 1,000 μm.

**[0031]** In some instances, one or more of the first porous carbonaceous region or the second porous carbonaceous region may also include a selectively permeable shell configured to form a separated liquid phase on the first porous carbonaceous region or the second porous carbonaceous region, respectively. In some aspects, the first porous carbonaceous region has an electrical conductivity in an approximate range between 500 S/m to 20,000 S/m at a pressure of 12,000 pounds per square in (psi). In other aspects, the second porous carbonaceous region has an electrical conductivity in an approximate range between 0 S/m to 500 S/m at a pressure of 12,000 pounds per square in (psi). In some other aspects, one or more of the first plurality of agglomerates or second plurality of agglomerates may include aggregates connected to each other with one or more polymer-based binders.

**[0032]** In some implementations, each of the tri-zone particles may include a first porosity region located around a center of each of the tri-zone particles, the first porosity region including first pores, and a second porosity region surrounding the first porosity region, the second porosity region including second pores. In some instances, the first pores define a first pore density, and the second pores define a second pore density different the first pore density. In other implementations, the cathode may also include one or more additional porous carbonaceous regions, at least one additional porous carbonaceous region coupled with the second porous carbonaceous region. In some instances, one or more additional porous carbonaceous regions are arranged in order of incrementally decreasing concentration levels of carbonaceous materials away from the first porous carbonaceous region.

**[0033]** Another innovative aspect of the subject matter described in this disclosure may be implemented as a composition of matter including a plurality of pores. In various implementations, the composition of matter may include a plurality of non-tri-zone particles, a plurality of aggregates, each aggregate including a multitude of the tri-zone particles joined together, each aggregate having a principal dimension in a range between 10 nanometers (nm) and 10 micrometers (μm), a plurality of mesopores interspersed throughout the plurality of aggregates, each mesopore having a principal dimension between 3.3 nanometers (nm) and 19.3 nm, a plurality of agglomerates, each agglomerate including a multitude of the aggregates joined to each other, each agglomerate having a principal dimension in an approximate range between 0.1 μm and 1,000 μm, and a plurality of macropores interspersed

throughout the plurality of aggregates, each macropore having a principal dimension between 0.1 μm and 1,000 μm. In some implementations, each tri-zone particle may include a plurality of carbon fragments intertwined with each other and separated from one another by mesopores, and a deformable perimeter configured to coalesce with one or more adjacent non-tri-zone particles or tri-zone particles. in some aspects, each of the pores has a principal dimension in an approximate range between 0 nanometers (nm) and 32.3 nm. In other aspects, the composition of matter has an electrical conductivity in an approximate range between 100 S/m to 20,000 S/m at a pressure of 12,000 pounds per square in (psi).

**[0034]** In various implementations, the composition of matter may also include a selectively permeable shell configured to form a separated liquid phase on one or more exposed surfaces of the composition of matter. In other implementations, the composition of matter may also include an electrolyte dispersed within the composition of matter. In some instances, at least some agglomerates are connected to each other with one or more polymer-based binders.

**[0035]** Details of one or more implementations of the subject matter described in this disclosure are set forth in the accompanying drawings and the description below. Other features, aspects, and advantages will become apparent from the description, the drawings, and the claims. Note that the relative dimensions of the following figures may not be drawn to scale.

## BRIEF DESCRIPTION OF THE DRAWINGS

**[0036]** Figure 1 shows a diagram depicting an example battery, according to some implementations.

**[0037]** Figure 2 shows a diagram depicting another example battery, according to some implementations.

**[0038]** Figure 3 shows a diagram of an example electrode of a battery, according to some implementations.

**[0039]** Figure 4 shows a diagram a diagram of a portion of an example battery that includes a protective lattice, according to some implementations.

**[0040]** Figure 5 shows a diagram of an anode structure including a tin fluoride ($SnF_2$) layer, according to some implementations.

**[0041]** Figure 6 shows a diagram of an enlarged portion of the anode structure of Figure 5, according to some implementations.

**[0042]** Figure 7 shows a diagram of a polymeric network of a battery, according to some implementations.

**[0043]** Figure 8A shows a diagram of an example carbonaceous particle with graded porosity, according to some implementations.

**[0044]** Figure 8B shows a diagram of an example of a tri-zone particle, according to some implementations.

**[0045]** Figure 8C shows an example step function representative of the tri-zone particle of Figure 8B, according to some implementations.

**[0046]** Figure 8D shows a graph depicting an example distribution of pore volume versus pore width of an example carbonaceous particle, according to some implementations.

**[0047]** Figures 9A and 9B show electron micrographs of example carbonaceous particles, aggregates, and/or agglomerates depicted in Figure 8A and/or Figure 8B, according to some implementations.

**[0048]** Figures 10A and 10B show transmission electron microscope (TEM) images of carbonaceous particles treated with carbon dioxide ($CO_2$), according to some implementation.

**[0049]** Figure 11 shows a diagram depicting carbon porosity types prevalent in the anodes and/or the cathodes of the present disclosure, according to some implementations.

**[0050]** Figure 12 shows a graph depicting cumulative pore volume versus pore width for micropores and mesopores dispersed throughout the anode or cathode of a battery, according to some implementations.

**[0051]** Figure 13 shows graphs depicting battery performance per cycle number, according to some implementations.

**[0052]** Figure 14 shows a bar chart depicting capacity per cycle number, according to some implementations.

**[0053]** Figure 15 shows graphs depicting battery performance per cycle number, according to some implementations.

**[0054]** Figure 16 shows a graph depicting battery discharge capacity per cycle number, according to some implementations.

**[0055]** Figure 17 shows a graph depicting battery discharge capacity per cycle number, according to some implementations.

**[0056]** Figure 18 shows a graph depicting battery specific discharge capacity for various TBT-containing electrolyte mixtures, according to some implementations.

**[0057]** Figure 19 shows graphs depicting battery specific discharge capacity per cycle number for the battery of Figure 1, according to some implementations.

**[0058]** Figure 20 shows graphs depicting battery specific discharge capacity and discharge capacity retention per cycle number for the battery of Figure 2, according to other implementations.

**[0059]** Figure 21 shows graphs depicting battery specific discharge capacity and discharge capacity retention per cycle number for the battery of Figure 2, according to some other implementations.

**[0060]** Figure 22 shows a diagram of an example cathode of a battery, according to some implementations.

**[0061]** Like reference numbers and designations in the various drawings indicate like elements.

## DETAILED DESCRIPTION

**[0062]** The following description is directed to some example implementations for the purposes of describing innovative aspects of this disclosure. However, a person having ordinary skill in the art will readily recognize that the teachings herein can be applied in a multitude of different ways. The described implementations can be implemented in any type of electrochemical cell, battery, or battery pack, and can be used to compensate for various performance related deficiencies. As such, the disclosed implementations are not to be limited by the examples provided herein, but rather encompass all implementations contemplated by the attached claims. Additionally, well-known elements of the disclosure will not be described in detail or will be omitted so as not to obscure the relevant details of the disclosure.

**[0063]** Batteries typically include several electrochemical cells that can be connected to each other to provide electric power to a wide variety of devices such as (but not limited to) mobile phones, laptops, electric vehicles (EVs), factories, and buildings. Certain types of batteries, such as lithium-ion or lithium-sulfur batteries, may be limited in performance by the type of electrolyte used or by uncontrolled battery side reactions. As a result, optimization of the electrolyte may improve the cyclability, the specific discharge capacity, the discharge capacity retention, the safety, and the lifespan of a respective battery. For example, in an unused or "fresh" battery, lithium ions are transported freely from the anode to the cathode upon activation and later during initial and subsequent discharge cycles. Then, during battery charge cycles, lithium ions may be forced to migrate back from their electrochemically favored positions in the cathode to the anode, where they are stored for subsequent use. This cyclical discharge-charge process associated with rechargeable batteries can result in the generation of undesirable chemical species that can interfere with the transport of lithium ions to and from the cathode during respective discharge and charge of the battery. Specifically, lithium-containing polysulfide intermediate species (referred to herein as "polysulfides") are generated when lithium ions interact with elemental sulfur (or, in some configurations, lithium sulfide, $Li_2S$) present in the cathode. These polysulfides are soluble in the electrolyte and, as a result, diffuse throughout the battery during operational cycling, thereby resulting in loss of active material from cathode. Generation of excessive concentration levels of polysulfides can result in unwanted battery capacity decay and cell failure during operational cycling, potentially reducing the driving range for electric vehicles (EVs) and increasing the frequency with which such EVs need recharging.

**[0064]** In some cases, polysulfides participate in the formation of inorganic layers in a solid electrolyte interphase (SEI) provided in the battery. In one example, the anode may be protected by a stable inorganic layer formed in the electrolyte and containing 0.020 M $Li_2S_5$ (0.10 M sulfur) and 5.0 wt. % $LiNO_3$. The anode with a lithium fluoride and polysulfides (LiF-$Li_2S_x$) may enrich the SEI and result in a stable Coulombic efficiency of 95% after 233 cycles for Li-Cu half cells, while preventing formation of lithium dendrites or other uncontrolled lithium growths that can extend from the anode to the cathode and result in a failed or ruptured cell. However, when polysulfides are generated at certain concentrations (such as greater than 0.50 M sulfur), formation of the SEI may be hindered. As a result, lithium metal from the anode may be undesirably etched, creating a rough and imperfect surface exposed to the electrolyte. This unwanted deterioration (etching) of the anode due to a relatively high concentration of polysulfides may indicate that polysulfide dissolution and diffusion may be limiting battery performance.

**[0065]** In some implementations, the porosity of a carbonaceous cathode may be adjusted to achieve a desired balance between maximizing energy density and inhibiting the migration of polysulfides into and/or throughout the battery's electrolyte. As used herein, carbonaceous may refer to materials containing or formed of one or more types or configuration of carbon. For example, cathode porosity may be higher in sulfur and carbon composite cathodes than in conventional lithium-ion battery electrodes. Denser electrodes with relatively low porosity may minimize electrolyte intake, parasitic weight, and cost. Sulfur utilization may be limited by the solubility of polysulfides and conversion from those polysulfides into lithium sulfide ($Li_2S$). The conversion of polysulfides into lithium sulfide may be based on the accessible surface area of the cathode. Aspects of the present disclosure recognize that cathode porosity may be adjusted based on electrolyte constituent materials to maximize battery volumetric energy density. In addition, or in the alternative, one or more protective layers or regions can be added to surfaces of the cathode and/or the anode exposed to the electrolyte to adjust cathode porosity levels. In some aspects, these protective layers or regions can inhibit the undesirable migration of polysulfides throughout the battery.

**[0066]** Various aspects of the subject matter disclosed herein relate to a lithium-sulfur battery including a liquid-phase electrolyte, which may include a ternary solvent package and one or more additives. In some implementations, the lithium-sulfur battery may include a cathode, an anode positioned opposite to the cathode, and an electrolyte. The cathode may include several regions, where each region may be defined by two or more carbonaceous

structures adjacent to and in contact with each other. In some instances, the electrolyte may be interspersed throughout the cathode and in contact with the anode. In some aspects, the electrolyte may include a ternary solvent package and 4,4'-thiobisbenzenethiol (TBT). In other instances, the electrolyte may include the ternary solvent package and 2-mercaptobenzothiazole (MBT).

**[0067]** In various implementations, the ternary solvent package may include 1,2-Dimethoxyethane (DME), 1,3-Dioxolane (DOL), tetraethylene glycol dimethyl ether (TEGDME) and one or more additives, which may include a lithium nitrate ($LiNO_3$), all which may be in a liquid-phase. In some implementations, the ternary solvent package may be prepared by mixing approximately 5,800 microliters (μL) of DME, 2,900 microliters (μL) of DOL, and 1,300 microliters (μL) of TEGDME with one another to create a mixture. Approximately 0.01 mol of lithium bis(trifluoromethanesulfonyl)imide (LiTFSI) may be dissolved into the ternary solvent package to produce an approximate dilution level of 1 M LiTFSI in DME:DOL:TEGDME at a volume ratio of 2:1:1 including approximately 2 weight percent (wt. %) lithium nitrate. In other implementations, the ternary solvent package may be prepared with 2,000 microliters (μL) of DME, 8,000 microliters (μL) of DOL, and 2,000 microliters (μL) of TEGDME and include approximately 0.01 mol of dissolved lithium bis(trifluoromethanesulfonyl)imide (LiTFSI). In some aspects, the ternary solvent package may be prepared at a first approximate dilution level of 1 molar (M) LiTFSI in a mixture of DME:DOL:TEGDME. In other instances, the ternary solvent package may be prepared at a second approximate dilution level of approximately 1 M LiTFSI in DME:DOL:TEGDME at an approximate volume ratio of 1:4:1 and include either an addition of 5M TBT solution or an addition of 5M MBT solution, or an addition of other additives and/or chemical substances.

**[0068]** In various implementations, each carbonaceous structure may include a relatively high-density outer shell region and a relatively low-density core region. In some aspects, the core region may be formed within an interior portion of the outer shell region. The outer shell region may have a carbon density between approximately 1.0 grams per cubic centimeter (g/cc) and 3.5 g/cc. The core region may have a carbon density of between approximately 0.0 g/cc and 1.0 g/cc or some other range lower than the first carbon density. In other implementations, each carbonaceous structure may include an outer shell region and core region having the same or similar densities, for example, such that the carbonaceous structure does not include a graded porosity.

**[0069]** Various regions of the cathode may include microporous channels, mesoporous channels, and macroporous channels interconnected to each other to form a porous network extending from the outer shell region to the core region. For example, in some aspects, the porous network may include pores that each have a principal dimension of approximately 1.5 nm.

**[0070]** In some implementations, one or more portions of the porous network may temporarily micro-confine electroactive materials such as (but not limited to) elemental sulfur within the cathode, which may increase battery specific capacity by complexing with lithium ions. In some aspects, the ternary solvent package may have a tunable polarity, a tunable solubility, and be capable of transporting lithium ions. In addition, the ternary solvent package may at least temporarily suspend polysulfides (PS) during charge-discharge cycles of the battery.

**[0071]** Particular implementations of the subject matter described in this disclosure can be implemented to realize one or more potential advantages. In some implementations, the porous network formed by the interconnection of microporous, mesoporous, and macroporous channels within the cathode may include a plurality of pores having a multitude of different pore sizes. In some implementations, the plurality of pores may include micropores having a pore size less than approximately 2 nm, may include mesopores having a pore size between approximately 5 and 50 nm, and may include macropores having a pore size greater than approximately 50 nm. The micropores, mesopores, and macropores may collectively mitigate the undesirable migration or diffusion of polysulfides throughout the electrolyte. Since the polysulfide shuttle effect may result in the loss of active material from the cathode, the ability to mitigate or reduce the polysulfide shuttle effect can increase battery performance.

**[0072]** In one implementation, the micropores may have a pore size of approximately 1.5 nm selected to micro-confine elemental sulfur ($S_8$, or smaller chains/fragments of sulfur, for example in the form of $S_2$,$S_4$ or $S_6$) pre-loaded into the cathode. The micro-confinement of elemental sulfur within the cathode may allow TBT or MBT complexes generated during battery cycling to inhibit the migration of long-chain polysulfides within the mesopores of the cathode. Accumulation of these long-chain polysulfides within the mesopores of the cathode may cause the cathode to volumetrically expand to retain the polysulfides and thereby reduce the polysulfide shuttle effect. Accordingly, lithium ions may continue to transport freely between the anode and the cathode via the electrolyte without being blocked or impeded by

the polysulfides. The free movement of lithium ions throughout the electrolyte without interference by polysulfides can increase battery performance.

**[0073]** In addition, or the alternative, one or more protective layers, sheaths, films, and/or regions (collectively referred to herein as "protective layers") may be disposed on the anode and/or the cathode and/or the separator and in contact with the electrolyte. The protective layers may include materials capable of binding with polysulfides to impede polysulfide migration and prevent lithium dendrite formation. In some aspects, the protective layers may be arranged in different configurations and used with any of the electrolyte chemistries and/or compositions disclosed herein, which in turn may result in complete tunability of the battery.

**[0074]** In one implementation, carbonaceous materials may be grafted with fluorinated polymer chains and deposited on one or more exposed surfaces of the anode. The fluorinated polymer chains can be cross-linked into a polymeric network on contact with Lithium metal from the anode surface via the Wurtz reaction. The cross-linked polymeric network formation may, in turn, suppress Lithium metal dendrite formation associated with the anode, and may also generate Lithium fluoride. Fluorinated polymers within the polymeric network may participate in chemical reactions during battery operational cycling to yield Lithium fluoride. Formation of the lithium fluoride may involve the chemical binding of lithium ions from the electrolyte with fluorine ions.

**[0075]** In addition, or the alternative, the polymeric network may be combined with any of the electrolyte chemistries and/or compositions disclosed herein and/or a protective sheath disposed on the cathode. In one implementation, the protective sheath can be formed by combining compounds containing di-functional, or higher functionality Epoxy and Amine or Amide compounds. Their intermolecular cross-linking would result in formation of 3D network with high chemical resistance to dissolution in electrolyte. Composition, for example, may include a tri-functional epoxy compound and a di-amine oligomer-based compound, which may react with each other to produce a protective lattice that can bind to polysulfides generated in the cathode and prevent their migration or diffusion into the electrolyte. In addition, the protective lattice may diffuse through one or more cracks that may form in the cathode due to battery cycling. The protective lattice, when diffused throughout such cracks formed in the cathode, may increase the structural integrity of the cathode, and reduce potential rupture of the cathode associated with volumetric expansion.

**[0076]** In various implementations, one or more of the disclosed battery components may be combined with a conformal coating disposed on edges or surfaces of the anode exposed to

the electrolyte. In some implementations, the conformal coating may include a graded interface layer that may replace the polymeric network. In some aspects, the graded interface layer may include a tin fluoride layer and a tin-lithium alloy region formed between the tin fluoride layer and the anode. The tin-lithium alloy region may form a layer of lithium fluoride uniformly dispersed between the anode and the tin-fluoride layer in response to operational cycling of the battery.

**[0077]** In various implementations, a lithium-sulfur battery employing various aspects of the present disclosure may include an electroactive material extracted from an external source, e.g., a subterranean source and/or an extraterrestrial subterranean source. In such implementations, the cathode may be prepared as a sulfur-free cathode including functional pores that may micro-confine the electroactive material within the cathode. In some aspects, the cathode may include aggregates including a multitude of carbonaceous particles joined together, and may include agglomerates including a multitude of the aggregates joined together. In one implementation, the carbonaceous materials used to form the cathode (and/or the anode) may be tuned to define unique pore sizes, size ranges, and volumes. In some implementations, the carbonaceous particles may include non-tri-zone particles with and without tri-zone particles. In other implementations, the carbonaceous particles may not include tri-zone particles. Each tri-zone particle may include micropores, mesopores, and macropores, and both the non-tri-zone and tri-zone particles may each have a principal dimension in an approximate range of 20 nm to 300 nm. Each of the carbonaceous particles may include carbonaceous fragments nested within each other and separated from immediate adjacent carbonaceous fragments by mesopores. In some aspects, each of the carbonaceous particles may have a deformable perimeter that changes in shape and coalesces with adjacent materials.

**[0078]** Some of the pores may be distributed throughout the plurality of carbonaceous fragments and/or the deformable perimeters of the carbonaceous particles. In various implementations, mesopores may be interspersed throughout the aggregates, and macropores may be interspersed throughout the plurality of agglomerates. In one implementation, each mesopore may have a principal dimension between 3.3 nanometers (nm) and 19.3 nm, each aggregate may have a principal dimension in an approximate range between 10 nm and 10 micrometers (μm), and each agglomerate may have a principal dimension in an approximate range between 0.1 μm and 1,000 μm. As further described below, specific combinations of pore sizes matched with unique electrolyte formulations and protective layers can be used to

reduce or mitigate the harmful effects of unwanted polysulfide diffusion, which may further increase battery performance.

**[0079]** Figure 1 shows an example battery 100, according to some implementations. The battery 100 may be a lithium-sulfur electrochemical cell, a lithium-ion battery, or a lithium-sulfur battery. The battery 100 may have a body 105 that includes a first substrate 101, a second substrate 102, a cathode 110, an anode 120 positioned opposite to the cathode 110, and an electrolyte 130. In some aspects, the first substrate 101 may function as a current collector for the anode 120, and the second substrate 102 may function as a current collector for the cathode 110. The cathode 110 may include a first thin film 111 deposited onto the second substrate 102, and may include a second thin film 112 deposited onto the first thin film 111. In some implementations, the electrolyte 130 may be a liquid-phase electrolyte including one or more additives such as lithium nitrate, tin fluoride, lithium iodide, lithium bis(oxalate)borate (LiBOB), cesium nitrate, cesium fluoride, ionic liquids, lithium fluoride, fluorinated ether, TBT, MBT, DPT and/or the like. Suitable solvent packages for these example additives may include various dilution ratios, including 1:1:1 of 1,3-dioxolane (DOL), 1,2-dimethoxyethane, (DME), tetraethylene glycol dimethyl ether (TEGDME), and/or the like.

**[0080]** Although not shown for simplicity, in one implementation, a lithium layer may be electrodeposited on one or more exposed carbon surfaces of the anode 120. In some instances, the lithium layer may include elemental lithium provided by the ex-situ electrodeposition of lithium onto exposed surfaces of the anode 120. In some aspects, the lithium layer may include lithium, calcium, potassium, magnesium, sodium, and/or cesium, where each metal may be ex-situ deposited onto exposed carbon surfaces of the anode 120. The lithium layer may provide lithium ions available for transport to-and-from the cathode 110 during operational cycling of the battery 100. As a result, the battery 100 may not need an additional lithium source for operation. Instead of using lithium sulfide, elemental sulfur ($S_8$) may be pre-loaded in various pores or porous networks formed in the cathode 110. During operational cycling of the battery, the elemental sulfur may form lithium-sulfur complexes that can micro-confine (at least temporarily) greater amounts of lithium than conventional cathode designs. As a result, the battery 100 may outperform batteries that rely on such conventional cathode designs.

**[0081]** In various implementations, the lithium layer may dissociate and/or separate into lithium ions 125 and electrons 174 during a discharge cycle of the battery 100. The lithium

ions 125 may migrate from the anode 120 towards the cathode 110 through the electrolyte 130 to their electrochemically favored positions within the cathode 110, as depicted in the example of Figure 1. As the lithium ions 125 move through the electrolyte 130, electrons 174 are released from lithium ions 125 and become available to carry charge, and therefore conduct an electric current, between the anode 120 and cathode 110. As a result, the electrons 174 may travel from the anode 120 to the cathode 110 through an external circuit to power a load 172. The load 172 may be any suitable circuit, device, or system such as (but not limited to) a lightbulb, consumer electronics, or an electric vehicle (EV).

**[0082]** In some implementations, the battery 100 may include a solid-electrolyte interphase layer 140. The solid-electrolyte interphase layer 140 may, in some instances, be formed artificially on the anode 120 during operational cycling of the battery 100. In such instances, the solid-electrolyte interphase layer 140 may also be referred to as an artificial solid-electrolyte interphase, or A-SEI. The solid-electrolyte interphase layer 140, when formed as an A-SEI, may include tin, manganese, molybdenum, and/or fluorine compounds. Specifically, the molybdenum may provide cations, and the fluorine compounds may provide anions. The cations and anions may interact with each other to produce salts such as tin fluoride, manganese fluoride, silicon nitride, lithium nitride, lithium nitrate, lithium phosphate, manganese oxide, lithium lanthanum zirconium oxide (*LLZO*, $Li_7La_3Zr_2O_{12}$), etc. In some instances, the A-SEI may be formed in response to exposure of lithium ions 125 to the electrolyte 130, which may include solvent-based solutions including tin and/or fluorine.

**[0083]** In various implementations, the solid-electrolyte interphase layer 140 may be artificially provided on the anode 120 prior to activation of the battery 100. Alternatively, in one implementation, the solid-electrolyte interphase layer 140 may form naturally, e.g., during operational cycling of the battery 100, on the anode 120. In some instances, the solid-electrolyte interphase layer 140 may include an outer layer of shielding material that can be applied to the anode 120 as a micro-coating. In this way, formation of the solid-electrolyte interphase layer 140 on portions of the anode 120 facing the electrolyte 130 may result from electrochemical reduction of the electrolyte 130, which in turn may reduce uncontrolled decomposition of the anode 120.

**[0084]** In some implementations, the battery 100 may include a barrier layer 142 that flanks the solid-electrolyte interphase layer 140, for example, as shown in Figure 1. The barrier layer 142 may include a mechanical strength enhancer 144 coated and/or deposited on the anode 120. In some aspects, the mechanical strength enhancer 144 may provide structural

support for the battery 100, may prevent lithium dendrite formation from the anode 120, and/or may prevent protrusion of lithium dendrite throughout the battery 100. In some implementations, the mechanical strength enhancer 144 may be formed as a protective coating over the anode 120, and may include one or more carbon allotropes, carbon nano-onions (CNOs), nanotubes (CNTs), reduced graphene oxide, graphene oxide (GO), and/or carbon nano-diamonds. In some instances, the solid-electrolyte interphase layer 140 may be formed within the mechanical strength enhancer 144.

**[0085]** In some implementations, the first substrate 101 and/or the second substrate 102 may be a solid copper metal foil and may influence the energy capacity, rate capability, lifespan, and long-term stability of the battery 100. For example, to control energy capacity and other performance attributes of the battery 100, the first substrate 101 and/or the second substrate 102 may be subject to etching, carbon coating, or other suitable treatment to increase electrochemical stability and/or electrical conductivity of the battery 100. In other implementations, the first substrate 101 and/or the second substrate 102 may include or may be formed from a selection of aluminum, copper, nickel, titanium, stainless steel and/or carbonaceous materials depending on end-use applications and/or performance requirements of the battery 100. For example, the first substrate 101 and/or the second substrate 102 may be individually tuned or tailored such that the battery 100 meets one or more performance requirements or metrics.

**[0086]** In some aspects, the first substrate 101 and/or the second substrate 102 may be at least partially foam-based or foam-derived, and can be selected from any one or more of metal foam, metal web, metal screen, perforated metal, or sheet-based three-dimensional (3D) structures. In other aspects, the first substrate 101 and/or the second substrate 102 may be a metal fiber mat, metal nanowire mat, conductive polymer nanofiber mat, conductive polymer foam, conductive polymer-coated fiber foam, carbon foam, graphite foam, or carbon aerogel. In some other aspects, the first substrate 101 and/or second substrate 102 may be carbon xerogel, graphene foam, graphene oxide foam, reduced graphene oxide foam, carbon fiber foam, graphite fiber foam, exfoliated graphite foam, or any combination thereof.

**[0087]** Figure 2 shows another example battery 200, according to some implementations. The battery 200 may be similar to the battery 100 of Figure 1 in many respects, such that description of like elements is not repeated herein. In some implementations, the battery 200 may be a next-generation battery, such as a lithium-metal battery and/or a solid-state battery featuring a solid-state electrolyte. In other implementations, the battery 200 may include a

liquid-phase electrolyte 230 and may therefore include any of the protective layers and/or electrolyte chemistries or compositions disclosed herein.

**[0088]** In some other implementations, the electrolyte 230 may be solid or substantially solid. For example, in some instances, the electrolyte 230 may begin in a gel phase and then later solidify upon activation of the battery 200. The battery 200 may reduce specific capacity or energy losses associated with the polysulfide shuttle effect by replacing conventional carbon scaffolded anodes with a single solid metal layer of lithium deposited in an initially empty cavity. For example, while the anode 120 of the battery 100 of Figure 1 may include carbon scaffolds, the anode 220 of the battery 200 of Figure 2 may be a lithium-metal anode devoid of any carbon material. In one implementation, the lithium-metal anode may be formed as a single solid lithium metal layer and referred to as a "lithium metal anode."

**[0089]** Energy density gains associated with various cathode materials may be based on whether lithium metal is pre-loaded into the cathode 210 and/or is prevalent in the electrolyte 230. Either the cathode 210 and/or the electrolyte 230 may provide lithium available for lithiation of the anode 220. For example, batteries having high-capacity cathodes may need thicker or energetically denser anodes in order to supply the increased quantities of lithium needed for usage by the high-capacity cathodes. In some implementations, the anode 220 may include scaffolded carbonaceous structures capable of being incrementally filled with lithium deposited therein. These carbonaceous structures may be capable of retaining greater amounts of lithium within the anode 220 as compared to conventional graphitic anodes, which may be limited to solely hosting lithium intercalated between alternating graphene layers or may be electroplated with lithium. For example, conventional graphitic anodes may use six carbon atoms to hold a single lithium atom. In contrast, by using a pure lithium metal anode, such as the anode 220, batteries disclosed herein may reduce or even eliminate carbon use in the anode 220, which may allow the anode 220 to store greater amounts of lithium in a relatively smaller volume than conventional graphitic anodes. In this way, the energy density of the battery 200 may be greater than conventional batteries of a similar size.

**[0090]** Lithium metal anodes, such as the anode 220, may be prepared to function with a solid-state electrolyte designed to inhibit the formation and growth of lithium dendrites from the anode. In some aspects, a separator 250 may further limit dendrite formation and growth. The separator 250 may have a similar ionic conductivity as the electrolyte 130 of Figure 1 yet still reduce lithium dendrite formation. In some aspects, the separator 250 may be formed

from a ceramic containing material and may, as a result, fail to chemically react with metallic lithium. As a result, the separator 250 may be used to control lithium ion transport through pores dispersed across the separator 250 while concurrently preventing a short-circuit by impeding the flow or passage of electrons through the electrolyte 230.

**[0091]** In one implementation, a void space (not shown for simplicity) may be formed within the battery 200 at or near the anode 220. Operational cycling of the battery 200 in this implementation may result in the deposition of lithium into the void space. As a result, the void space may become or transform into a lithium-containing region (such as a solid lithium metal layer) and function as the anode 220. In some aspects, the void space may be created in response to chemical reactions between a metal-containing electrically inactive component and a graphene-containing component of the battery 200. Specifically, the graphene-containing component may chemically react with lithium deposited into the void space during operational cycling and produce lithiated graphite ($LiC_6$) or a patterned lithium metal. The lithiated graphite produced by the chemical reactions may generate or lead to the generation and/or liberation of lithium ions and/or electrons that can be used to carry electric charge or a "current" between the anode 220 and the cathode 210 during discharge cycles of the battery 200.

**[0092]** And, in implementations for which the anode 220 is a solid lithium metal layer, the battery 200 may be able to hold more electroactive material and/or lithium per unit volume (as compared to batteries with scaffolded carbon and/or intercalated lithiated graphite anodes). In some aspects, the anode 220, when prepared as a solid lithium metal layer, may result in the battery 200 having a higher energy density and/or specific capacity than batteries with scaffolded carbon and/or intercalated lithiated graphite anodes, thereby resulting in longer discharge cycle times and additional power output per unit time. In instances for which use of a solid-state electrolyte is not desired or not optimal, the electrolyte 230 of the battery 200 of Figure 2 may be prepared with any of the liquid-phase electrolyte chemistries and/or compositions disclosed herein. In addition, or in the alternative, the electrolyte 230 may include lithium and/or lithium ions available for cyclical transport from the anode 220 to the cathode 210 and vice-versa during discharge and charge cycles, respectively.

**[0093]** To reduce the migration of polysulfides 282 generated from elemental sulfur 281 pre-loaded in the cathode 210 into the electrolyte 230, the battery 200 may include one or more unique polysulfide retention features. For example, given that polysulfides are soluble in the electrolyte 230, some polysulfides may be expected to drift or migrate from the cathode

210 towards the anode 220 due to differences in electrochemical potential, chemical gradients, and/or other phenomena. The migration of polysulfides 282, especially long-chain form polysulfides, may impede the transport of lithium ions from the anode 220 to the cathode 210, which in turn may reduce the number of electrons available to generate an electric current that can power a load 272, such as an electric vehicle (EV). In some aspects, lithium ions 225 may be transported from one or more start positions 226 in or near the anode 220 along transport pathways to one or more end positions 227 in or near the cathode 210, as depicted in the example of Figure 2.

**[0094]** In some implementations, a polymeric network 285 may be disposed on the anode 220 to reduce the uncontrolled migration of polysulfides 282 from the anode 220 to the cathode 210. The polymeric network 285 may include one or more layers of carbonaceous materials grafted with fluorinated polymer chains cross-linked with each other via the Wurtz reaction upon exposure to Lithium anode surface. The carbonaceous materials in the polymeric network 285, which may include (but are not limited to graphene, few layer graphene, FLG, many layer graphene, and MLG), may be chemically grafted with fluorinated polymer chains containing carbon-fluorine (C-F) bonds. These C-F bonds may chemically react with lithium metal from the surface of the anode 220 to produce highly ionic Carbon-Lithium bonds (C-Li). These formed C-Li bonds, in turn, may react with C-F bonds of polymer chains to form new Carbon-Carbon bonds that can also cross-link the polymer chains into (and thereby form) the polymeric network and generate lithium fluoride (LiF).

**[0095]** The resulting lithium fluoride may be uniformly distributed along the entire perimeter of the polymeric network 285, such that lithium ions are uniformly consumed to produce an interface layer 283 that may form or otherwise include lithium fluoride during battery cycling. The interface layer 283 may extend along a surface or portion of the anode 220 facing the cathode 210, as shown in Figure 2. As a result, the lithium ions 225 are less likely to combine and/or react with each other and are more likely to combine and/or react with fluorine atoms made available by the fluorinated polymer chains in the polymeric network 285. The resulting reduction of lithium-lithium chemical reactions decreases lithium-lithium bonding responsible for undesirable lithium-metal dendrite formation. In addition, in some implementations, the polymeric network 285 may replace the interphase layer 240 that either naturally or artificially develops between the anode 220 and the electrolyte 230.

**[0096]** In one implementation, the interface layer 283 of the polymeric network 285 is in contact with the anode 220, and a protective layer 284 is disposed on top of the interface layer 283 (such as between the interface layer 283 and the interphase layer 240). In some aspects, the interface layer 283 and the protective layer 284 may collectively define a gradient of cross-linked fluoropolymer chains of varying degrees of density, for example, as described with reference to Figure 7.

**[0097]** In some other implementations, the battery 200 may include a protective lattice 280 disposed on the cathode 210. The protective lattice 280 may include a tri-functional epoxy compound and a di-amine oligomer-based compound that may chemically react with each other to produce nitrogen and oxygen atoms. The nitrogen and oxygen atoms made available by the protective lattice 280 can bind with the polysulfides 282, thereby confining the polysulfides 282 within the cathode 210 and/or the protective lattice 280. Either of the cathode 210 and/or the protective lattice 280 may include carbon-carbon bonds and/or regions capable of flexing and/or volumetrically expanding during operational cycling of the battery 200, which may confine polysulfides 282 generated during the operational cycling to the cathode 210.

**[0098]** The electrolyte 130 of Figure 1 and the electrolyte 230 of Figure 2 may be prepared according to one or more recipes disclosed herein. For example, a ternary solvent package used in the electrolyte 130 and/or the electrolyte 230 may include DME, DOL and TEGDME. In one implementation, a solvent mixture may be prepared by mixing 5800 μL DME, 2900 μL DOL and 1300 μL TEGDME and stirring at room temperature (77°F or 25°C). Next, 0.01 mol (2,850.75 mg) of LiTFSI may be weighed. Afterwards, the 0.01 mol of LiTFSI may be dissolved in solvent mixture by stirring at room temperature to prepare approximately 10 mL 1 M LiTFSI in DME:DOL:TEGDME (volume: volume: volume 1:4:1). Finally, approximately 223 mg $LiNO_3$ may be added to 10 mL solution to produce 10 mL 1 M LiTFSI in DME:DOL:TEGDME (volume: volume: volume = 58:29:13) with approximately 2 wt.% $LiNO_3$.

**[0099]** In addition, or the alternative, a ternary solvent package used in the electrolyte 130 and/or the electrolyte 230 may include DME, DOL, TEGDME, and TBT or MBT. A solvent mixture may be prepared by mixing 2,000 μL DME, 8,000 μL DOL and 2,000 μL TEGDME and stirring at room temperature (68°F or 25°C). Next, 0.01 mol (2,850.75 mg) of LiTFSI may be weighed and dissolved in approximately 3 mL of the solvent mixture by stirring at room temperature. Next, the dissolved LiTFSI and an additional solvent mixture

(~ 8,056 mg) may be mixed in a 10 mL volumetric flask to produce approximately 1 M LiTFSI in DME:DOL:TEGDME (volume: volume: volume 1:4:1). Finally, approximately 0.05 mmol (~12.5 mg) TBT or MBT may be added to the 10 mL solution to produce 10 mL of 5M TBT or MBT solution.

**[0100]** Figure 3 shows an example electrode 300, according to some implementations. In various implementations, the electrode 300 may be one example of the cathode 110 and/or the anode 120 of the battery 100 of Figure 1. In some other implementations, the electrode 300 may be one example of the cathode 210 of the battery 200 of Figure 2. When the electrode 300 is implemented as a cathode (such as the cathode 110 of the battery 100 of Figure 1), the electrode 300 may temporarily micro-confine an electroactive material, such as elemental sulfur, which may decrease the amount of sulfur available for reacting with lithium to produce polysulfides. In some aspects, the electrode 300 may provide an excess supply of lithium and/or lithium ions that can compensate for first-cycle operational losses associated with lithium-based batteries.

**[0101]** In some implementations, the electrode 300 may be porous and receptive of a liquid-phase electrolyte, such as the electrolyte 130 of Figure 1. Electroactive species, such as lithium ions 125 suspended in the electrolyte 130, may chemically react with elemental sulfur pre-loaded into pores of the electrode 300 to produce polysulfides, which in turn may be trapped in the electrode 300 during battery cycling. In some aspects, the electrode 300 may expand in volume along one or more flexure points to retain additional quantities of polysulfides created during battery cycling. By confining the polysulfides within the electrode 300, aspects of the subject matter disclosed herein may allow the lithium ions 125 to flow freely through the electrolyte 130 from the anode 120 to the cathode 110 during discharge cycles of the battery 100 (e.g., without being impeded by the polysulfides). For example, when lithium ions 125 reach the cathode 110 and react with elemental sulfur contained in or associated with the cathode 110, sulfur is reduced to lithium polysulfides ($Li_2S_x$) at decreasing chain lengths according to the order $Li_2S_8 \rightarrow Li_2S_6 \rightarrow Li_2S_4 \rightarrow Li_2S_2 \rightarrow Li_2S$, where $2 \leq x \leq 8$). Higher order polysulfides may be soluble in various types of solvents and/or electrolytes, thereby interfering with the lithium ion transport necessary for healthy battery operation. Retention of such higher order polysulfides by the electrode 300 thereby allows the lithium ions 125 to flow more freely through the electrolyte 130, which in turn may increase the number of electrons available to carry charge from the anode 120 to the cathode 110.

**[0102]** The electrode 300 may include a body 301 defined by a width 305, and may include a first thin film 310 and a second thin film 320. The first thin film 310 may include a plurality of first aggregates 312 that join together to form a first porous structure 316 of the electrode 300. In some instances, the first porous structure 316 may have an electrical conductivity between approximately 0 and 500 S/m. In other instances, the first electrical conductivity may be between approximately 500 and 1,000 S/m. In some other instances, the first electrical conductivity may be greater than 1,000 S/m. In some aspects, the first aggregates 312 may include carbon nano-tubes (CNTs), carbon nano-onions (CNOs), flaky graphene, crinkled graphene, graphene grown on carbonaceous materials, and/or graphene grown on graphene.

**[0103]** In some implementations, the first aggregates 312 may be decorated with a plurality of first nanoparticles 314. In some instances, the first nanoparticles 314 may include tin, lithium alloy, iron, silver, cobalt, semiconducting materials and/or metals such as silicon and/or the like. In some aspects, CNTs, due to their ability to provide high exposed surface areas per unit volume and stability at relatively high temperatures (such as above 77°F or 25°C), may be used as a support material for the first nanoparticles 314. For example, the first nanoparticles 314 may be immobilized (such as by decoration, deposition, surface modification or the like) onto exposed surfaces of CNTs and/or other carbonaceous materials. The first nanoparticles 314 may react with chemically available carbon on exposed surfaces of the CNTs and/or other carbonaceous materials.

**[0104]** The second thin film 320 may include a plurality of second aggregates 322 that join together to form a second porous structure 326. In some instances, the electrical conductivities of the first porous structure 316 and/or the second porous structure 326 may be between approximately 0 S/m and 250 S/m. In instances for which the first porous structure 316 includes a higher concentration of aggregates than the second porous structure 326, the first porous structure 316 may have a higher electrical conductivity than the second porous structure 326. In one implementation, the first electrical conductivity may be between approximately 250 S/m and 500 S/m, while the second electrical conductivity may be between approximately 100 S/m and 250 S/m. In another implementation, the second electrical conductivity may be between approximately 250 S/m and 500 S/m. In yet another implementation, the second electrical conductivity may be greater than 500 S/m. In some aspects, the second aggregates 322 may include CNTs, CNOs, flaky graphene, crinkled graphene, graphene grown on carbonaceous materials, and/or graphene grown on graphene.

**[0105]** The second aggregates 322 may be decorated with a plurality of second nanoparticles 324. In some implementations, the second nanoparticles 324 may include iron, silver, cobalt, semiconducting materials and/or metals such as silicon and/or the like. In some instances, CNTs may also be used as a support material for the second nanoparticles 324. For example, the second nanoparticles 324 may be immobilized (such as by decoration, deposition, surface modification or the like) onto exposed surfaces of CNTs and/or other carbonaceous materials. The second nanoparticles 324 may react with chemically available carbon on exposed surfaces of the CNTs and/or other carbonaceous materials.

**[0106]** In some aspects, the first thin film 310 and/or the second thin film 320 (as well as any additional thin films disposed on their respective immediately preceding thin film) may be created as a layer or region of material and/or aggregates. The layer or region may range from fractions of a nanometer to several microns in thickness, such as between approximately 0 and 5 microns, between approximately 5 and 10 microns, between approximately 10 and 15 microns, or greater than 15 microns. Any of the materials and/or aggregates disclosed herein, such as CNOs, may be incorporated into the first thin film 310 and/or the second thin film 320 to result in the described thickness levels.

**[0107]** In some implementations, the first thin film 310 may be deposited onto the second substrate 102 of Figure 1 by chemical deposition, physical deposition, or grown layer-by-layer through techniques such as Frank-van der Merwe growth, Stranski-Krastonov growth, Volmer-Weber growth and/or the like. In other implementations, the first thin film 310 may be deposited onto the second substrate 102 by epitaxy or other suitable thin-film deposition process involving the epitaxial growth of materials. The second thin film 320 and/or subsequent thin films may be deposited onto their respective immediately preceding thin film in a manner similar to that described with reference to the first thin film 310.

**[0108]** In various implementations, each of the first aggregates 312 and/or the second aggregates 322 may be a relatively large particle formed by many relatively small particles bonded or fused together. As a result, the external surface area of the relatively large particle may be significantly smaller than combined surface areas of the many relatively small particles. The forces holding an aggregate together may be, for example, covalent, ionic bonds, or other types of chemical bonds resulting from the sintering or complex physical entanglement of former primary particles.

**[0109]** As discussed above, the first aggregates 312 may join together to form the first porous structure 316, and the second aggregates 322 may join together to form the second

porous structure 326. The electrical conductivity of the first porous structure 316 may be based on the concentration level of the first aggregates 312 within the first porous structure 316, and the electrical conductivity of the second porous structure 326 may be based on the concentration level of the second aggregates 322 within the second porous structure 326. In some aspects, the concentration level of the first aggregates 312 may cause the first porous structure 316 to have a relatively high electrical conductivity, and the concentration level of the second aggregates 322 may cause the second porous structure 326 to have a relatively low electrical conductivity (such that the first porous structure 316 has a greater electrical conductivity than the second porous structure 326). The resulting differences in electrical conductivities of the first porous structure 316 and the second porous structure 326 may create an electrical conductivity gradient across the electrode 300. In some implementations, the electrical conductivity gradient may be used to control or adjust electrical conduction throughout the electrode 300 and/or one or more operations of the battery 100 of Figure 1.

**[0110]** As used herein, the relatively small source particles may be referred to as "primary particles," and the relatively large aggregates formed by the primary particles may be referred to as "secondary particles." As shown in Figure 1, Figures 8 to 10, and elsewhere throughout the present disclosure, the primary particles may be or include multiple graphene sheets, layers, regions, and/or nanoplatelets fused and/or joined together. Thus, in some instances, carbon nano-onions (CNOs), carbon nano-tubes (CNTs), and/or other tunable carbon materials may be used to form the primary particles. In some aspects, some aggregates may have a principal dimension (such as a length, a width, and/or a diameter) between approximately 500 nm and 25 μm. Also, some aggregates may include innately-formed smaller collections of primary particles, referred to as "innate particles," of graphene sheets, layers, regions, and/or nanoplatelets joined together at orthogonal angles. In some instances, these innate particles may each have a respective dimension between approximately 50 nm and 250 nm.

**[0111]** The surface area and/or porosity of these innate particles may be imparted by secondary processes, such as carbon-activation by a thermal, plasma, or combined thermal-plasma process using one or more of steam, hydrogen gas, carbon dioxide, oxygen, ozone, KOH, ZnCl2, H3PO4, or other similar chemical agents alone or in combination.. In some implementations, the first porous structure 316 and/or the second porous structure 326 may be produced from a carbonaceous gaseous species that can be controlled by gas-solid reactions under non-equilibrium conditions. Producing the first porous structure 316 and/or

the second porous structure 326 in this manner may involve recombination of carbon-containing radicals formed from the controlled cooling of carbon-containing plasma species (which can be generated by excitement or compaction of feedstock carbon-containing gaseous and/or plasma species in a suitable chemical reactor).

**[0112]** In some implementations, the first aggregates 312 and/or the second aggregates 322 may have a percentage of carbon to other elements, except hydrogen, within each respective aggregate of greater than 99%. In some instances, a median size of each aggregate may be between approximately 0.1 microns and 50 microns. The first aggregates 312 and/or the second aggregates 322 may also include metal organic frameworks (MOFs).

**[0113]** In some implementations, the first porous structure 316 and second porous structure 326 may collectively define a host structure 328, for example, as shown in Figure 3. In some instances, the host structure 328 may be based on a carbon scaffold and/or may include decorated carbons, for example, as shown in Figure 8. The host structure 328 may provide structural definition to the electrode 300. In some instances, the host structure 328 may be fabricated as a positive electrode and used in the cathode 110 of Figure 1. In other implementations, the host structure 328 may be fabricated as a negative electrode and used in the anode 120 of Figure 1. In some other implementations, the host structure 328 may include pores having different sizes, such as micropores, mesopores, and/or macropores defined by the IUPAC. In some instances, at least some of the micropores may have a width of approximately 1.5 nm, which may be large enough to allow sulfur to be pre-loaded into the electrode 300 and yet small enough to confine polysulfides within the electrode 300.

**[0114]** The host structure 328, when provided within the electrode 300 as shown in Figure 3, may include microporous, mesoporous, and/or macroporous pathways created by exposed surfaces and/or contours of the first porous structure 316 and/or the second porous structure 326. These pathways may allow the host structure 328 to receive an electrolyte, for example, by transporting lithium ions towards the cathode 110 of the battery 100. Specifically, the electrolyte 130 may infiltrate the various porous pathways of the host structure 328 and uniformly disperse throughout the electrode 300 and/or other portions of the battery 100. Infiltration of the electrolyte 130 into such regions of the host structure 328 may allow the lithium ions 125 migrating from the anode 120 towards the cathode 110 to react with elemental sulfur associated with the cathode 110 to form lithium-sulfur complexes. As a result, the elemental sulfur may retain additional quantities of lithium ions that would

otherwise be achievable using non-sulfur chemistries such as lithium cobalt oxide (LiCoO) or other lithium-ion cells.

**[0115]** In some aspects, each of the first porous structure 316 and/or the second porous structure 326 may have a porosity based on one or more of a thermal, plasma, or combined thermal-plasma process using one or more of steam, hydrogen gas, carbon dioxide, oxygen, ozone, KOH, ZnCl2, H3PO4, or other similar chemical agents alone or in combination. For example, in one implementation, the macroporous pathways may have a principal dimension greater than 50 nm, the mesoporous pathways may have a principal dimension between approximately 20 nm and 50 nm, and the microporous pathways may have a principal dimension less than 4 nm. As such, the macroporous pathways and mesoporous pathways can provide tunable conduits for transporting lithium ions 125, and the microporous pathways may confine active materials within the electrode 300.

**[0116]** In some implementations, the electrode 300 may include one or more additional thin films (not shown for simplicity). Each of the one or more additional thin films may include individual aggregates interconnected with each other across different thin films, with at least some of the thin films having different concentration levels of aggregates. As a result, the concentration levels of any thin film may be varied (such as by gradation) to achieve particular electrical resistance (or conductance) values. For example, in some implementations, the concentration levels of aggregates may progressively decline between the first thin film 310 and the last thin film (such as in a direction 195 depicted in Figure 1), and/or the individual thin films may have an average thickness between approximately 10 microns and approximately 200 microns. In addition, or in the alternative, the first thin film 310 may have a relatively high concentration of carbonaceous aggregates, and the second thin film 320 may have a relatively low concentration of carbonaceous aggregates. In some aspects, the relatively high concentration of aggregates corresponds to a relatively low electrical resistance, and the relatively low concentration of aggregates corresponds to a relatively high electrical resistance.

**[0117]** The host structure 328 may be prepared with multiple active sites on exposed surfaces of the first aggregates 312 and/or the second aggregates 322. These active sites, as well as the exposed surfaces of the first aggregates 312 and/or the second aggregates 322, may facilitate ex-situ electrodeposition prior to incorporation of the electrode 300 into the battery 100. Electroplating is a process that can create a lithium layer 330 (including lithium on exposed surfaces of the host structure 328) through chemical reduction of metal cations by

application and/or modulation of an electric current. In implementations for which the electrode 300 serves as the anode 120 of the battery 100 in Figure 1, the host structure 328 may be electroplated such that the lithium layer 330 has a thickness between approximately 1 and 5 micrometers (μm), 5 μm and 20 μm, or greater than 20 μm. In some instances, ex-situ electrodeposition may be performed at a location separate from the battery 100 prior to the assembly of the battery 100.

**[0118]** In various implementations, excess lithium provided by the lithium layer 330 may increase the number of lithium ions 125 available for transport in the battery 100, thereby increasing the storage capacity, longevity, and performance of the battery 100 (as compared with traditional lithium-ion and/or lithium-sulfur batteries).

**[0119]** In some aspects, the lithium layer 330 may produce lithium-intercalated graphite ($LiC_6$) and/or lithiated graphite based on chemical reactions with the first aggregates 312 and/or the second aggregates 322. Lithium intercalated between alternating graphene layers may migrate or be transported within the electrode 300 due to differences in electrochemical gradients during operational cycling of the battery 100, which in turn may increase the energy storage and power delivery of the battery 100.

**[0120]** Figure 4 shows a diagram of a portion of an example battery 400 that includes a protective lattice 402, according to some implementations. In some implementations, the protective lattice 402 may be disposed on the anode 220 of the battery 200. In other implementations, the protective lattice 402 may be disposed on the cathode 210 of the battery 200 (or other suitable batteries). In some aspects, the protective lattice 402 may be one example of the protective lattice 280 of Figure 2. The protective lattice 402 may function with many components (e.g., anode, cathode, current collectors associated, carbonaceous materials, electrolyte, and separator) in a manner similar to the battery 100 of Figure 1 and/or the battery 200 of Figure 2.

**[0121]** The protective lattice 402 may include a tri-functional epoxy compound and a di-amine oligomer-based compound that can chemically react with each other to produce a 3D lattice structure (e.g., as shown in Figure 6 and Figure 8). In some aspects, the protective lattice 402 may prevent polysulfide migration within the battery 400 by providing nitrogen and oxygen atoms that can chemically bind with lithium present in the polysulfides, thereby impeding the migration of polysulfides through the electrolyte 130. As a result, lithium ions 125 can be more freely transported from the anode 120 and the cathode 110 of Figure 1, thereby increasing battery performance metrics.

**[0122]** Cyclical usage of the cathode 110 may cause the formation of cracks 404 that at least partially extend into the cathode 110. In one implementation, the protective lattice 402 may disperse throughout the cracks 404, thereby reducing susceptibility of the cathode 110 to rupture during volumetric expansion of the cathode 110 caused by the retention of polysulfides within the cathode 110 during cyclical usage. In one implementation, the protective lattice 402 of Figure 4 may have a cross-linked, 3D structure based on chemical reactions between di-functional, or higher functionality Epoxy and Amine or Amide compounds.. For example, the di-functional, or higher functionality Epoxy compound may be trimethylolpropane triglycidyl ether (TMPTE), tris(4-hydroxyphenyl)methane triglycidyl ether, or tris(2,3-epoxypropyl) isocyanurate, and di-functional, or higher functionality Amine compound may be dihydrazide sulfoxide (DHSO) or one of polyetheramines, for example JEFFAMINE ® D-230 characterized by repeating oxypropylene units in the backbone.

**[0123]** In various implementations, the chemical compounds may be combined and reacted with each other in any number of quantities, amounts, ratios and/or compositions to achieve different performance capabilities relating to binding with polysulfides generated during operation of the battery 400. For example, in one implementation, 113 mg of TMPTE and 134 mg of JEFFAMINE ® D-230 polyetheramine may be mixed together and diluted with 1 mL to 10 mL of tetrahydrofuran (THF), or any other solvent. Additional amounts of TMPTE and/or JEFFAMINE may be mixed together and diluted in THF, or any other solvent, at an example ratio of 113 mg of TMPTE for every 134 mg of JEFFAMINE ® D-230 polyetheramine. For this implementation, proof-of-concept (POC) data shows that the protective lattice 402 of Figure 4 has a defined weight of approximately 2.6 wt.% of the cathode 110 of Figure 1 or the cathode 210 of Figure 2. In other implementations, the protective lattice 402 may have a weight of approximately 2 wt.% to 21 wt. % of the cathode 110 and/or the cathode 210, where an impedance increases of the cathode 110 and/or the cathode 210 may be expected at a weight level of approximately 10 wt.% or more for the protective lattice 402.

**[0124]** In various implementations, the protective lattice 402 may be fabricated based on a mole and/or molar ratio of $-NH_2$ group and epoxy groups and may further accommodate various forms of cross-linking between di-functional, or higher functionality Epoxy and Amine or Amide compound. In some aspects, such forms of cross-linking may include a fully cross-linked stage, e.g., where one $-NH_2$ group is chemically bonded with two epoxy groups and may further extend to configurations including one $NH_2$ group chemically bonded

with only one epoxy group. Still further, in one or more implementations, mixtures including excess quantities (above the ratios presented here) of -$NH_2$ groups may be prepared to provide additional polysulfide binding capability for the protective lattice 402.

**[0125]** In some other implementations, the protective lattice 402 may be prepared by mixing 201g of TMPTE with between 109g and 283g of JEFFAMINE ® D-230 polyetheramine. The resulting mixture may be then diluted with 1 L to 20 L of a selected solvent (such as THF). The resultant diluted solution may be deposited and/or otherwise disposed on the cathode 110 to achieve a crosslinker content between 1 wt.% to 10 wt.%. Additional TMPTE and/or JEFFAMINE may be mixed together and diluted in THF, or another suitable solvent, at an example ratio of 201g of TMPTE for every 109g to 283g of JEFFAMINE ® D-230 polyetheramine.

**[0126]** In still other implementations, the protective lattice 402 may be prepared by mixing 201g of TMPTE with between 74g and 278g DHSO. The resulting mixture may be then diluted with 1 L to 20 L of a selected solvent (such as THF). The resultant diluted solution may be deposited and/or otherwise disposed on the cathode 110 to achieve a crosslinker content between 1 wt.% to 10 wt.%. Additional TMPTE and/or JEFFAMINE may be mixed together and diluted in THF, or another suitable solvent, at an example ratio of 201g of TMPTE for every 201g to 278g of JEFFAMINE ® D-230 polyetheramine.

**[0127]** In one implementation, di-functional, or higher functionality Epoxy compound may chemically react with di-functional, or higher functionality amine compound to produce the protective lattice 402 in a 3D cross-linked form, which may include both functional epoxy compounds and amine containing molecules. In some aspects, the protective lattice 402, when deposited on the cathode 110 of Figure 1 or the cathode 210 of Figure 2, may have a thickness between approximately 1 nm and 5 μm.

**[0128]** In some implementations, the protective lattice 402 may increase the structural integrity of the cathode 110 or the cathode 210, may reduce surface roughness, and may retain polysulfides in the cathode. For example, in one implementation, the protective lattice 402 may serve as sheath on exposed surfaces of the cathode and bind with polysulfides to prevent their migration and diffusion into the electrolyte 130. In this way, aspects of the subject matter disclosed herein may prevent (or at least reduce) battery capacity decay by suppressing the polysulfide shuttle effect. In some aspects, the protective lattice 402 may also fill the cracks 404 formed in the cathode of Figure 4 to improve cathode coating integrity. In various implementations, the protective lattice 402 may be prepared by drop

casting processes in the presence of a solvent, where the resultant solution can penetrate in cracks 404 of the cathode 110 and bind with polysulfides in the cathode 110 to prevent their migration and/or diffusion throughout the electrolyte 130.

**[0129]** In various implementations, the protective lattice 402 may provide nitrogen atoms and/or oxygen atoms that can chemically bond with lithium in the polysulfides generated during operational battery cycling. In one example, the polysulfides may bond with available nitrogen atoms provided by, for example, DHSO. In another example, the polysulfides may bond with available oxygen atoms provided by, for example, DHSO. In yet another example, the polysulfides may bond with other available oxygen atoms.

**[0130]** In some other implementations, the recipes described above may be altered by replacing TMPTE with a tris(4-hydroxyphenyl)methane triglycidyl ether 910 and/or a tris(2,3-epoxypropyl) isocyanurate. In various implementations, the di-amine oligomer-based compound may be (or may include) a JEFFAMINE ® D-230, or other polyetheramines containing polyether backbone normally based on either propylene oxide (PO), ethylene oxide (EO), or mixed PO/EO structure, for example JEFFAMINE ® D-400, JEFFAMINE ® T-403. The protective lattice 402 may also include various concentration levels of inert molecules, e.g., polyethylene glycol chains of various lengths, which may allow to fine-tune mechanical properties of protective lattice and the chemical bonding of various atoms to lithium present in the polysulfides.

**[0131]** Figure 5 shows a diagram of an anode structure 500 that includes a tin fluoride ($SnF_2$) layer, according to some implementations. Specifically, the diagram depicts a cut-away schematic view of the anode structure 500 in which all of the components associated with a first region A have identical counterparts in a second region B, where the first and second regions A and B have opposite orientations around a current collector 520. As such, the description below with reference to the components of first region A is equally applicable to the components of second region B. In some aspects, the anode 502 may be one example of the anode 120 of Figure 1 and/or the anode 220 of Figure 2.

**[0132]** As discussed, lithium-sulfur batteries, such as the battery 100 of Figure 1 and the battery 200 of Figure 2, operate as conversion-chemistry type electrochemical cells in that sulfur pre-loaded into the cathode may dissolve rapidly into the electrolyte prior to and during operation. Lithium, which may be provided by lithiated anodes and/or may be prevalent in the electrolyte, dissociates into lithium ions (Li+) suitable for transport from the anode to the cathode through the electrolyte. The production of lithium ions is associated with a

corresponding release of electrons, which may flow through an external circuit to power a load, as described with reference to Figure 1. However, when lithium disassociates into lithium ions and electrons, some of the lithium ions may undesirably react with polysulfides produced in the cathode, and therefore may no longer be available to generate an output current or voltage. This consumption of lithium ions by polysulfides reduces the overall capacity of the host cell or battery, and may also facilitate corrosion of the anode, which can result in cell failure.

**[0133]** In some implementations, the protective layer 516 may be provided as passivation coating that can reduce the chemical reactivity of the anode 502 during cell assembly or formation. In some aspects, the protective layer 516 may be permeable to lithium ions while concurrently protecting the anode 502 from corrosion caused by chemical reactions between lithium ions and polysulfides. In other implementations, the protective layer 516 may be an artificial solid-electrolyte interphase (A-SEI) that can replace naturally occurring SEIs and/or other types of conventional A-SEIs. In various implementations, the protective layer 516 may be deposited as a liner on top of one or more films disposed on the anode 502. In some aspects, the protective layer 516 may be a self-generating layer that forms during electrochemical reactions associated with operational cycling of the battery. In some aspects, the protective layer 516 may have a thickness that is less than 5 microns. In other aspects, the protective layer 516 may have a thickness between 0.1 and 1.0 microns.

**[0134]** In various implementations, one or more engineered additives that may facilitate the formation and/or deposition of the protective layer 516 on the anode 502 may be provided within the electrolyte of the battery. In other implementations, the engineered additives may be an active ingredient of the protective layer 516. In some aspects, the protective layer 516 may provide tin ions and/or fluoride ions that can prevent undesirable lithium growths from a first edge $518_1$ and a second edge $518_2$ of the anode.

**[0135]** A graded layer 514 may be formed and/or deposited onto the anode 502 beneath the protective layer 516. In various implementations, the graded layer 514 may prevent lithium contained in or associated with the anode 502 from participating in undesirable chemical interactions and/or reactions with the electrolyte 540 that can lead to the growth of lithium-containing dendrites from the anode 502. The graded layer 514 may also facilitate the production of lithium fluoride based on chemical reactions between dissociated lithium ions and fluoride ions. As discussed, the presence of lithium fluoride in or near the anode 502 can decrease the polysulfide shuttle effect. For example, formation of lithium fluoride

(e.g., form available lithium ions and fluorine ions) may occur uniformly across the entirety of the first edge $518_1$ and/or the second edge $518_2$ of the anode. In this way, localized regions of high lithium concentration in the electrolyte 540 near the anode 502 are substantially inhibited. As a result, lithium-lithium bonds contributing to the formation of lithium containing dendritic structures extending length-wise from the anode are correspondingly inhibited, thereby yielding free passage of lithium ions from the anode 502 into the electrolyte (e.g., as encountered during battery operational cycling). In some aspects, the uniform distribution of lithium throughout the graded layer 514 can increase a uniformity of a lithium-ion flux during battery operational cycling. In some aspects, the graded layer 514 may be approximately 5 nanometers (nm) in thickness.

**[0136]** In one or more implementations, the graded layer 514 may structurally reinforce the host battery in a manner that not only decreases or prevents lithium-containing dendritic growth from the anode 502 but also increases the ability of the anode 502 to expand and contract during operational cycling of the host battery without rupturing. In some aspects, the graded layer 514 has a 3D architecture with a graded concentration gradient (e.g., of one or more formative materials and/or ingredients including carbon, tin, and/or fluorine), which facilitates rapid lithium-ion transport. As a result, the graded layer 514 markedly improves overall battery efficiency and performance.

**[0137]** In some implementations, the graded layer 514 may provide an electrochemically desirable surface upon which the protective layer 516 may be grown or deposited. For example, in some aspects, the graded layer 514 may include compounds and/or organometallic compounds including (but not limited to) aluminum, gallium, indium, nickel, zinc, chromium, vanadium, titanium, and/or other metals. In other aspects, the graded layer 514 may include oxides, carbides and/or nitrides of aluminum, gallium, indium, nickel, zinc, chromium, vanadium, titanium, and/or other metals.

**[0138]** In some implementations, the graded layer 514 may include carbonaceous materials including (but not limited to) flaky graphene, few layer graphene (FLG), carbon nano onions (CNOs), graphene nanoplatelets, or carbon nanotubes (CNTs). In other implementations, the graded layer 514 may include carbon, oxygen, hydrogen, tin, fluorine and/or other suitable chemical compounds and/or molecules derived from tin fluoride and one or more carbonaceous materials. The graded layer 514 may be prepared and/or deposited either directly or indirectly on the anode 502 at a different concentration levels. For example, the graded layer 514 may include 5 wt. % carbonaceous materials with a balance of 95 wt. %

tin fluoride, which may result in a relatively uniform disassociation of fluorine atoms and/or fluoride ions from the tin fluoride.

**[0139]** Other suitable ratios include: 5% carbonaceous materials with 95% tin fluoride; 10% carbonaceous materials with 90% tin fluoride, 15% carbonaceous materials with 85% tin fluoride, 20% carbonaceous materials with 80% tin fluoride, 25% carbonaceous materials with 75% tin fluoride, 30% carbonaceous materials with 70% tin fluoride, 35% carbonaceous materials with 65% tin fluoride, 40% carbonaceous materials with 60% tin fluoride, 45% carbonaceous materials with 55% tin fluoride, 50% carbonaceous materials with 50% tin fluoride, 55% carbonaceous materials with 45% tin fluoride, 55% carbonaceous materials with 45% tin fluoride, 60% carbonaceous materials with 40% tin fluoride, 65% carbonaceous materials with 35% tin fluoride, 70% carbonaceous materials with 30% tin fluoride, 75% carbonaceous materials with 25% tin fluoride, 80% carbonaceous materials with 20% tin fluoride, 85% carbonaceous materials with 15% tin fluoride, 90% carbonaceous materials with 10% tin fluoride, 95% carbonaceous materials with 5% tin fluoride. The fluorine atoms and/or fluoride ions may then uniformly react and combine with lithium ions to form lithium fluoride, as further discussed below.

**[0140]** In some implementations, lithium ions cycling between the anode 502 and the cathode (not shown in Figure 5) may produce a tin-lithium alloy region 512 within the graded layer 514. In some aspects, operational cycling of the host battery may result in a uniform dispersion of lithium fluoride within the tin-lithium alloy region 512. The uniform dispersion of lithium fluoride may facilitate a defluorination reaction of at least some of tin (II) fluoride ($SnF_2$) within the tin fluoride layer 510 (and additional tin fluoride which may have dispersed into the graded layer 514 and/or the protective layer). The fluorine atoms and/or fluoride ions made available by the defluorination reaction may chemically bond with at least some of the lithium ions present in or near the anode 502, to create lithium fluoride (LiF) and correspondingly thereby prevent at least some of the lithium ions from bonding with each other and creating a lithium dendritic growth from the anode 502.

**[0141]** For example, at least a portion of the fluorine atoms and/or fluoride ions present in the tin fluoride may dissociate from the protective layer 516 and produce tin ions ($Sn^{2+}$) and fluorine ions ($2F^-$) via one or more chemical reactions. The fluorine atoms and/or fluoride ions dissociated from the protective layer 516 may chemically bond to at least some of the lithium ions present in the electrolyte 540 and/or dispersed throughout the protective layer 516 or the graded layer 514. In some aspects, the dissociated fluorine atoms may form Li—F

bonds or Li—F compounds in the tin-lithium alloy region 512. In other aspects, the dissociated fluorine atoms may form a tin fluoride layer 510 within the graded layer 514.

**[0142]** In addition, in one implementation, at least some of the defluorinated tin fluoride may disperse uniformly throughout the graded layer 514 to produce lithium fluoride (LiF) crystals. The lithium fluoride crystals may act as an electrical insulator and prevent the flow of electrons from the anode 502 into the electrolyte 540 through the first edge $518_1$ and/or the second edge $518_2$ of the anode 502.

**[0143]** In various implementations, the graded layer 514 may be deposited on the anode 502 by one or more of atomic layer deposition (ALD), chemical vapor deposition (CVD), or physical vapor deposition (PVD). For example, ALD may be used to deposit protective films on the anode 502 such as, for example, an ALD film that at least partially reacts with the electrolyte 540 during high-pressure bonding processes. Accordingly, the ALD film may be used to produce the protective layer 516 or the graded layer 514 using an atomic plane available for lithium transfer. Such lithium transfer may be similar in principle to that observed for few layer graphene (FLG) or graphite, where alternating graphene layers in FLG or graphite intercalate lithium ions in various forms including as lithium titanium oxide (LTO), lithium iron phosphate ($PO_3$) (LFP). The described forms of intercalated lithium, e.g., LTO and/or LFP, may be oriented to facilitate rapid lithium atom and/or lithium ion transport and/or diffusion, which may be conducive for the formation and/or synthesis of lithium fluoride (e.g., in the tin fluoride layer 510 and/or elsewhere), as described earlier. Additional forms of intercalated lithium, e.g., perovskite lithium lanthanum titanate (LLTO), may also function to store lithium within the anode 502.

**[0144]** In some implementations, the graded layer 514 may include various distinct types and/or forms of carbon and/or carbonaceous materials, each having one or more physical attributes that can be selected or configured to adjust the reactivity of carbon with contaminants (such as polysulfides) present in the electrolyte 540 and/or the anode 502. In some aspects, the selectable physical attributes may include (but are not limited to) porosity, surface area, surface functionalization, or electric conductivity. In addition, the graded layer 514 may include binders or other additives that can be used to adjust one or more physical attributes of the carbonaceous materials to achieve a desired reactivity of carbon supplied by the carbonaceous materials with polysulfides present in the electrolyte 540 and/or the anode 502.

**[0145]** In one implementation, carbonaceous materials within the graded layer 514 may

capture unwanted contaminants and thereby prevent the contaminants from chemically reacting with lithium available at exposed surfaces of the anode 502. Instead, the unwanted contaminants (e.g., polysulfides) may chemically react with various exposed surfaces of the carbonaceous materials within the graded layer 514 (e.g., through carbon – lithium interactions). In some implementations, the carbonaceous materials within the graded layer 514 may cohere to the available lithium. The degree of cohesion between the carbonaceous materials and the lithium ions may be selected or modified via chemical reactions induced during preparation of the graded layer 514.

**[0146]** In some implementations, various carbon allotropes may be incorporated within the graded layer 514 (such as in one or more portions of the tin-lithium alloy region 512 and/or the tin fluoride layer 510). These carbon allotropes may be functionalized with one or more reactants and used to form a sealant layer and/or region at an interface of carbon nanodiamonds within the graded layer 514 and the electrolyte 540. In some aspects, the carbon nanodiamonds may increase the mechanical robustness of the anode 502 and/or the graded layer 514. In other aspects, the carbon nanodiamonds may also provide exposed carbonaceous surfaces that may be used to decrease the polysulfide shuttle effect by micro-confining and/or bonding with polysulfides present in the electrolyte 540 in a manner that retains the polysulfides within defined regions of the battery external to the anode 502.

**[0147]** Alternatively, in other implementations, the carbon nanodiamonds within the graded layer 514 may be replaced with carbons and/or carbonaceous materials including surfaces and/or regions having a specific $L_A$ dimensions (e.g., $sp^2$ hybridized carbon), reduced graphene oxide (rGO), and/or graphene. In some aspects, employing the carbonaceous materials disclosed herein within a battery may increase carbon stacking and layer formation within the graded layer 514. Exfoliated and oxidized carbonaceous materials may also yield more uniform layered structures within the graded layer 514 (as compared to carbonaceous materials that have not been exfoliated and oxidized). In some aspects, solvents such as tetrabutylammonium hydroxide (TBA) and/or dimethyl formamide (DMF) treatments may be applied to the carbonaceous materials disclosed herein to increase the wetting of exposed carbonaceous surfaces within the graded layer 514.

**[0148]** In some implementations, slurries used to form the graded layer 514 may be doped to improve or otherwise influence the crystalline structure of carbonaceous materials within the graded layer 514. For example, addition of certain dopants may influence the crystalline structure of the carbonaceous materials in a certain corresponding way, and

functional groups may be added (e.g., via grafting onto exposed carbon atoms within the carbonaceous materials) within the graded layer 514.

**[0149]** In some implementations, carbonaceous materials having exposed surfaces functionalized with one or more of fluorine-containing or silicon-containing functional groups may be included within the graded layer 514. In other implementations, carbonaceous materials having exposed surfaces functionalized with one or more of fluorine-containing or silicon-containing functional groups may be deposited beneath the graded layer 514 to form a stable SEI on at an interface between the graded layer 514 and the anode 502. In one implementation, the stable SEI may replace the protective layer 516. In some implementations, the graded layer 514 may be slurry cast and/or deposited using other techniques onto the anode 502 with lithium and carbon interphases, any of which may be functionalized with silicon and/or nitrogen to inhibit the diffusion and migration of polysulfides towards exposed surfaces of the anode 502. In addition, specific polymers and/or crosslinkers may be incorporated within the graded layer 514 to mechanically strengthen the graded layer 514, to improve lithium ion transport across the graded layer 514, or to increase the uniformity of lithium ion flux across the graded layer 514. Example polymers and/or polymeric materials suitable for incorporation within the graded layer 514 may include poly(ethylene oxide) and poly(ethyleneimine). Example crosslinkers suitable for incorporation within the graded layer 514 may include inorganic linkers (e.g., borate, aluminate, silicate), multifunctional organic molecules (e.g., diamines, diols), polyurea, or high molecular weight (MW) (e.g., >10,000 daltons) carboxymethyl cellulose (CMC).

**[0150]** Various fabrication methods may be employed to produce the graded layer 514. In one implementation, direct coating of the interface between the anode 502 and the electrolyte 540 prior to the deposition and/or formation of the graded layer 514 may be performed with a dispersion of carbonaceous materials and other chemicals dissolved in a carrier (e.g., a solvent, binder, polymer). In another implementation, deposition of the graded layer 514 may be performed as a separate operation, or may be added to various other active ingredients (e.g., metals, carbonaceous materials, tin fluoride and/or the like) into a slurry that can be cast onto the anode 502. Alternatively, in another implementation, the protective layer 516 may be transferred directly onto the anode 502 by a calendar roll lamination processes. The protective layer 516 and/or the graded layer 514 may also incorporate partially-cured lithium ion conductive epoxies to, for example, increase adhesion with lithium better during the calendar roll lamination processes.

**[0151]** In one implementation, a carbon-inclusive layered structure (not shown in Figure 5) may be disposed on the anode 502 as a replacement for the graded layer 514. The carbon-inclusive layered structure may include an atomic plane available for lithium transfer, and may uniformly transport lithium ions provided by the electrolyte 540 throughout the protective layer 516 in a manner that can guide the formation of lithium fluoride in various portions of the battery. In various implementations, the carbon-inclusive layered structure may include one or more arrangements of few layer graphene (FLG) or graphite and/or may intercalate with lithium and produce one or more reaction products including lithium tin oxide (LTO), lithium iron phosphate (LFP), or perovskite lithium lanthanum titanate (LLTO).

**[0152]** In some implementations, the tin fluoride layer 510 may function as a protection layer against corrosion, including corrosion of copper-inclusive surfaces and/or regions of the protective layer 516, the graded layer 514, or the anode 502. In some aspects, the tin fluoride layer 510 may also provide a uniform seed layer suitable for lithium deposition, and thereby inhibiting dendrite formation. In addition, in some implementations, the tin fluoride layer 510 may include one or more lithium ion intercalating compounds, any one or more having a low voltage penalty. Suitable lithium ion intercalating compounds may include graphitic carbon (e.g., graphite, graphene, reduced graphene oxide, rGO). In one implementation, during fabrication of the anode 502, lithium ions may tend to intercalate prior to plating onto exposed carbonaceous surfaces within the tin fluoride layer 510. In this way, the tin fluoride layer 510 will have a uniform Li distribution ready to act as a seed layer prior to initiation of lithium plating and/or electroplating operations.

**[0153]** In one implementation, one or more conformal coatings may be applied over portions of the anode 502 such that the resulting conformal coating contacts and conforms to the first edge $518_1$ and/or the second edge $518_2$ of the anode 502. In some aspects, the conformal coating may begin as a first spacer edge protection region $530_1$ and a second spacer edge protection region $530_2$ that react or otherwise combine with one or more of the protective layer 516, the tin-lithium alloy region 512, and/or the tin fluoride layer 510 to form a conformal coating 544 that at least partially seals and protects surfaces and/or interfaces between lithium in the anode 502 and various substances suspended in the electrolyte, e.g., copper (Cu). In some aspects, the dissociation of fluorine atoms from tin fluoride present in the conformal coating 544 may react with lithium in the anode 502 to form lithium fluoride, rather than form or grow into lithium dendrites. In this way, the conformal coating 544 may decrease lithium dendrite formation or growth from the anode 502.

**[0154]** The conformal coating 544 may be deposited or disposed over the anode 502 at any number of different thicknesses. In some aspects, the conformal coating 544 may be less than 5 μm thick. In other aspects, the conformal coating 544 may be less than 2 μm thick. In some other aspects, the conformal coating 544 may be less than 1μm thick. These thickness levels may impede the migration of polysulfides towards the anode 502 during battery cycling, thereby preventing at least some of the lithium ions from reacting with the polysulfides. Lithium ions that do not react with the polysulfides are available for transport from the anode to the cathode during discharge cycles of the battery.

**[0155]** The conformal coating 544 (as well as the protective layer 516 and the graded layer 514) can uniquely regulate lithium ion flux toward the first edge $518_1$ and/or the second edge $518_2$ of the anode 502, and thereby prevent corrosion of the anode 502. Such regulation may function in a similar manner to gate spacers used during the fabrication of polysilicon (poly-Si) gates. Specifically, gate spacer or gate sidewall constructs may be used to protect and mechanically support polysilicon gates during the fabrication of integrated circuits (ICs). Similarly, edge protection provided by the conformal coating 544 for the anode 502 of Figure 5 regulates lithium ion flux toward the first edge $518_1$ and/or the second edge $518_2$ of the anode 502, and thereby prevents corrosion of the anode 502. This type of edge protection provided by the conformal coating 544 for the anode 502 may equally apply to other battery and/or electrical cell formats and/or configurations such as (but not limited to) cylindrical cells, stacked cells, and/or the like, with various constructs engineered specifically to fit within the parameters of each of these designs.

**[0156]** In some implementations, fabrication and/or deposition of the conformal coating 544, the protective layer 516, and/or the graded layer 514 on the anode 502 may depend on the type of battery or cell construct in which the anode 502 is incorporated, e.g., cylindrical cells compared to pouch cells and/or prismatic cells. In one implementation, for cylindrical cells, metal anodes may be constructed from an electroactive material, typically metallic lithium, and/or lithium-containing alloys, such as graphitic and/or other carbonaceous composited including lithium, as well as any plenary uniform or multi-layer sheet of material. In one example, a solid metal lithium foil used as the anode 502 may be attached to a copper substrate used as the current collector 520 to facilitate electron transfer through a tab 546 to an external load, as depicted in the example of Figure 5. In other implementations, the battery 500 may include the anode 502 without the current collector 520, where carbonaceous materials contained within the anode 502 may provide an electrically conductive medium

coupled to a circuit.

**[0157]** In some implementations, the anode structure 500 may be incorporated into electrochemical cells and/or batteries by winding around a mandrel. Cylindrical cell layouts typically use double-sided anodes, such as the anode structure 500. In some implementations, cylindrical cell constructions employing the anode structure 500 may use the conformal coating 544 to protect the first edge $518_1$ and/or the second edge $518_2$ of the anode 502. The uniform protection provided by the conformal coating 544 may be referred to herein as "edge protection." In one implementation, edge protection can be incorporated into a cell employing the anode structure 500 by extending the size and/or area of the protective layer 516 to overlap beyond any geometrically induced edge effects, e.g., surface roughness, of the anode.

**[0158]** In other implementations, the anode structure 500 may be incorporated into pouch cells and/or prismatic cells. Generally, two constructs of pouch and/or prismatic cells may be manufactured, including (1): jelly-roll type cells (e.g., seen in industry as lithium-polymer batteries), two mandrel wound electrodes may be produced in a manner similar to cylindrical cells as discussed earlier; and (2): stacked plate type cells, which may be cut from a sheet of a pre-cast and/or pre-laminated prepared anode, leaving an unprotected edge of, for example, the anode 502 (when prepared in a stacked-plate type configuration) exposed and vulnerable to corrosion, fast ion fluxes and exposure within the cells. The conformal coating 544, in a stacked-plate type configuration, may protect the anode 502 and prevent lithium over-saturation in the electrolyte 540. In this way, the conformal coating 544 can control lithium plating on the anode 502 during operational cycling of the battery.

**[0159]** In some implementations, one or more chemical reactions may occur between the electrolyte 540 and the anode 502 (involving solvent decomposition and/or additive reactions) during cell assembly or cell rest period. These chemical reactions may assist in the production of the conformal coating 544. In some aspects, elevated and/or reduced temperatures (e.g., relative to room temperature and/or 20°C) may be used as a stimulus for lithium-induced polymerization of the conformal coating 544. For example, the lithium-induced polymerization may occur in the presence of one or more catalysts and/or by using lithium metal, and its associated chemical reactivity, as an inducing agent to initiate free-radical based polymerization of constituent species within any one or more layers of the anode structure 500 and/or the conformal coating 544. In addition, electrochemical reactions under electrical bias in either the forward or reverse direction may be used to fabricate and/or

deposit the conformal coating 544 onto the anode 502, as well as usage of secondary metals and/or salts as additives that may decompose to form an alloy on the first edge $518_1$ and/or the second edge $518_2$ of metallic lithium in the anode 502 exposed to the electrolyte 540. For example, suitable additives may contain one or more metallic species, e.g., desired for co-alloying with lithium or to be used as a blocking layer to reduce lithium transfer to the first edge $518_1$ and/or the second edge $518_2$ of the anode 502.

**[0160]** Figure 6 shows a schematic diagram of an enlarged portion 600 of the anode structure 500 of Figure 5, according to some implementations. The enlarged portion 600 illustrates placement of the first spacer edge protection region $530_1$ and the second spacer edge protection region $530_2$ (collectively referred to as the edge protection region 530 in Figure 6) in a direction orthogonal to the first edge $518_1$ and/or the second edge $518_2$, as shown in Figure 5. As a result, the edge protection region 530, which may include the carbonaceous materials 610 organized into structures and/or lattices, may block lithium ions from undesirably escaping the anode 502 across the edge protection region 530. In this way, lithium ion dissociation, flux, transport, and/or other movement may be channeled effectively throughout the enlarged portion 600 of Figure 6 (as well as the anode structure 500 of Figure 5), thereby yielding optimal battery operational cycling. In some implementations, carbonaceous materials 610 used to produce the edge protection region may include few layer graphene (FLG), multi-layer graphene (MLG), graphite, carbon nano-tubes (CNTs), carbon nano-onions (CNOs) and/or the like. The carbonaceous materials 610 (e.g., shown in Figure 8A, Figure 8B, Figure 9A, Figure 9B, Figure 10A and/or Figure 10B) may be synthesized, self-nucleated, or otherwise joined together at varying concentration levels to provide for complete tunability of the edge protection region 530. For example, the density, thickness, and/or compositions of may be designed to reduce lithium ion permeation more than the protective layer 516 or the graded layer 514 to direct lithium ion permeation accordingly. In some implementations, the edge protection region 530 may be less than 5 μm thick. In other aspects, the edge protection region 530 may be less than 2 μm thick. In some other aspects, the edge protection region 530 may be less than 1μm thick. In some implementations, a conductive additive 640 may be added to the carbonaceous materials 610, as well as a binder 620.

**[0161]** Figure 7 shows a diagram of a polymeric network 710, according to some implementations. In some aspects, the polymeric network 710 may be one example of the polymeric network 285 of Figure 2. The polymeric network 710 may be disposed on an

anode 702. The anode 702 may be formed as an alkali metal layer having one or more exposed surfaces that include any number of alkali metal-containing nanostructures or microstructures. The alkali metal may include (but is not limited to) lithium, sodium, zinc, indium and/or gallium. The anode 702 may release alkali ions during operational cycling of the battery.

**[0162]** A layer 714 of carbonaceous materials may be grafted with fluorinated polymer chains and deposited over one or more exposed surfaces of the anode 702. The grafting may be based on (e.g., initiated by) activation of carbonaceous material with one or more radical initiators, for example, benzoyl peroxide (BPO) or azobisisobutyronitrile (AIBN), followed by reaction with monomer molecules. The polymeric network 710 may be based on the fluorinated polymer chains cross-linked with one another and carbonaceous materials of the layer 714 such that the layer 714 is consumed during generation of the polymeric network 710. In some implementations, the polymeric network 710 may have a thickness approximately between 0.001 μm and 5 μm and include between approximately 0.001 wt.% to 2 wt.% of the fluorinated polymer chains. In some other implementations, the polymeric network 710 may include between approximately 5 wt.% to 100 wt.% of the plurality of carbonaceous materials grafted with fluorinated polymer chains and a balance of fluorinated polymers, or one or more non-fluorinated polymers, or one or more cross-linkable monomers, or combinations thereof. In one implementation, carbonaceous materials grafted with fluorinated polymer chains may include 5 wt.% to 50 wt.% of fluorinated polymer chains and a balance of carbonaceous material.

**[0163]** During battery cycling, carbon-fluorine bonds within the polymeric network 710 may chemically react with newly forming Lithium metal and convert into carbon-Lithium bonds (C-Li). These C-Li bonds may, in turn, react with carbon-fluorine bonds within the polymeric network 710 via a Wurtz reaction 750, to further cross-link polymeric network by newly formed C-C bonds and to form an alkali-metal containing fluoride (such as lithium fluoride (LiF)). Additional polymeric network cross-linking leading to uniform formation of the alkali-metal containing fluoride may thereby suppress alkali metal dendrite formation 740 associated with the anode 702, thereby improving battery performance and longevity. In one implementation, grafting of fluorinated m/acrylate (FMA) to one or more exposed graphene surfaces of carbonaceous materials in the layer 714 may be performed in an organic solution, e.g., leading to the formation of graphene-graft-poly-FMA and/or the like. Incorporation of carbon-fluorine bonds on exposed graphene surfaces may enable the Wurtz reaction 750 to

occur between carbon-fluorine bonds and metallic surface of an alkali metal (e.g., lithium) provided by the anode 702. In this way, completion of the Wurtz reaction 750 may result in the formation of the polymeric network 710. In some aspects, the polymeric network 710 may include a density gradient 716 pursuant to completion of the Wurtz reaction 750. The density gradient 716 may include interconnected graphene flakes and may be infused with one or more metal-fluoride salts formed in-situ. In addition, layer porosity and/or mechanical properties may be tuned by carbon loading and/or a combination of functionalized carbons, each having a unique and/or distinct physical structure.

**[0164]** In some implementations, carbonaceous materials within the density gradient 716 may include one or more of flat graphene, wrinkled graphene, a plurality of carbon nano-tubes (CNTs), or a plurality of carbon nano-onions (CNOs) (e.g., as depicted in Figure 8A and/ Figure 8B and as shown in the micrographs of Figures 9A-9B and Figures 10A-10B). In one implementation, graphene nanoplatelets may be dispersed throughout and isolated from each other within the polymeric network 710. The dispersion of the graphene nanoplatelets includes one or more different concentration levels. In one implementation, the dispersion of the graphene nanoplatelets may include at least some of the carbonaceous materials functionalized with at least some of the fluorinated polymer chains.

**[0165]** For example, the fluorinated polymer chains may include one or more acrylate or methacrylate monomers including 2,2,3,3,4,4,5,5,6,6,7,7-Dodecafluoroheptyl acrylate (DFHA), 3,3,4,4,5,5,6,6,7,7,8,8,9,9,10,10,10-Heptadecafluorodecyl methacrylate (HDFDMA), 2,2,3,3,4,4,5,5-Octafluoropentyl methacrylate (OFPMA), Tetrafluoropropyl methacrylate (TFPM), 3-[3,3,3-Trifluoro-2-hydroxy-2-(trifluoromethyl)propyl]bicyclo[2.2.1]hept-2-yl methacrylate (HFA monomer), or vinyl-based monomers including 2,3,4,5,6-Pentafluorostyrene (PFSt).

**[0166]** In some implementations, fluorinated polymer chains may be grafted to a surface of the layer of carbonaceous materials and may thereby chemically interact with the one or more surfaces of the alkali metal of the anode via the Wurtz reaction 750. In organic chemistry, organometallic chemistry, and inorganic main-group polymers, the Wurtz reaction is a coupling reaction, whereby two alkyl halides are reacted with sodium metal (or some other metal) in dry ether solution to form a higher alkane. In this reaction alkyl halides are treated with alkali metal, for example, sodium metal in dry ethereal (free from moisture) solution to produce higher alkanes. In case of Sodium intermediate product of the Wurtz reaction are highly polar and highly reactive Carbon-Sodium metal bonds, which in turn are

chemically reacting with Carbon-Halide bonds to yield newly formed C-C bonds and Sodium Halide. A formation of new Carbon-Carbon bonds allows to use the Wurtz reaction for the preparation of higher alkanes containing even number of carbon atoms, for example:

$$2\ R{-}X + 2\ Na \rightarrow R{-}R + 2\ Na^{+}X^{-} \qquad \text{(Eq. 1)}$$

**[0167]** Other metals have also been used to influence Wurtz coupling, among them silver, zinc, iron, activated copper, indium and a mixture of manganese and copper chloride. The related reaction dealing with aryl halides is called the Wurtz–Fittig reaction. This can be explained by the formation of free radical intermediate and its subsequent disproportionation to give alkene. The Wurtz reaction 750 occurs through a free-radical mechanism that makes possible side reactions producing alkene products. In some implementations, chemical interactions associated with the Wurtz reaction described above may form an alkali metal fluoride, e.g., lithium fluoride.

**[0168]** In one implementation, the polymeric network 710 may include an interface layer 718 in contact with the anode 702. A protective layer 720 may be disposed on top of the interface layer 718, which may be based on the Wurtz reaction 750 at an interface between the anode 702 and the polymeric network 710. The interface layer 718 may have a relatively high cross-linking density (e.g., of fluorinated polymers and/or the like), a high metal-fluoride concentration, and a relatively low carbon-fluorine bond concentration. In contrast to the interface layer 718, the protective layer 720 may have a relatively low cross-linking density, a low metal-fluoride concentration, and a high carbon-fluorine bond concentration.

**[0169]** In some implementations, the interface layer 718 may include cross-linkable monomers such as methacrylate (MA), acrylate, vinyl functional groups, or a combination of epoxy and amine functional groups. In one implementation, the protective layer 720 may be characterized by the density gradient 716. In this way, the density gradient 716 may be associated with one or more self-healing properties of the protective layer 720 and/or may strengthen the polymeric network 710. In some implementations, the protective layer 720 may further suppress alkali metal dendrite formation 740 from the anode 702 during battery cycling.

**[0170]** Operationally, the interface layer 718 may suppress alkali metal dendrite formation 740 associated with the anode 702 by uniformly producing metal-fluorides, e.g., lithium fluoride, at an interface across the length of the anode 702. The uniform production of metal fluorides causes dendrite surface dissolution, e.g., via conversion into metal-fluorides, ultimately suppressing alkali metal dendrite formation 740. In addition, cross-

linking of fluorinated polymer chains over remaining dendrites may further suppress alkali metal dendrite formation 740. In some implementations, the density gradient 716 may be tuned to control the degree of cross-linking between the fluorinated polymer chains.

**[0171]** Figure 8A shows a simplified cutaway view of an example carbonaceous particle 800 with graded porosity, according to some implementations. The carbonaceous particle 800 may be synthesized in a reactor, and output in a controlled manner to produce the cathode 110 and/or anode 120 of Figure 1, the cathode 210 and/or anode 220 of Figure 2, or the electrode 300 of Figure 3. The carbonaceous particle 800, which may also be referred to as a composition of matter, includes a plurality of regions nested within each other. Each region may include at least a first porosity region 811 and a second porosity region 812. The first porosity region 811 may include a plurality of first pores 801, and the second porosity region 812 may include a plurality of second pores 802. In some aspects, each region may be separated from immediate adjacent regions by at least some of the first pores 801. The first pores 801 may be dispersed throughout the first porosity region 811 of the carbonaceous particle 800, and the second pores 802 may be dispersed throughout the second porosity region 812 of the carbonaceous particle 800. In this way, the first pores 801 may be associated with a first pore density, and the second pores 802 may be associated with a second pore density that is different than the first pore density. In some aspects, the first pore density may be between approximately 0.0 cubic centimeters (cc)/g and 2.0 cc/g, and the second pore density may be between approximately 1.5 and 5.0 cc/g. In some aspects, the first pores 801 may be configured to retain polysulfides 820, and the second pores 802 may provide exit pathways from the carbonaceous particle 800.

**[0172]** A group of carbonaceous particles 800 may be joined together to form a carbonaceous aggregate (not shown for simplicity), and a group of carbonaceous aggregates may be joined together to form a carbonaceous agglomerate (not shown for simplicity). In some implementations, the first pores 801 and second pores 802 may be dispersed throughout aggregates formed by respective groups of the carbonaceous particles 800. In some aspects, the first porosity region 811 may be at least partially encapsulated by the second porosity region 812 such that a respective agglomerate may include some of the first pores 801 and/or some of the second pores 802.

**[0173]** In some implementations, the carbonaceous particle 800 may have a principal dimension "A" in an approximate range between 20 nm and 150 nm, an aggregate formed by a group of the carbonaceous particle 800 may have a principal dimension in an approximate

range between 20 nm and 10 μm, and an agglomerate formed by a group of aggregates may have a principal dimension in an approximate range between 0.1 μm and 1,000 μm. In some aspects, at least some of the first pores 801 and the second pores 802 has a principal dimension in an approximate range between 1.3 nm and 32.3 nm. In one implementation, each of the first pores 801 has a principal dimension in an approximate range between 0 nm and 100 nm.

**[0174]** The carbonaceous particle 800 may also include a plurality of deformable regions 813 distributed along a perimeter 810 of the carbonaceous particle 800. The carbonaceous particle 800 may conduct electricity along joined boundaries with (such as the perimeter 810) one or more other carbonaceous particles. The carbonaceous particle 800 may also confine polysulfides 820 within the first pores 801 and/or at one or more blocking regions 822, thereby inhibiting the migration of polysulfides 820 towards the anode and increasing the rate at which lithium ions can be transported from the anode to the cathode of a host battery.

**[0175]** In some implementations, the carbonaceous particle 800 may have a surface area of exposed carbon surfaces in an approximate range between 10 $m^2/g$ to 3,000 $m^2/g$. In other implementations, the carbonaceous particle 800 may have a composite surface area including sulfur 824 micro-confined within a number of the first pores 801 and/or a number of the second pores 802. As used herein, the first pores 801 and/or the second pores 802 that micro-confine the polysulfides 820 may be referred to as "functional pores." In some aspects, one or more of the carbonaceous particles, the aggregates formed by corresponding groups of carbonaceous particles, or the agglomerates formed by corresponding groups of aggregates may include one or more exposed carbon surfaces configured to nucleate the sulfur 824. The composite surface area may be in an approximate range between 10 $m^2/g$ to 3,000 $m^2/g$, and the carbonaceous particle 800 may have a sulfur to carbon weight ratio between approximately 1:5 to 10:1. In some aspects, the carbonaceous particle 800 may have an electrical conductivity in an approximate range between 100 S/m to 20,000 S/m at a pressure of 12,000 pounds per square in (psi).

**[0176]** In some implementations, the carbonaceous particle 800 may include a surfactant or a polymer that includes one or more of styrene butadiene rubber, polyvinylidene fluoride, poly acrylic acid, carboxyl methyl cellulose, polyvinylpyrrolidone, and/or polyvinyl acetate that can act as a binder to join a group of the carbonaceous particles 800 together. In other implementations, the carbonaceous particle 800 may include a gel-phase electrolyte or a solid-phase electrolyte disposed within at least some of the first pores 801 or second pores

802.

**[0177]** Figure 8B shows a diagram of an example of a tri-zone particle 850, according to some implementations. In various implementations, the tri-zone particle 850 may be one example of the carbonaceous particle 800 of Figure 8A. The tri-zone particle 850 may include three discrete zones such as (but not limited to) a first zone 851, a second zone 852, and a third zone 853. In some aspects, each of the zones 851–853 surrounds and/or encapsulates a preceding zone. For example, the first zone 851 may be surrounded by or encapsulated by the second zone 852, and the second zone 852 may be surrounded by or encapsulated by the third zone 853. The first zone 851 may correspond to an inner region of the tri-zone particle 850, the second zone 852 may correspond to an intermediate transition region of the tri-zone particle 850, and the third zone 853 may correspond to an outer region of the tri-zone particle 850. In some aspects, the tri-zone particle 850 may include a permeable shell 855 that deforms in response to contact with one or more adjacent non-tri-zone particles and/or tri-zone particles 850.

**[0178]** In some implementations, the first zone 851 may have a relatively low density, a relatively low electrical conductivity, and a relatively high porosity, the second zone 852 may have an intermediate density, an intermediate electrical conductivity, and an intermediate porosity, and the third zone 853 may have a relatively high density, a relatively high electrical conductivity, and a relatively low porosity. In some aspects, the first zone 851 may have a density of carbonaceous material between approximately 1.5 g/cc and 5.0 g/cc, the second zone 852 may have a density of carbonaceous material between approximately 0.5 g/cc and 3.0 g/cc, and the third zone 853 may have a density of carbonaceous material between approximately 0.0 and 1.5 g/cc. In other aspects, the first zone 851 may include pores having a width between approximately 0 and 40 nm, the second zone 852 may include pores having a width between approximately 0 and 35 nm, and the third zone 853 may include pores having a width between approximately 0 and 30 nm. In some other implementations, the second zone 852 may not be defined for the tri-zone particle 850. In one implementation, the first zone 851 may have a principal dimension $D_1$ between approximately 0 nm and 100 nm, the second zone 852 may have a principal dimension $D_2$ between approximately 20 nm and 150 nm, and the third zone 853 may have a principal dimension $D_3$ of approximately 200 nm.

**[0179]** Aspects of the present disclosure recognize that the unique layout of the tri-zone particle 850 and the relative dimensions, porosities, and electrical conductivities of the first

zone 851, the second zone 852, and the third zone 853 can be selected and/or modified achieve a desired balance between minimizing the polysulfide shuttle effect and maximizing the specific capacity of a host battery. Specifically, in some aspects, the pores may decrease in size and volume from one zone to other. In some implementations, the tri-zone particle may consist entirely of one zone with a range of pore sizes and pores distributions (e.g., pore density). For the example of Figure 8B, the pores 861 associated with the first zone 851 or the first porosity region have relatively large widths and may be defined as macropores, the pores 862 associated with the second zone 852 or the second porosity region have intermediate-sized widths and may be defined as mesopores, and the pores 863 associated with the third zone 853 or the third porosity region have relatively small widths and may be defined as micropores.

**[0180]** A group of tri-zone particles 850 may be joined together to form an aggregate (not shown for simplicity), and a group of the aggregates may be joined together to form an agglomerate (not shown for simplicity). In some implementations, a plurality of mesopores may be interspersed throughout the aggregates formed by respective groups of the carbonaceous particles 800. In some aspects, the first porosity region 811 may be at least partially encapsulated by the second porosity region 812 such that a respective aggregate may include one or more mesopores and one or more macropores. In one implementation, each mesopore may have a principal dimension between 3.3 nanometers (nm) and 19.3 nm, and each macropore may have a principal dimension between 0.1 μm and 1,000 μm. In some instances, the tri-zone particle 850 may include carbon fragments intertwined with each other and separated from one another by at least some of the mesopores.

**[0181]** In some implementations, the tri-zone particle 850 may include a surfactant or a polymer that includes one or more of styrene butadiene rubber, polyvinylidene fluoride, poly acrylic acid, carboxyl methyl cellulose, polyvinylpyrrolidone, and/or polyvinyl acetate that can act as a binder to join a group of the carbonaceous materials together. In other implementations, the tri-zone particle 850 may include a gel-phase electrolyte or a solid-phase electrolyte disposed within at least some of the pores.

**[0182]** In some implementations, the tri-zone particle 850 may have a surface area of exposed carbonaceous surfaces in an approximate range between 10 $m^2/g$ to 3,000 $m^2/g$ and/or a composite surface area (including sulfur micro-confined within pores) in an approximate range between 10 $m^2/g$ to 3,000 $m^2/g$. In one implementation, a composition of matter including a multitude of tri-zone particles 850 may have an electrical conductivity in

an approximate range between 100 S/m to 20,000 S/m at a pressure of 12,000 pounds per square in (psi) and a sulfur to carbon weight ratio between approximately 1:5 to 10:1.

**[0183]** Figure 8C shows an example step function 800C representative of the average pore volumes in each of the regions of the tri-zone particle 850 of Figure 8B, according to some implementations. As discussed, the pores distributed throughout the tri-zone particle 850 may have different sizes, volumes, or distributions. In some implementations, the average pore volume may decrease based on a distance between a center of the tri-zone particle 850 and an adjacent zonae, for example, such that pores associated with the first zone 851 or the first porosity region have a relatively large volume or pore size, pores associated with the second zone 852 or the second porosity region have an intermediate volume, and pores associated with the third zone 853 or the third porosity region have a relatively small volume. The interior region has a higher pore volume than the regions near the periphery. The region with higher pore volume provides for high sulfur loading whereas the lower pore volume outer regions mitigate the migration of polysulfides during cell cycling. In the example of Figure 8C, the average pore volume in the inner region is approximately 3 cc/g, the average pore volume in the outermost region is -0.5 cc/g and the average pore volume in the intermediate region is between 0.5 cc/g and 3 cc/g.

**[0184]** Figure 8D shows a graph 800D depicting an example distribution of pore volume versus pore width of carbonaceous particles described herein. As depicted in the graph 800D, pores associated with a relatively high pore volume may have a relatively low pore width, for example, such that the pore width generally increases as the pore volume decreases. In some aspects, pores having a pore width less than approximately 1.0 nm may be referred to as micropores, pores having a pore width between approximately 3 and 11 nm may be referred to as mesopores, and pores having a pore width greater than approximately 24 nm may be referred to as macropores.

**[0185]** Figure 9A shows a micrograph 900 of a plurality of carbonaceous structures 902, according to some implementations. In some implementations, each of the carbonaceous structures 902 may have a substantially hollow a core region surrounded by various monolithic carbon growths and/or layering. In some aspects, the monolithic carbon growths and/or layering may be examples of the monolithic carbon growths and/or layering described with reference to Figures 8A and 8B. In some instances, the carbonaceous structures 902 may include several concentric multi-layered fullerenes and/or similarly shaped carbonaceous structures organized at varying levels of density and/or concentration. For example, the

actual final shape, size, and graphene configuration of each of the carbonaceous structures 902 may depend on various manufacturing processes. The carbonaceous structures 902 may, in some aspects, demonstrate poor water solubility. As such, in some implementations, non-covalent functionalization may be utilized to alter one or more dispersibility properties of the carbonaceous structures 902 without affecting the intrinsic properties of the underlying carbon nanomaterial. In some aspects, the underlying carbon nanomaterial may be formative a $sp^2$ carbon nanomaterial. In some implementations, each of the carbonaceous structures 902 may have a diameter between approximately20 and 500 nm. In various implementations, groups of the carbonaceous structures 902 may coalesce and/or join together to form the aggregates 904. In addition, groups of the aggregates 904 may coalesce and/or join together to form the agglomerates 906. In some aspects, one or more of the carbonaceous structures 902, the aggregates 904, and/or the agglomerates 906 may be used to form the anode and/or the cathode of the battery 100 of Figure 1, the battery 200 of Figure 2, or the electrode 300 of Figure 3.

**[0186]** Figure 9B shows a micrograph 950 of an aggregate formed of carbonaceous material, according to some implementations. In some implementations, the aggregate 960 may be an example of one of the aggregates 904 of Figure 9A. In one implementation, exterior carbonaceous shell-type structures 952 may fuse together with carbons provided by other carbonaceous shell-type structures 954 to form a carbonaceous structure 956. A group of the carbonaceous structures 956 may coalesce and/or join with one another to form the aggregate 1010. In some aspects, a core region 958 of each of the carbonaceous structures 956 may be tunable, for example, in that the core region 958 may include various defined concentration levels of interconnected graphene structures, as described with reference to Figure 8A and/or Figure 8B. In some implementations, some of the carbonaceous structures 956 may have a first concentration of interconnected carbons approximately between 0.1 g/cc and 2.3 g/cc at or near the exterior carbonaceous shell-type structure 952. Each of the carbonaceous structures 956 may have pores to transport lithium ions extending inwardly from toward the core region 1008.

**[0187]** In some implementations, the pores in each of the carbonaceous structures 956 may have a width or dimension between approximately 0.0 nm and 0.5 nm, between approximately 0.0 and 0.1 nm, between approximately 0.0 and 6.0 nm, or between approximately 0.0 and 35 nm. Each carbonaceous structures 956 may also have a second concentration at or near the core region 958 that is different than the first concentration. For

example, the second concentration may include several relatively lower-density carbonaceous regions arranged concentrically. In one implementation, the second concentration may be lower than the first concentration at between approximately 0.0 g/cc and 1.0 g/cc or between approximately 1.0 g/cc and 1.5 g/cc. In some aspects, the relationship between the first concentration and the second concentration may be used to achieve a balance between confining sulfur or polysulfides within a respective electrode and maximizing the transport of lithium ions. For example, sulfur and/or polysulfides may travel through the first concentration and be at least temporarily confined within and/or interspersed throughout the second concentration during operational cycling of a lithium-sulfur battery.

**[0188]** In some implementations, at least some of the carbonaceous structures 956 may include CNO oxides organized as a monolithic and/or interconnected growths and be produced in a thermal reactor. For example, the carbonaceous structures 956 may be decorated with cobalt nanoparticles according to the following example recipe: cobalt(II) acetate ($C_4H_6CoO_4$), the cobalt salt of acetic acid (often found as tetrahydrate $Co(CH_3CO_2)_2 \cdot 4\ H_2O$, which may be abbreviated as $Co(OAc)_2 \cdot 4\ H_2O$, may be flowed into the thermal reactor at a ratio of approximately 59.60 wt% corresponding to 40.40 wt% carbon (referring to carbon in CNO form), resulting in the functionalization of active sites on the CNO oxides with cobalt, showing cobalt-decorated CNOs at a 15,000x level, respectively. In some implementations, suitable gas mixtures used to produce Carbon #29 and/or the cobalt-decorated CNOs may include the following steps:

- Ar purge 0.75 standard cubic feet per minute (scfm) for 30 min;
- Ar purge changed to 0.25 scfm for run;
- temperature increase: 25°C to 300°C 20 mins; and
- temperature increase: 300° – 500°C 15 mins.

**[0189]** Carbonaceous materials described with reference to Figures 9A and 9B may include or otherwise be formed from one or more instances of graphene, which may include a single layer of carbon atoms with each atom bound to three neighbors in a honeycomb structure. The single layer may be a discrete material restricted in one dimension, such as within or at a surface of a condensed phase. For example, graphene may grow outwardly only in the x and y planes (and not in the z plane). In this way, graphene may be a two-dimensional (2D) material, including one or several layers with the atoms in each layer

strongly bonded (such as by a plurality of carbon-carbon bonds) to neighboring atoms in the same layer.

**[0190]** In some implementations, graphene nanoplatelets (e.g., formative structures included in each of the carbonaceous structures 956) may include multiple instances of graphene, such as a first graphene layer, a second graphene layer, and a third graphene layer, all stacked on top of each other in a vertical direction. Each of the graphene nanoplatelets, which may be referred to as a GNP, may have a thickness between 1 nm and 3 nm, and may have lateral dimensions ranging from approximately 100 nm to 100 μm. In some implementations, graphene nanoplatelets may be produced by multiple plasma spray torches arranged sequentially by roll-to-roll (R2R) production. In some aspects, R2R production may include deposition upon a continuous substrate that is processed as a rolled sheet, including transfer of 2D material(s) to a separate substrate. In some instances, the R2R production may be used to form the first thin film 310 and/or the second thin film 320 of the electrode 300 of Figure 3, for example, such that the concentration level of the first aggregates 312 within the first thin film 310 is different than the concentration level of the second aggregates 322 within the second thin film 320. That is, the plasma spray torches used in the R2R processes may spray carbonaceous materials at different concentration levels to create the first thin film 310 and/or the second thin film 320 using specific concentration levels of graphene nanoplatelets. Therefore, R2R processes may provide a fine level of tunability for the battery 100 of Figure 1 and/or the battery 200 or Figure 2.

**[0191]** Figures 10A and 10B show transmission electron microscope (TEM) images 1000 and 1050, respectively, of carbonaceous particles treated with carbon dioxide ($CO_2$), according to some implementations. The carbonaceous particles shown in Figures 10A and 10B may include or otherwise be formed from one or more instances of graphene, which may include a single layer of carbon atoms with each atom bound to three neighbors in a honeycomb structure.

**[0192]** Figure 11 shows a diagram 1100 depicting carbon porosity types of various carbonaceous aggregates, according to some implementations. In various implementations, the carbonaceous aggregates described with reference to Figure 11 may be examples of the aggregates 904 of Figure 9A and/or the carbonaceous structures 956 of Figure 9B. In some aspects, the carbonaceous aggregates described with reference to Figure 11 may be used to form the electrode 300 of Figure 3. As discussed, the aggregates may be formed from or may include a group of carbonaceous structures such as the carbonaceous structure 902 of Figure

9A or the carbonaceous structures 956 of Figure 9B. In some aspects, the carbonaceous structures may be CNOs.

**[0193]** The carbonaceous structures may be used to form an electrode (such as the electrode 300 of Figure 3) having any of the porosity types shown in the diagram 1100. For example, the electrode may include any of a porosity type 1 1110, a porosity type II 1120, and a porosity type III 1130. In some implementations, the porosity type 1 1110 may include a first pore 1111, a second pore 1112, and a third pore 1113, all sized with a principal dimension of less than 5 nm to retain polysulfides within the electrode. Some polysulfides may grow in size upon forming larger complexes and become immovably lodged within pores of the porosity type I 1110. In some implementations, aggregates may be joined together to create pores of the porosity type II 1120 and/or porosity type III 1130 that can retain larger polysulfides and/or polysulfide complexes.

**[0194]** Figure 12 shows a graph 1200 depicting pore size versus pore distribution of an example electrode, according to some implementations. As used herein, "Carbon 1" refers to structured carbonaceous materials including mostly micropores (such as less than 5 nm in principal dimension), and "Carbon 2" refers to structured carbonaceous materials including mostly mesopores (such as between approximately 20 nm to 50 nm in principal dimension). In some implementations, an electrode suitable for use in one of the batteries disclosed herein may be prepared to have the pore size versus pore distribution depicted in the graph 1200.

**[0195]** Figure 13 shows a first graph 1300 and a second graph 1310 depicting battery performance per cycle number, according to some implementations. Specifically, the first graph 1300 shows the specific discharge capacity of an example battery employing an electrolyte 1302 disclosed herein relative to the specific discharge capacity of a conventional battery employing a conventional electrolyte. The second graph shows the capacity retention of the battery employing the electrolyte 1302 relative to the capacity retention of the battery employing the conventional electrolyte. In some aspects, the electrolyte 1302 may be one example of the electrolyte 130 of Figure 1 or the electrolyte 230 of Figure 2. In the first graph 1300 and the second graph 1310, the conventional electrolyte is prepared as 1 M LiTFSI in DME:DOL:TEGDME (volume: volume: volume = 1:1:1) with 2 wt.% $LiNO_3$.

**[0196]** Figure 14 shows a bar chart 1400 depicting battery performance per cycle number, according to some implementations. Specifically, the bar chart 1400 depicts the specific discharge capacity per cycle number of an example battery employing an electrolyte 1402 disclosed herein relative to the specific discharge capacity per cycle number of a

conventional battery employing a conventional electrolyte. In some aspects, the electrolyte 1402 may be one example of the electrolyte 130 of Figure 1 or the electrolyte 230 of Figure 2. In the bar chart 1400, the conventional electrolyte is prepared as 1 M LiTFSI in DME:DOL:TEGDME (volume: volume: volume = 1:1:1). The bar chart 1400 shows that employing the electrolyte 1402 in an example battery (such as the battery 100 of Figure 1 or the battery 200 of Figure 2) may increase the specific discharge capacity of the battery by approximately 28% at the 3$^{rd}$ cycle number, by approximately 30% at the 50$^{th}$ cycle number, and by approximately 39% at the 60$^{th}$ as compared to a battery employing the conventional electrolyte.

**[0197]** Figure 15 shows a first graph 1500 and a second graph 1510 depicting battery performance per cycle number, according to some implementations. Specifically, the first graph 1500 shows the electrode discharge capacity per cycle number of an example lithium-sulfur coin cell employing an electrolyte 1502 disclosed herein relative to the electrode discharge capacity per cycle number of an example lithium-sulfur coin cell battery employing a conventional electrolyte, and the second graph 1510 shows the capacity retention per cycle number of the lithium-sulfur coin cell battery employing the electrolyte 1502 relative to the electrode discharge capacity per cycle number of the lithium-sulfur coin cell battery employing the conventional electrolyte. In some aspects, the electrolyte 1502 may be one example of the electrolyte 130 of Figure 1 or the electrolyte 230 of Figure 2. The lithium-sulfur coin cell battery is cycled at a discharge rate of 1C (such as fully discharged within one hour), at 100% depth-of-discharge (DOD) and is kept at approximately at room temperature (68°F or 20°C). The conventional electrolyte is prepared as 1 M LiTFSI in DME:DOL:TEGDME (volume: volume: volume = 1:1:1) with 2 wt.% $LiNO_3$.

**[0198]** Figure 16 shows a graph 1600 depicting electrode discharge capacity per cycle number, according to some implementations. Specifically, the graph 1600 depicts the electrode discharge capacity per cycle number of an example battery employing an electrolyte 1602 disclosed herein relative to the electrode discharge capacity of a conventional battery employing a conventional electrolyte. In some aspects, the electrolyte 1602 may be one example of the electrolyte 130 of Figure 1 or the electrolyte 230 of Figure 2. The conventional electrolyte is prepared as 1 M LiTFSI in DME:DOL:TEGDME (volume: volume: volume = 1:1:1) with 2 wt.% $LiNO_3$, and the electrolyte 1602 is prepared as 1 M LiTFSI in DME:DOL:TEGDME (volume: volume: volume = 58:29:13) with approximately 2 wt.% $LiNO_3$.

**[0199]** Figure 17 shows another graph 1700 depicting electrode discharge capacity per cycle number, according to some implementations. Specifically, the graph 1700 depicts the electrode discharge capacity per cycle number of an example battery employing an electrolyte 1702 and solvent package 1704 disclosed herein relative to the electrode discharge capacity of a conventional battery employing a conventional electrolyte and solvent package. The conventional electrolyte is prepared as 1 M LiTFSI in DME:DOL:TEGDME (volume: volume: volume = 1:1:1) with approximately 2 wt.% $LiNO_3$, and the electrolyte 1702 is prepared as 1 M LiTFSI in DME:DOL:TEGDME (volume: volume: volume = 58:29:13) with 2 wt.% $LiNO_3$. The conventional solvent package is prepared as 1 M LiTFSI in DME:DOL:TEGDME (volume: volume: volume = 1:1:1), and the solvent package 1704 is prepared as 1 M LiTFSI in DME:DOL:TEGDME (volume: volume: volume = 58:29:13).

**[0200]** Figure 18 shows a graph 1800 depicting specific discharge capacity per cycle number for various TBT-containing electrolyte mixtures, according to some implementations. As shown in the graph 1800, "181" indicates an electrolyte without any TBT additions, resulting in a 0 M TBT concentration level, "181-25TBT" indicates an electrolyte prepared at a 25 M TBT concentration level and so on and so forth. In some implementations, a 5M TBT concentration level may result in an approximate 70 mAh/g discharge capacity increase relative to the electrolyte without any TBT additions.

**[0201]** Figure 19 shows a first graph 1900 depicting electrode discharge capacity per cycle number and a second graph 1910 depicting electrode capacity retention per cycle number, according to some implementations. Specifically, the first graph 1900 depicts the electrode discharge capacity per cycle number of an example battery that includes a protective lattice disclosed herein relative to the electrode discharge capacity of an example battery that does not include the protective lattice disclosed herein. The second graph 1910 depicts the electrode capacity retention per cycle number of an example battery that includes the protective lattice disclosed herein relative to the electrode capacity retention of an example battery that does not include the protective lattice disclosed herein. In some aspects, the protective lattice may be one example of the protective lattice 402 of Figure 4. Performance results for both the first graph 1900 and the second graph 1910 include usage of an electrolyte prepared with 1 M LiTFSI in DME:DOL:TEGDME (volume: volume: volume = 58:29:13) with 2 wt.% $LiNO_3$.

**[0202]** Figure 20 shows a first graph 2000 depicting electrode discharge capacity per cycle number and a second graph 2010 depicting electrode capacity retention per cycle

number, according to other implementations. Specifically, the first graph 2000 depicts the electrode discharge capacity per cycle number of an example battery that includes the polymeric network of Figure 7. The second graph 2010 depicts the discharge capacity retention per cycle number of an example battery that includes the polymeric network of Figure 7. The battery may be one example of the battery 100 of Figure 1 or the battery 200 of Figure 2. Performance results for both the first graph 2000 and the second graph 2010 include usage of an electrolyte prepared with 1 M LiTFSI in DME:DOL:TEGDME (volume: volume: volume = 58:29:13) with 2 wt.% $LiNO_3$.

**[0203]** Figure 21 shows a first graph 2100 depicting electrode discharge capacity per cycle number and a second graph 2110 depicting electrode capacity retention per cycle number, according to some other implementations. Specifically, the first graph 2100 depicts the electrode discharge capacity per cycle number of an example battery that includes the protective layer 516 of Figure 5. The second graph 2110 depicts the discharge capacity retention per cycle number of an example battery that includes the protective layer 516 of Figure 5. The battery may be one example of the battery 100 of Figure 1 or the battery 200 of Figure 2. Performance results for both the first graph 1900 and the second graph 1910 include usage of an electrolyte prepared with 1 M LiTFSI in DME:DOL:TEGDME (volume: volume: volume = 58:29:13) with 2 wt.% $LiNO_3$.

**[0204]** Figure 22 shows an example cathode 2200 having a body 2201 and a width 2205, according to some implementations. In some implementations, the cathode 2200 may be one example of the electrode 300 of Figure 3. The cathode 2200 may be similar to the electrode 300 of Figure 3 in many respects, such that description of like elements is not repeated herein. In one implementation, the cathode 2200 includes a first porous carbonaceous region 2210 and a second porous carbonaceous region 2220 positioned adjacent to the first porous carbonaceous region 2210. The first porous carbonaceous region 2210 may be formed of a first concentration level of carbonaceous materials, and the second porous carbonaceous region 2220 formed of a second concentration level of carbonaceous materials dissimilar to the first concentration level of carbonaceous materials. For example, the second porous carbonaceous region 2220 may have a lower concentration level of carbonaceous materials than the first porous carbonaceous region 2210 as shown in Figure 22. In some aspects, additional porous carbonaceous regions (not shown in Figure 22 for simplicity) maybe coupled with at least the second porous carbonaceous region.

**[0205]** Specifically, these additional porous carbonaceous regions may be arranged in order of incrementally decreasing concentration levels of carbonaceous materials in a direction away from the first porous carbonaceous region 2210 to provide for complete ionic transport and electrical current tunability. That is, in one implementation, the second porous carbonaceous region 2220 may face a bulk electrolyte (e.g., provided in the liquid phase) and the first porous carbonaceous region 2210 of the cathode 2200 may be coupled with a current collector (not shown in Figure 22 for simplicity). In this way, denser carbonaceous regions, such as the first porous carbonaceous region 2210, may facilitate higher levels of electrical conduction (shown in Figure 22 as "$e^-$") between adjacent contact points of carbonaceous materials, while sparser carbonaceous regions, such as the second porous carbonaceous region 2220, may facilitate higher levels of lithium ion transport associated with improved lithium-sulfur battery discharge-charge cycling relative to conventional lithium ion batteries. In some implementations, additional carbonaceous regions coupled with and positioned adjacent to the second porous carbonaceous region 2220 may have a lower density of carbonaceous materials than the second porous carbonaceous region 2220. In this way, the additional carbonaceous regions of lower density may accommodate higher levels of lithium ion transport to, for example, permit for tuning of various performance characteristics of the electrode 300.

**[0206]** In one implementation, the first porous carbonaceous region 2210 may include first non-tri-zone particles 2211. The configuration of the first non-tri-zone particles 2211 within the first porous carbonaceous region is one example configuration. Other placements, orientations, alignments and/or the like are possible for the non-tri-zone particles. In some aspects, each non-tri-zone particle may be an example of one or more carbonaceous materials disclosed elsewhere in the present disclosure. The first porous carbonaceous region 2210 may also include first tri-zone particles 2212 interspersed throughout the first non-tri-zone particles 2211 as shown in Figure 22, or positioned in any other placement, orientation, or configuration. Each first tri-zone particle 2212 may be one example of the tri-zone particle 850 of Figure 8B. In addition, or the alternative, each of the first tri-zone-particles 2212 may include first carbon fragments 2213 intertwined with each other and separated from one another by mesopores 2214. Each tri-zone-particle may have a first deformable perimeter 2215 configured to coalesce with adjacent first non-tri-zone particles 2211 and/or first tri-zone particles 2212.

**[0207]** The first porous carbonaceous region 2210 may also include first aggregates 2216, where each aggregate includes a multitude of the first tri-zone particles 2212 joined together. In one or more particular examples, each first aggregate may have a principal dimension in a range between 10 nanometers (nm) and 10 micrometers (μm). The mesopores 2214 may be interspersed throughout the first plurality of aggregates, where each mesopore has a principal dimension between 3.3 nanometers (nm) and 19.3 nm. In addition, the first porous carbonaceous region 2210 may include first agglomerates 2217, where each agglomerate includes a multitude of the first aggregates 2216 joined to each other. In some aspects, each first agglomerate 2217 may have a principal dimension in an approximate range between 0.1 μm and 1,000 μm. Macropores 2218 may be interspersed throughout the first aggregates 2216, where each macropore may have a principal dimension between 0.1 μm and 1,000 μm. In some implementations, one or more of the above-discussed carbonaceous materials, allotropes and/or structures may be one or more examples of that shown in Figures 9A and 9B.

**[0208]** The second porous carbonaceous may include second non-tri-zone particles 2221, which may be one example of the first non-tri-zone particles 2211. The second porous carbonaceous region 2220 may include second tri-zone particles 2222, which may each be one example of each of the first tri-zone particles 2212 and/or may be one example of the tri-zone particle 850 of Figure 8B. In addition, or the alternative, each second tri-zone particle 2222 may include second carbon fragments 2223 intertwined with each other and separated from one another by the mesopores 2214. Each second tri-zone particle 2222 may have a second deformable perimeter 2225 configured to coalesce with one or more adjacent second non-tri-zone particles 2221 or second tri-zone particles 2222.

**[0209]** In addition, the second porous carbonaceous region 2220 may include second aggregates 2226, where each second aggregate 2226 may include a multitude of the second tri-zone particles 2222 joined together. In one or more particular examples, each second aggregate 2226 may have a principal dimension in a range between 10 nanometers (nm) and 10 micrometers (μm). The mesopores 2214 may be interspersed throughout the second aggregates 2226, each mesopore may have a principal dimension between 3.3 nanometers (nm) and 19.3 nm. Further, the second porous carbonaceous region 2220 may include second agglomerates 2227, each second agglomerate 2227 may include a multitude of the second aggregates 2226 joined to each other, where each agglomerate may have a principal dimension in an approximate range between 0.1 μm and 1,000 μm. The macropores 2218

may be interspersed throughout the second plurality of aggregates, where each macropore having a principal dimension between 0.1 μm and 1,000 μm. In some implementations, one or more of the above-discussed carbonaceous materials, allotropes and/or structures may be one or more examples of that shown in Figures 9A and 9B.

**[0210]** In one implementation, the first porous carbonaceous region 2210 and/or the second porous carbonaceous region 2220 may include a selectively permeable shell (not shown in Figure 22 for simplicity), which may form a separated liquid phase on the first porous carbonaceous region 2210 or the second porous carbonaceous region 2220, respectively. An electrolyte, such as any of the electrolytes disclosed in the present disclosure, may be dispersed within the first porous carbonaceous region and/or the second porous carbonaceous region for lithium ion transport associated with lithium-sulfur battery discharge-charge operational cycling.

**[0211]** In one or more particular examples, the first porous carbonaceous region 2210 may have an electrical conductivity in an approximate range between 500 S/m to 20,000 S/m at a pressure of 12,000 pounds per square in (psi). The second porous carbonaceous region 2220 may have an electrical conductivity in an approximate range between 0 S/m to 500 S/m at a pressure of 12,000 pounds per square in (psi). The first agglomerates 2217 and/or second agglomerates 2227 may include aggregates connected to each other with one or more polymer-based binders.

**[0212]** In some aspects, the first tri-zone particles 2212 or the second tri-zone particles 2222 may each include a first porosity region (not shown in Figure 22 for simplicity) located around a center of a respective first tri-zone particle 2212 or second tri-zone particle 2222. The first porosity region may include first pores. A second porosity region (not shown in Figure 22 for simplicity) may surround the first porosity region. The second porosity region may include second pores. In one implementation, the first pores may define a first pore density, and the second pores may define a second pore density that is different the first pore density.

**[0213]** In some aspects, the mesopores 2214 may be grouped into first mesopores and second mesopores (both not shown in Figure 22 for simplicity). In one or more particular examples, the first mesopores may have a first mesopore density, and the second mesopores may have a second mesopore density that is different than the first mesopore density. In addition, the macropores 2218 may be grouped into first macropores that may have a first

pore density, and second macropores (both not shown in Figure 22 for simplicity) that may have a second pore density different than the first pore density.

**[0214]** In one implementation, the first porous carbonaceous region 2210 and/or the second porous carbonaceous region 2220 may nucleate sulfur, such as that necessary to facilitate operational discharge-charge cycling of any of the lithium-sulfur batteries disclosed by the present disclosure. For example, the cathode 2200 may have a sulfur to carbon weight ratio between approximately 1:5 to 10:1. In some aspects, one or more electrically conductive additives may be dispersed within the first porous carbonaceous region 2210 and/or the second porous carbonaceous region 2220 to, for example, correspondingly influence discharge-charge cycling performance of the cathode 2200. In addition, a protective sheath, such as the protective lattice 402 of Figure 4, may be disposed on the cathode.

**[0215]** As used herein, a phrase referring to "at least one of" or "one or more of" a list of items refers to any combination of those items, including single members. For example, "at least one of: a, b, or c" is intended to cover the possibilities of: a only, b only, c only, a combination of a and b, a combination of a and c, a combination of b and c, and a combination of a and b and c.

**[0216]** The various illustrative components, logic, logical blocks, modules, circuits, operations, and algorithm processes described in connection with the implementations disclosed herein may be implemented as electronic hardware, firmware, software, or combinations of hardware, firmware, or software, including the structures disclosed in this specification and the structural equivalents thereof. The interchangeability of hardware, firmware and software has been described generally, in terms of functionality, and illustrated in the various illustrative components, blocks, modules, circuits and processes described above. Whether such functionality is implemented in hardware, firmware or software depends upon the application and design constraints imposed on the overall system.

**[0217]** Various modifications to the implementations described in this disclosure may be readily apparent to persons having ordinary skill in the art, and the generic principles defined herein may be applied to other implementations without departing from the spirit or scope of this disclosure. Thus, the claims are not intended to be limited to the implementations shown herein but are to be accorded the widest scope consistent with this disclosure, the principles and the novel features disclosed herein.

**[0218]** Additionally, various features that are described in this specification in the context of separate implementations also can be implemented in combination in a single implementation. Conversely, various features that are described in the context of a single implementation also can be implemented in multiple implementations separately or in any suitable subcombination. As such, although features may be described above in combination with one another, and even initially claimed as such, one or more features from a claimed combination can in some cases be excised from the combination, and the claimed combination may be directed to a subcombination or variation of a subcombination.

**[0219]** Similarly, while operations are depicted in the drawings in a particular order, this should not be understood as requiring that such operations be performed in the particular order shown or in sequential order, or that all illustrated operations be performed, to achieve desirable results. Further, the drawings may schematically depict one more example processes in the form of a flowchart or flow diagram. However, other operations that are not depicted can be incorporated in the example processes that are schematically illustrated. For example, one or more additional operations can be performed before, after, simultaneously, or between any of the illustrated operations. In some circumstances, multitasking and parallel processing may be advantageous. Moreover, the separation of various system components in the implementations described above should not be understood as requiring such separation in all implementations, and it should be understood that the described program components and systems can generally be integrated together in a single product or packaged into multiple products.

## CLAIMS

What is claimed is:

1. A composition of matter including a plurality of pores, the composition of matter comprising:

a plurality of particles, each of the particles including:

a first zone including a plurality of first pores, the plurality of first pores having a uniform pore size; and

a second zone including a plurality of second pores, the second zone concentrically positioned relative to the first zone and separated from the first zone by at least some of the plurality of first pores, wherein the plurality of second pores has a pore size that gradually decreases along a radial direction from the center of the particle to a boundary of the particle;

a plurality of aggregates, each including a multitude of the particles joined together; and

a plurality of agglomerates, each including a multitude of the aggregates joined together.

2. The composition of matter of claim 1, wherein each of the particles has a principal dimension in an approximate range between 20 nanometers (nm) and 150 nm.

3. The composition of matter of claim 1, wherein each of the aggregates has a principal dimension in an approximate range between 10 nanometers (nm) and 10 micrometers (μm).

4. The composition of matter of claim 1, wherein each of the agglomerates has a principal dimension in an approximate range between 0.1 micrometers (μm) and 1,000 μm.

5. The composition of matter of claim 1, wherein each of the pores has a principal dimension in an approximate range between 0 nanometers (nm) and 100 nm.

6. The composition of matter of claim 1, wherein the first zone has a first porosity and the second zone has a second porosity different than the first porosity.

7. The composition of matter of claim 1, wherein the first zone has a first density and the second zone has a second density different than the first density.

8. The composition of matter of claim 1, wherein the first zone has a first pore density between 0.0 cubic centimeters (cc)/g and 2.0 cc/g.

9. The composition of matter of claim 1, wherein the second zone has a second pore density between 1.5 cubic centimeters (cc)/g and 5.0 cc/g.

10. The composition of matter of claim 1, wherein the composition of matter has an electrical conductivity in an approximate range between 100 Siemens (S)/m to 20,000 S/m at a pressure of 12,000 pounds per square in (psi).

11. The composition of matter of claim 1, wherein at least some of the agglomerates are connected to each other with one or more polymer-based binders.

12. The composition of matter of claim 1, further including one or more electrically conductive additives dispersed within at least some of the plurality of pores.

13. The composition of matter of claim 1, wherein each of the particles includes one or more of flat graphene, wrinkled graphene, a plurality of carbon nano-tubes (CNTs), or a plurality of carbon nano-onions (CNOs).

14. The composition of matter of claim 1, wherein each of the particles further includes a third zone concentrically disposed on the second zone to the center of the respective particle and is separated from the second zone by at least some of the plurality of pores, the third zone including a plurality of third pores.

15. The composition of matter of claim 1, wherein the plurality of first pores are macropores, the plurality of second pores are mesopores, and the plurality of third pores are micropores.

16. The composition of matter of claim 1, wherein each of the particles further includes one or more additional zones concentrically disposed on the second zone to the center of the respective particle and each of the one or more additional zones is separated from an immediately adjacent zone by at least some of the plurality of pores.

17. The composition of matter of claim 1, wherein the pore sizes of pores of the plurality of second pores gradually decreases along the radial direction.

18. A battery comprising:

an anode including an alkali metal configured to release a plurality of alkali ions during cycling of the battery;

a polymeric network deposited over one or more exposed surfaces of the anode, the polymeric network including carbonaceous materials grafted with a plurality of fluorinated polymer chains cross-linked with each other, the plurality of fluorinated polymer chains configured to produce an alkali-metal fluoride in response to operational cycling of the battery, the alkali-metal fluoride configured to suppress alkali metal dendrite formation from the anode, wherein the carbonaceous materials include one or more of flat graphene, wrinkled graphene, a plurality of carbon nano-tubes (CNTs), or a plurality of carbon nano-onions (CNOs);

a cathode positioned opposite to the anode;

an electrolyte at least partially dispersed throughout the cathode and in contact with the anode, the electrolyte configured to transport the plurality of alkali ions between the cathode and the anode; and

a separator positioned between the anode and the cathode.

19. The battery of claim 18, wherein the plurality of fluorinated polymer chains include a plurality of monomers, one or more monomers including 2,2,3,3,4,4,5,5,6,6,7,7-Dodecafluoroheptyl acrylate (DFHA), 3,3,4,4,5,5,6,6,7,7,8,8,9,9,10,10,10-Heptadecafluorodecyl methacrylate (HDFDMA), 2,2,3,3,4,4,5,5-Octafluoropentyl methacrylate (OFPMA), Tetrafluoropropyl methacrylate (TFPM), 3-[3,3,3-Trifluoro-2-hydroxy-2-(trifluoromethyl)propyl]bicyclo[2.2.1]hept-2-yl methacrylate (HFA monomer), or vinyl-based monomers including 2,3,4,5,6-Pentafluorostyrene (PFSt).

20. The battery of claim 18, wherein the polymeric network has a thickness approximately between 0.001 μm and 5 μm.

21. The battery of claim 18, wherein the plurality of fluorinated polymer chains are grafted to a surface of the carbonaceous materials.

22. The battery of claim 21, wherein the grafting is based on one or more radical initiators including at least one of benzoyl peroxide (BPO) or azobisisobutyronitrile (AIBN).

23. The battery of claim 21, wherein the anode includes at least some adjacent graphene sheets configured to intercalate alkali metal ions (AIBN).

24. The battery of claim 18, wherein the plurality of fluorinated polymer chains are configured to chemically interact with at least some alkali metal ions via a Wurtz reaction.

25. The battery of claim 24, wherein the Wurtz reaction is associated with production of the alkali-metal fluoride.

26. The battery of claim 18, further including a plurality of graphene nanoplatelets dispersed throughout the polymeric network, wherein the graphene nanoplatelets are isolated from each other within the polymeric network.

27. The battery of claim 26, wherein dispersion of the graphene nanoplatelets includes one or more different concentration levels.

28. The battery of claim 27, wherein dispersion of the graphene nanoplatelets further includes at least some of the carbonaceous materials functionalized with at least some of the plurality of fluorinated polymer chains.

29. The battery of claim 18, wherein the polymeric network includes between approximately 0.001 wt.% to 2 wt.% of the fluorinated polymer chains.

30. The battery of claim 18, wherein the polymeric network further comprises:

an interface layer in contact with the anode; and

a protective layer disposed on top of the interface layer.

31. The battery of claim 30, wherein the interface layer includes one or more of a plurality of cross-linkable monomers including methacrylate (MA), acrylate, vinyl functional groups, or a combination of epoxy and amine functional groups.

32. The battery of claim 31, wherein the protective layer is characterized by a density gradient.

33. The battery of claim 32, wherein the density gradient is associated with one or more self-healing properties of the protective layer.

34. The battery of claim 32, wherein the density gradient is configured to strengthen the polymeric network.

35. The battery of claim 32, wherein the polymeric network is configured to suppress dendritic growth from the anode.

36. The battery of claim 18, wherein the anode is an alkali metal layer.

37. The battery of claim 18, further including a film disposed on the cathode, the film including a lattice including a tri-functional epoxy compound and a di-amine oligomer compound chemically bonded to each other, wherein the film is associated with chemical bonding of alkali metal containing polysulfide intermediates generated during cycling of the battery.

38. The battery of claim 18, wherein the polymeric network includes between approximately 5 wt.% to 100 wt.% of the plurality of carbonaceous materials grafted with the fluorinated polymer chains and a balance of fluorinated polymers, one or more non-fluorinated polymers, one or more cross-linkable monomers, or any combination thereof.

39. The battery of claim 18, wherein the plurality of carbonaceous materials grafted with the fluorinated polymer chains includes 5 wt.% to 50 wt.% of the fluorinated polymer chains and a balance of carbonaceous material.

40. A battery comprising:

an anode including a polymeric network including carbonaceous materials grafted with a plurality of fluorinated polymer chains cross-linked into a lattice, the anode configured to output a plurality of alkali ions during operational cycling of the battery;

a cathode positioned opposite to the anode;

a protective sheath disposed on the cathode, the protective sheath including a tri-functional epoxy compound and a di-amine oligomer-based compound configured to chemically react with each other;

an electrolyte at least partially dispersed throughout the cathode and in contact with the anode, the electrolyte configured to transport the plurality of alkali ions between the cathode and the anode; and

a separator positioned between the anode and the cathode.

41. The battery of claim 40, wherein the lattice is configured to produce an alkali metal fluoride in response to operational cycling of the battery, the alkali metal fluoride configured to suppress alkali metal dendrite formation from the anode.

42. The battery of claim 40, wherein the polymeric network is deposited over one or more exposed surfaces of the anode.

43. The battery of claim 40, wherein the carbonaceous materials include one or more of flat graphene, wrinkled graphene, a plurality of carbon nano-tubes (CNTs), or a plurality of carbon nano-onions (CNOs).

44. The battery of claim 40, wherein the plurality of fluorinated polymer chains includes a plurality of monomers, one or more monomers including 2,2,3,3,4,4,5,5,6,6,7,7-Dodecafluoroheptyl acrylate (DFHA), 3,3,4,4,5,5,6,6,7,7,8,8,9,9,10,10,10-Heptadecafluorodecyl methacrylate (HDFDMA), 2,2,3,3,4,4,5,5-Octafluoropentyl methacrylate (OFPMA), Tetrafluoropropyl methacrylate (TFPM), 3-[3,3,3-Trifluoro-2-

hydroxy-2-(trifluoromethyl)propyl]bicyclo[2.2.1]hept-2-yl methacrylate (HFA monomer), or vinyl-based monomers including 2,3,4,5,6-Pentafluorostyrene (PFSt).

45. The battery of claim 40, wherein the polymeric network has a thickness approximately between 0.001 μm and 5 μm.

46. The battery of claim 40, wherein at least some of the plurality of fluorinated polymer chains are grafted to a surface of a respective one of the carbonaceous materials.

47. The battery of claim 40, wherein the plurality of fluorinated polymer chains is configured to chemically interact with the one or more surfaces of the alkali metal of the anode via a Wurtz reaction.

48. The battery of claim 40, wherein the carbonaceous materials include a plurality of graphene nanoplatelets dispersed throughout the polymeric network, wherein the graphene nanoplatelets are isolated from each other within the polymeric network.

49. The battery of claim 48, wherein dispersion of the plurality of graphene nanoplatelets throughout the polymeric network includes one or more different concentration levels.

50. The battery of claim 48, wherein at least some of the plurality of graphene nanoplatelets are functionalized with at least some of the plurality of fluorinated polymer chains.

51. The battery of claim 40, wherein the polymeric network includes between approximately 0.001 wt.% to 2 wt.% of the fluorinated polymer chains.

52. The battery of claim 40, wherein the polymeric network further includes:
an interphase region in contact with the anode; and
a protective region disposed on top of the interphase region.

53. The battery of claim 52, wherein the interphase region is based on a Wurtz reaction at an interface between the anode and the polymeric network.

54. The battery of claim 52, wherein the interphase region includes one or more of a plurality of cross-linkable monomers including methacrylate (MA), acrylate, vinyl functional groups, or a combination of epoxy and one or more amine functional groups.

55. The battery of claim 52, wherein the protective region is characterized by a density gradient.

56. The battery of claim 55, wherein the density gradient is associated with one or more self-healing properties of the protective region.

57. The battery of claim 55, wherein the density gradient is configured to strengthen the polymeric network.

58. The battery of claim 40, wherein the polymeric network is configured to suppress dendritic growth from the anode.

59. The battery of claim 40, wherein the anode further includes one or more exposed surfaces, each exposed surface including one or more alkali metal-containing nanostructures or microstructures.

60. The battery of claim 59, wherein each of the one or more alkali metal-containing nanostructures or microstructures includes at least some of the carbonaceous materials.

61. The battery of claim 40, wherein the anode includes a three-dimensional (3D) structure.

62. A battery comprising:

an anode arranged in a lattice configuration and including one or more carbonaceous materials;

a cathode positioned opposite to the anode;

a separator disposed between the anode and cathode;

a protective sheath disposed on the cathode, the protective sheath including a tri-functional epoxy compound and a di-amine oligomer-based compound configured to chemically react with each other; and

an electrolyte at least partially dispersed within the cathode and in contact with the anode.

63. The battery of claim 62, further including a polymeric network deposited over one or more exposed surfaces of the anode, the polymeric network including a plurality of fluorinated polymer chains grafted with the one or more carbonaceous materials and cross-linked with each another.

64. The battery of claim 63, wherein the polymeric network further includes an alkali-metal fluoride configured to suppress alkali metal dendrite formation associated with the anode.

65. The battery of claim 62, wherein the protective sheath is configured to prevent polysulfide migration within the battery based on chemical bonding between the protective sheath and one or more lithium-containing polysulfide intermediates.

66. The battery of claim 62, further including one or more cracks extending into the cathode, and wherein the protective sheath is dispersed throughout the one or more cracks.

67. The battery of claim 62, wherein the protective sheath is configured to reduce a susceptibility of the cathode to rupturing.

68. The battery of claim 62, wherein the protective sheath has a cross-linked, three-dimensional structure based on the tri-functional epoxy compound and the di-amine oligomer-based compound.

69. The battery of claim 68, wherein the tri-functional epoxy compound is one or more of trimethylolpropane triglycidyl ether (TMPTE), tris(4-hydroxyphenyl)methane triglycidyl ether, or tris(2,3-epoxypropyl) isocyanurate.

70. The battery of claim 69, wherein the di-amine oligomer-based compound is one or more of dihydrazide sulfoxide (DHSO) or JEFFAMINE® D-230 polyetheramine.

71. The battery of claim 62, wherein the protective sheath includes trimethylolpropane tris[poly(propylene glycol) and amine terminated ether.

72. The battery of claim 62, wherein the carbonaceous materials include one or more of flat graphene, wrinkled graphene, a plurality of carbon nano-tubes (CNTs), or a plurality of carbon nano-onions (CNOs).

73. The battery of claim 62, wherein the cathode includes a host structure including one or more of flat graphene, wrinkled graphene, carbon nanotubes (CNTs), or carbon nano-onions (CNOs), and the anode includes a solid lithium metal layer.

74. The battery of claim 62, further including:

a tin fluoride layer disposed on the anode; and

a lithium fluoride layer formed between the tin fluoride layer and the anode, wherein the lithium fluoride layer is associated with reactions between fluorine ions and lithium ions.

75. The battery of claim 74, wherein the lithium fluoride layer is configured to inhibit dendritic growth from the anode.

76. The battery of claim 62, further including a solid-electrolyte interphase layer disposed on the anode, the solid-electrolyte interphase layer including one or more of tin, manganese, molybdenum, fluorine compounds, tin fluoride, manganese fluoride, silicon nitride, lithium nitride, lithium nitrate, lithium phosphate, manganese oxide, or lithium lanthanum zirconium oxide (LLZO).

77. A battery comprising:

an anode configured to output a plurality of lithium ions during cycling of the battery;

a graded layer disposed on the anode, the graded layer containing a polymeric network including a density gradient formed of wrinkled graphene associated with graphene nanoplatelets dispersed throughout and isolated from one other within the polymeric network, at least some wrinkled graphene configured to expand in volume along one or more flexure

points and retain polysulfides generated during cycling of the battery, the polymeric network including:

a plurality of fluorinated poly(meth)acrylates grafted onto one of more flexure points of at least some wrinkled graphene;

a plurality of carbon-fluorine (C-F) bonds within the polymeric network, at least some of the plurality of carbon-fluorine (C-F) bonds configured to chemically react, by a Wurtz reaction, with at least some of the plurality of lithium ions and convert into carbon-lithium (C-Li) bonds by displacing fluorine ions ($F^-$);

a plurality of carbon-carbon (C-C) bonds formed during displacement of fluorine ions ($F^-$) during the Wurtz reaction, formation of carbon-carbon (C-C) bonds associated with cross-linking of the polymeric network; and

lithium fluoride (LiF) formed responsive to displacement of fluorine ions ($F^-$), lithium fluoride (LiF) associated with consumption of at least some of the plurality of lithium ions; and

a cathode positioned opposite to the anode;

an electrolyte dispersed throughout the cathode and dispersed the throughout the anode; and

a separator positioned between the anode and cathode.

78. The battery of claim 77, further including a solid-electrolyte interphase formed at a surface of the anode exposed to the electrolyte during cycling of the battery.

79. The battery of claim 78, wherein the graded layer is configured to grow the solid-electrolyte interphase during cycling of the battery.

80. The battery of claim 77, wherein the graded layer is deposited on the anode by one or more of atomic layer deposition (ALD), chemical vapor deposition (CVD), or physical vapor deposition (PVD).

81. A battery comprising:

an anode configured to output a plurality of lithium ions during cycling of the battery;

a graded layer disposed on the anode, the graded layer including a polymeric network including a density gradient formed of wrinkled graphene associated with graphene nanoplatelets dispersed throughout and isolated from one other within the polymeric network,

at least some wrinkled graphene configured to expand in volume along one or more flexure points and retain polysulfides generated during cycling of the battery, the polymeric network including:

a plurality of fluorinated poly(meth)acrylates grafted onto one of more flexure points of at least some wrinkled graphene;

a plurality of carbon-fluorine (C-F) bonds within the polymeric network, at least some of the plurality of carbon-fluorine (C-F) bonds configured to chemically react, by a Wurtz reaction, with at least some of the plurality of lithium ions and convert into carbon-lithium (C-Li) bonds by displacing fluorine ions ($F^-$); and

a plurality of carbon-carbon (C-C) bonds formed during displacement of fluorine ions ($F^-$) during the Wurtz reaction, formation of carbon-carbon (C-C) bonds associated with cross-linking of the polymeric network; and

lithium fluoride (LiF) formed responsive to formation of at least some of the plurality of carbon-carbon (C-C) bonds, lithium fluoride (LiF) associated with consumption of at least some of the plurality of lithium ions;

a cathode positioned opposite to the anode and containing a plurality of pores, the cathode further including:

a plurality of non-tri-zone particles;

a plurality of tri-zone particles, each tri-zone particle including:

a plurality of carbon fragments intertwined with each other and separated from one another by mesopores; and

a deformable perimeter configured to coalesce with one or more adjacent non-tri-zone particles or tri-zone particles;

a plurality of aggregates, each aggregate including a multitude of the tri-zone particles joined together;

a plurality of mesopores interspersed throughout the plurality of aggregates;

a plurality of agglomerates, each agglomerate including a multitude of the aggregates joined to each other; and

a plurality of macropores interspersed throughout the plurality of aggregates; and

an electrolyte dispersed throughout the cathode and the anode; and

a separator positioned between the anode and cathode.

82. The cathode of claim 81, wherein each aggregate has a principal dimension in

a range between 10 nanometers (nm) and 10 micrometers (μm).

83. The cathode of claim 81, wherein each mesopore has a principal dimension between 3.3 nanometers (nm) and 19.3 nm.

84. The cathode of claim 81, wherein each agglomerate has a principal dimension in an approximate range between 0.1 μm and 1,000 μm.

85. The cathode of claim 77, wherein each agglomerate has a principal dimension in an approximate range between 0.1 μm and 1,000 μm.

86. A cathode comprising:

a first porous carbonaceous region formed of a first concentration level of carbonaceous materials, the first porous carbonaceous region including:

a first plurality of non-tri-zone particles;

a first plurality of tri-zone particles, each tri-zone particle including:

a first plurality of carbon fragments intertwined with each other and separated from one another by mesopores; and

a first deformable perimeter configured to coalesce with one or more adjacent non-tri-zone particles or tri-zone particles;

a first plurality of aggregates, each aggregate including a multitude of the tri-zone particles joined together, each aggregate having a principal dimension in a range between 10 nanometers (nm) and 10 micrometers (μm);

a first plurality of mesopores interspersed throughout the first plurality of aggregates, each mesopore having a principal dimension between 3.3 nanometers (nm) and 19.3 nm;

a first plurality of agglomerates, each agglomerate including a multitude of the aggregates joined to each other, each agglomerate having a principal dimension in an approximate range between 0.1 μm and 1,000 μm; and

a first plurality of macropores interspersed throughout the first plurality of aggregates, each macropore having a principal dimension between 0.1 μm and 1,000 μm; and

a second porous carbonaceous region positioned adjacent to the first porous carbonaceous region, the second porous carbonaceous region formed of a second

concentration level of carbonaceous materials dissimilar to the first concentration level of carbonaceous materials, the second porous carbonaceous region including:

a second plurality of non-tri-zone particles;

a second plurality of tri-zone particles, each tri-zone particle including:

a second plurality of carbon fragments intertwined with each other and separated from one another by mesopores; and

a second deformable perimeter configured to coalesce with one or more adjacent non-tri-zone particles or tri-zone particles;

a second plurality of aggregates, each aggregate including a multitude of the tri-zone particles joined together, each aggregate having a principal dimension in a range between 10 nanometers (nm) and 10 micrometers (μm);

a second plurality of mesopores interspersed throughout the second plurality of aggregates, each mesopore having a principal dimension between 3.3 nanometers (nm) and 19.3 nm;

a second plurality of agglomerates, each agglomerate including a multitude of the aggregates joined to each other, each agglomerate having a principal dimension in an approximate range between 0.1 μm and 1,000 μm; and

a second plurality of macropores interspersed throughout the second plurality of aggregates, each macropore having a principal dimension between 0.1 μm and 1,000 μm.

87. The cathode of claim 86, wherein one or more of the first porous carbonaceous region or the second porous carbonaceous region further includes a selectively permeable shell configured to form a separated liquid phase on the first porous carbonaceous region or the second porous carbonaceous region, respectively.

88. The cathode of claim 86, further including an electrolyte dispersed within one or more of the first porous carbonaceous region or the second porous carbonaceous region.

89. The cathode of claim 86, wherein the first porous carbonaceous region has an electrical conductivity in an approximate range between 500 S/m to 20,000 S/m at a pressure of 12,000 pounds per square in (psi).

90. The cathode of claim 86, wherein the second porous carbonaceous region has an electrical conductivity in an approximate range between 0 S/m to 500 S/m at a pressure of 12,000 pounds per square in (psi).

91. The cathode of claim 86, wherein one or more of the first plurality of agglomerates or second plurality of agglomerates include aggregates connected to each other with one or more polymer-based binders.

92. The cathode of claim 86, wherein each of the tri-zone particles includes:

a first porosity region located around a center of each of the tri-zone particles, the first porosity region including first pores; and

a second porosity region surrounding the first porosity region, the second porosity region including second pores.

93. The cathode of claim 86, wherein the first pores define a first pore density, and the second pores define a second pore density different the first pore density.

94. The cathode of claim 86, further including one or more additional porous carbonaceous regions, at least one additional porous carbonaceous region coupled with the second porous carbonaceous region.

95. The cathode of claim 94, wherein one or more additional porous carbonaceous regions are arranged in order of incrementally decreasing concentration levels of carbonaceous materials away from the first porous carbonaceous region.

96. The cathode of claim 86, wherein the first plurality of mesopores has a first mesopore density, and the second plurality of mesopores has a second mesopore density different than the first mesopore density.

97. The cathode of claim 86, wherein the first plurality of macropores has a first pore density, and the second plurality of macropores has a second pore density different than the first pore density.

98. The cathode of claim 86, wherein one or more of the first porous carbonaceous region or the second porous carbonaceous region is configured to nucleate sulfur.

99. The cathode of claim 86, wherein the cathode has a sulfur to carbon weight ratio between approximately 1:5 to 10:1.

100. The cathode of claim 86, further including one or more electrically conductive additives dispersed within one or more of the first porous carbonaceous region or the second porous carbonaceous region.

101. The cathode of claim 86, further including a protective sheath disposed on the cathode.

102. The cathode of claim 101, wherein the protective sheath includes:

a tri-functional epoxy compound, and

a di-amine oligomer-based compound, both of which are configured to chemically react with each other.

103. The cathode of claim 102, wherein the cathode is incorporated into a lithium-sulfur battery.

104. The cathode of claim 103, wherein the tri-functional epoxy compound is one or more of trimethylolpropane triglycidyl ether (TMPTE), tris(4-hydroxyphenyl)methane triglycidyl ether, or tris(2,3-epoxypropyl) isocyanurate.

105. The cathode of claim 103, wherein the protective sheath is configured to prevent polysulfide migration within the lithium-sulfur battery based on chemical bonding between the protective sheath and one or more lithium-containing polysulfide intermediates generated during operational discharge-charge cycling of the lithium-sulfur battery.

106. A composition of matter including a plurality of pores, the composition of matter comprising:

a plurality of non-tri-zone particles;

a plurality of tri-zone particles, each tri-zone particle including:

a plurality of carbon fragments intertwined with each other and separated from one another by mesopores; and

a deformable perimeter configured to coalesce with one or more adjacent non-tri-zone particles or tri-zone particles;

a plurality of aggregates, each aggregate including a multitude of the tri-zone particles joined together, each aggregate having a principal dimension in a range between 10 nanometers (nm) and 10 micrometers (μm);

a plurality of mesopores interspersed throughout the plurality of aggregates, each mesopore having a principal dimension between 3.3 nanometers (nm) and 19.3 nm;

a plurality of agglomerates, each agglomerate including a multitude of the aggregates joined to each other, each agglomerate having a principal dimension in an approximate range between 0.1 μm and 1,000 μm; and

a plurality of macropores interspersed throughout the plurality of agglomerates, each macropore having a principal dimension between 0.1 μm and 1,000 μm.

107. The composition of matter of claim 106, further including a selectively permeable shell configured to form a separated liquid phase on one or more exposed surfaces of the composition of matter.

108. The composition of matter of claim 106, further including an electrolyte dispersed within the composition of matter.

109. The composition of matter of claim 106, wherein each of the pores has a principal dimension in an approximate range between 0 nanometers (nm) and 32.3 nm.

110. The composition of matter of claim 106, wherein the composition of matter has an electrical conductivity in an approximate range between 100 S/m to 20,000 S/m at a pressure of 12,000 pounds per square in (psi).

111. The composition of matter of claim 106, wherein at least some agglomerates are connected to each other with one or more polymer-based binders.

112. The composition of matter of claim 106, wherein each of the tri-zone particles includes:

a first porosity region located around a center of each of the tri-zone particles, the first porosity region including first pores; and

a second porosity region surrounding the first porosity region, the second porosity region including second pores.

113. The composition of matter of claim 112, wherein the first pores define a first pore density, and the second pores define a second pore density different the first pore density.

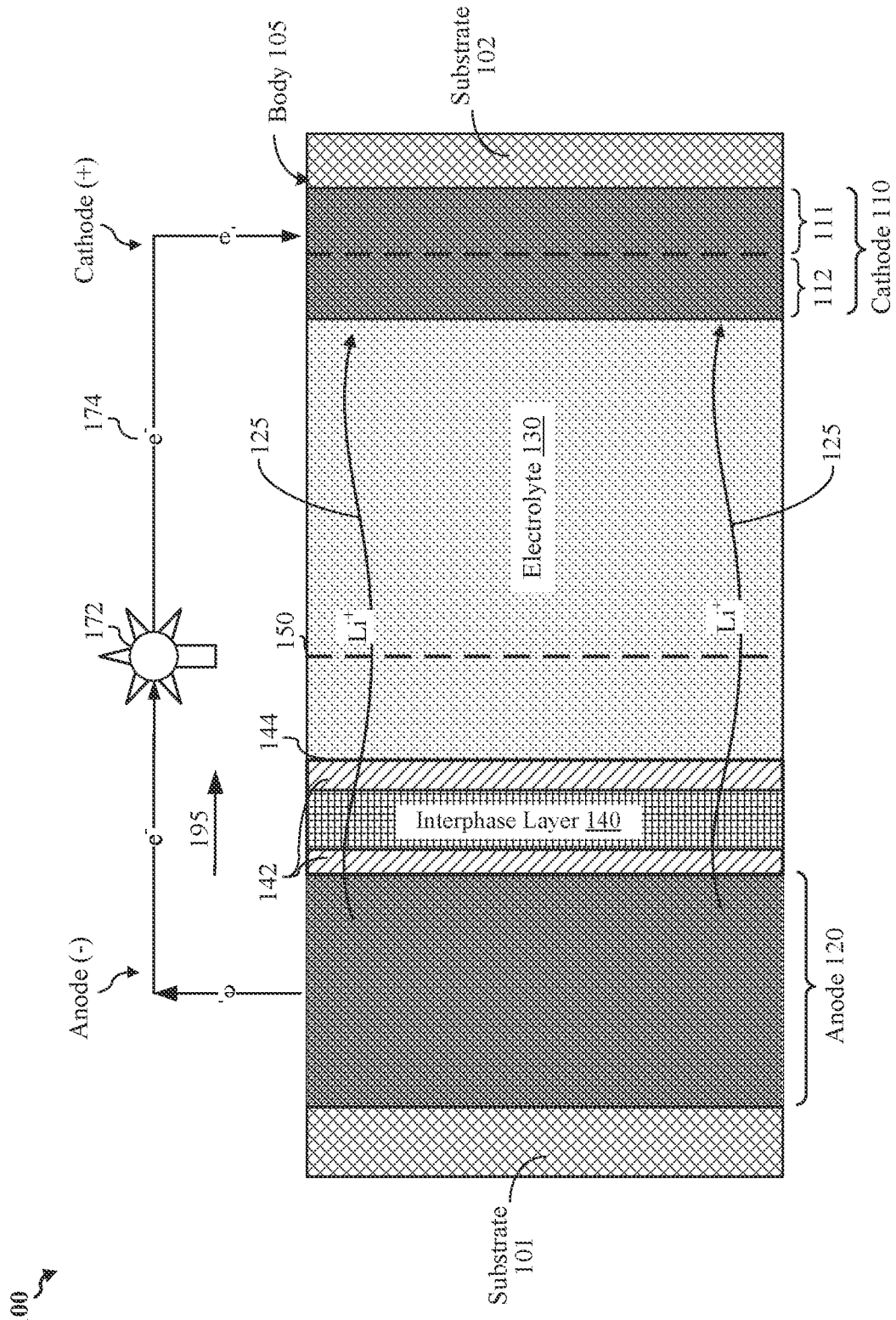
100
Cathode (+)
Anode (-)
174
172
195
Body 105
Substrate 102
Substrate 101
Cathode 110
111
112
125
125
Electrolyte 130
150
144
142
Interphase Layer 140
Anode 120
Li+
Li+

*Figure 1*

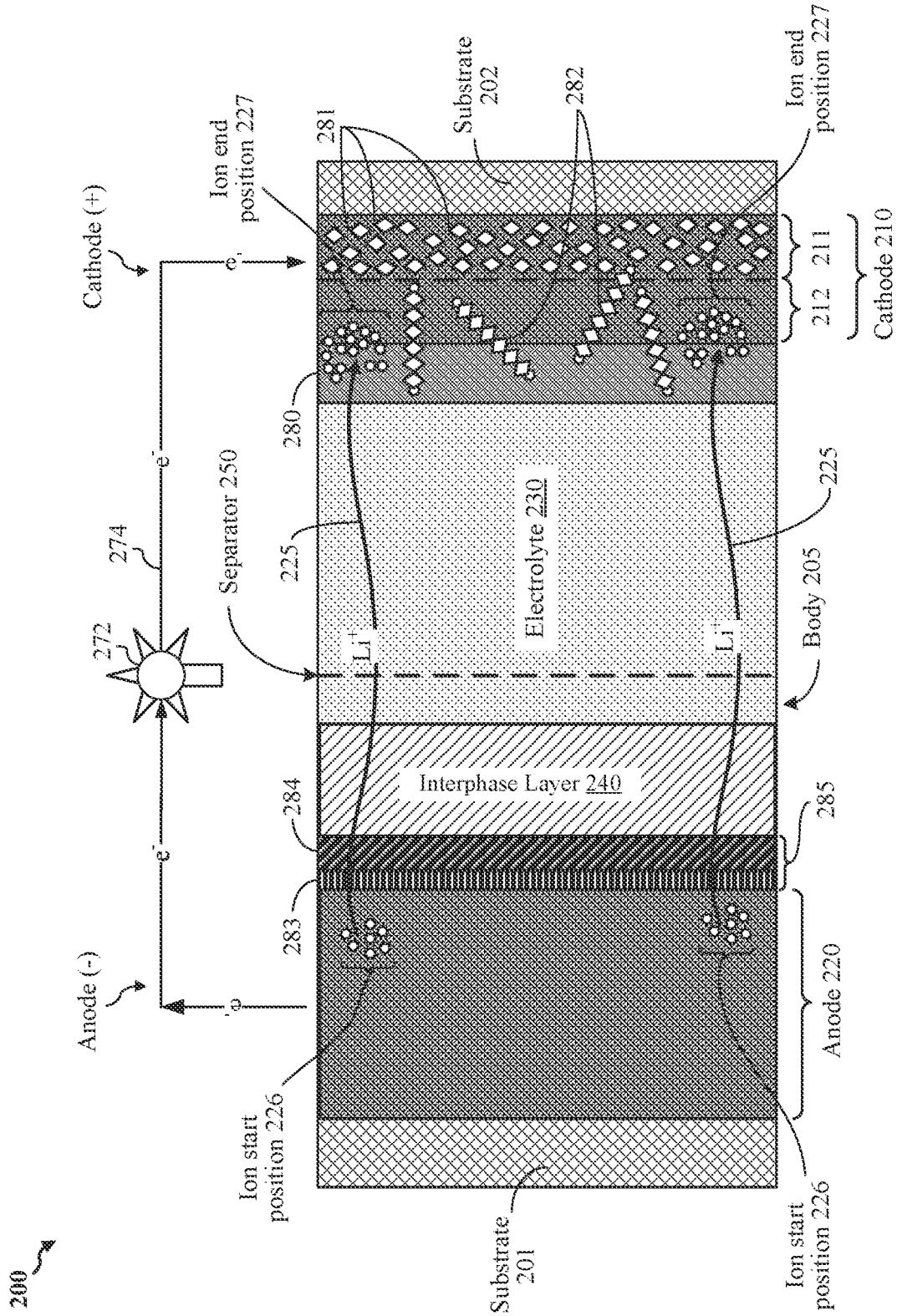
200
Cathode (+)
Anode (-)
e-
e-
e-
e-
274
272
Separator 250
Ion end position 227
Ion end position 227
281
Substrate 202
282
280
225
225
Electrolyte 230
Li+
Li+
Body 205
Interphase Layer 240
284
285
283
Anode 220
Ion start position 226
Ion start position 226
Substrate 201
211
212
Cathode 210

*Figure 2*

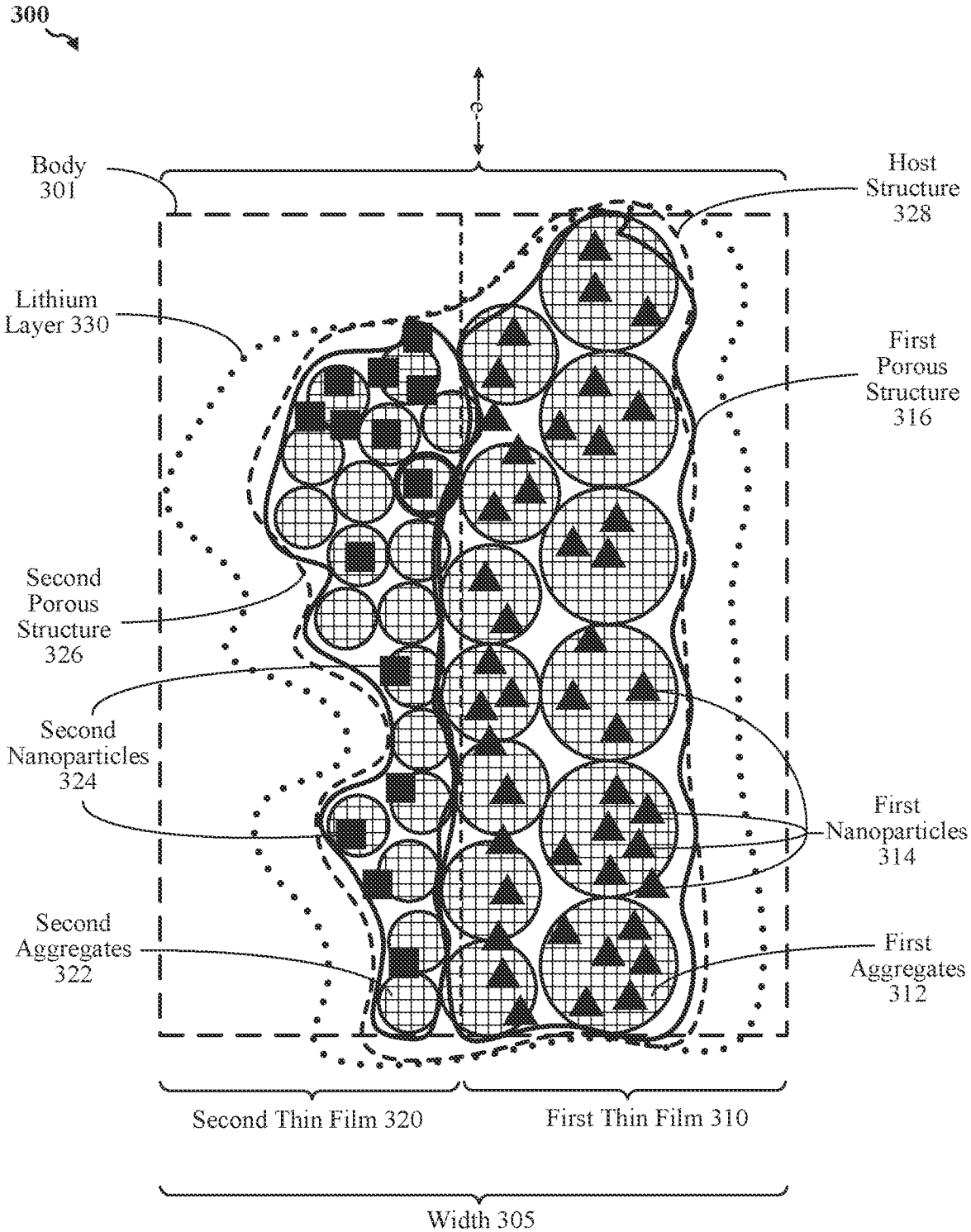
300
Body 301
Host Structure 328
Lithium Layer 330
First Porous Structure 316
Second Porous Structure 326
Second Nanoparticles 324
First Nanoparticles 314
Second Aggregates 322
First Aggregates 312
Second Thin Film 320
First Thin Film 310
Width 305

*Figure 3*

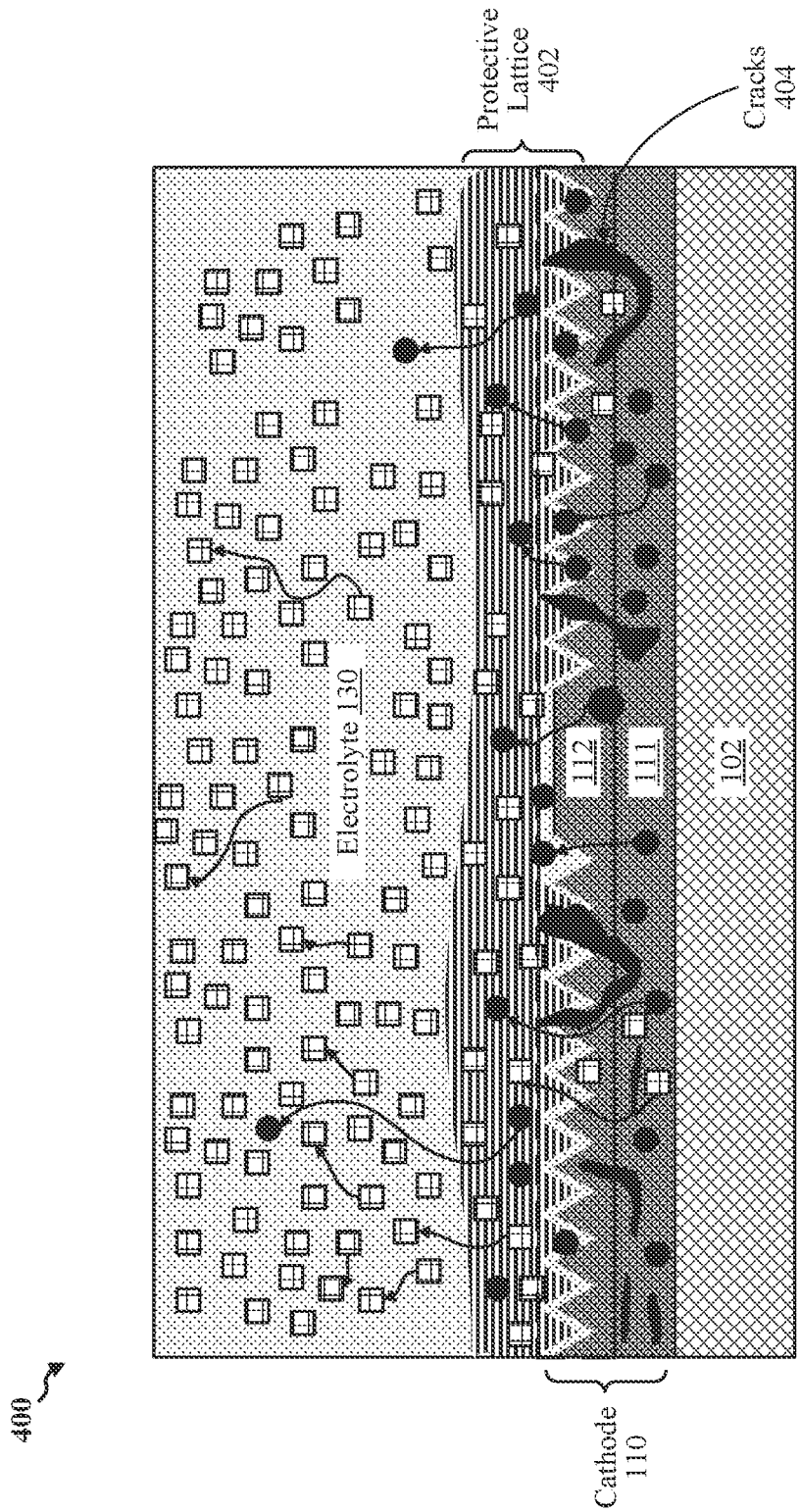
400
Protective Lattice 402
Cracks 404
Electrolyte 130
112
111
102
Cathode 110

*Figure 4*

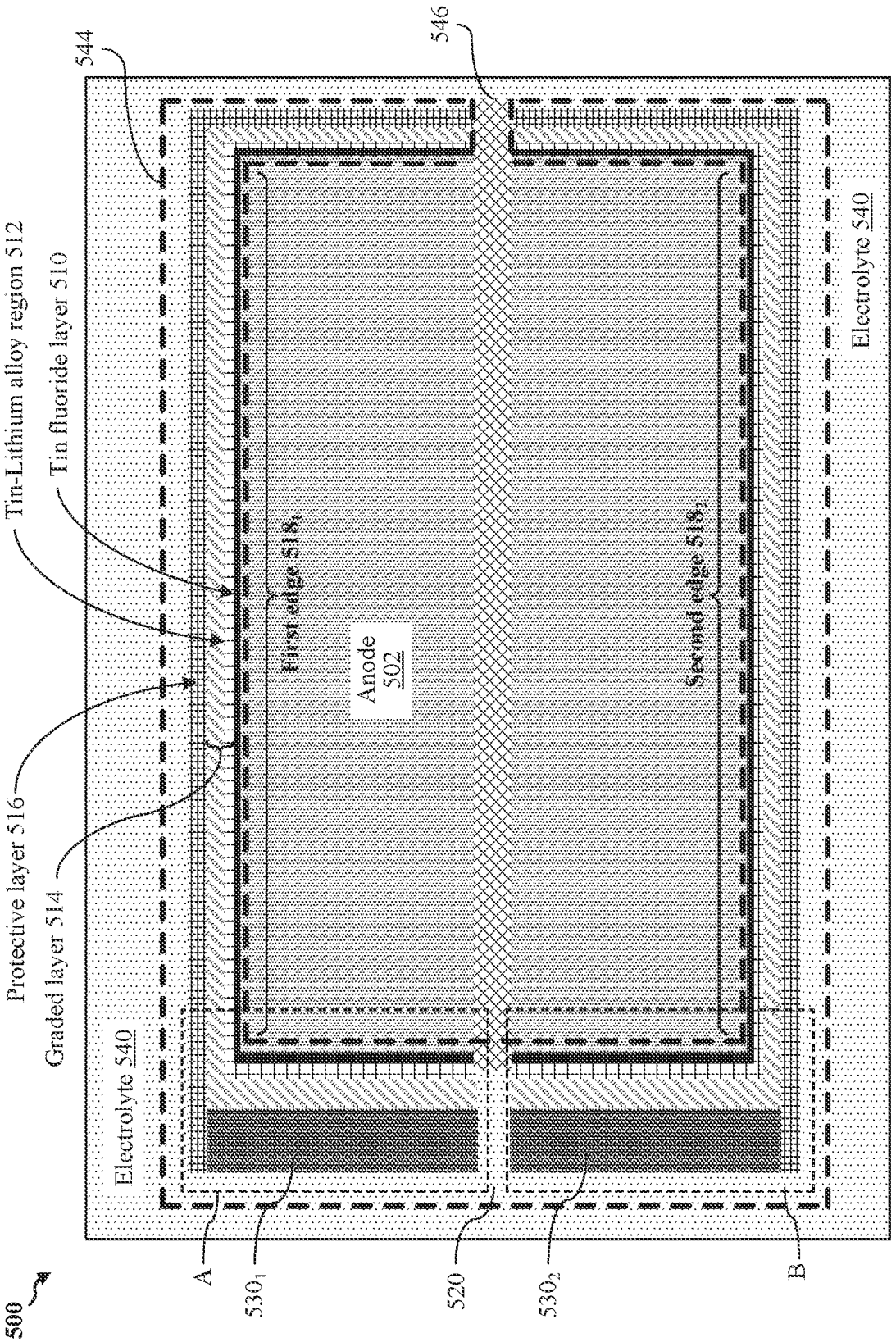
500
544
546
Tin-Lithium alloy region 512
Tin fluoride layer 510
Protective layer 516
Graded layer 514
Electrolyte 540
Electrolyte 540
First edge 518$_1$
Anode 502
Second edge 518$_2$
A
530$_1$
520
530$_2$
B

*Figure 5*

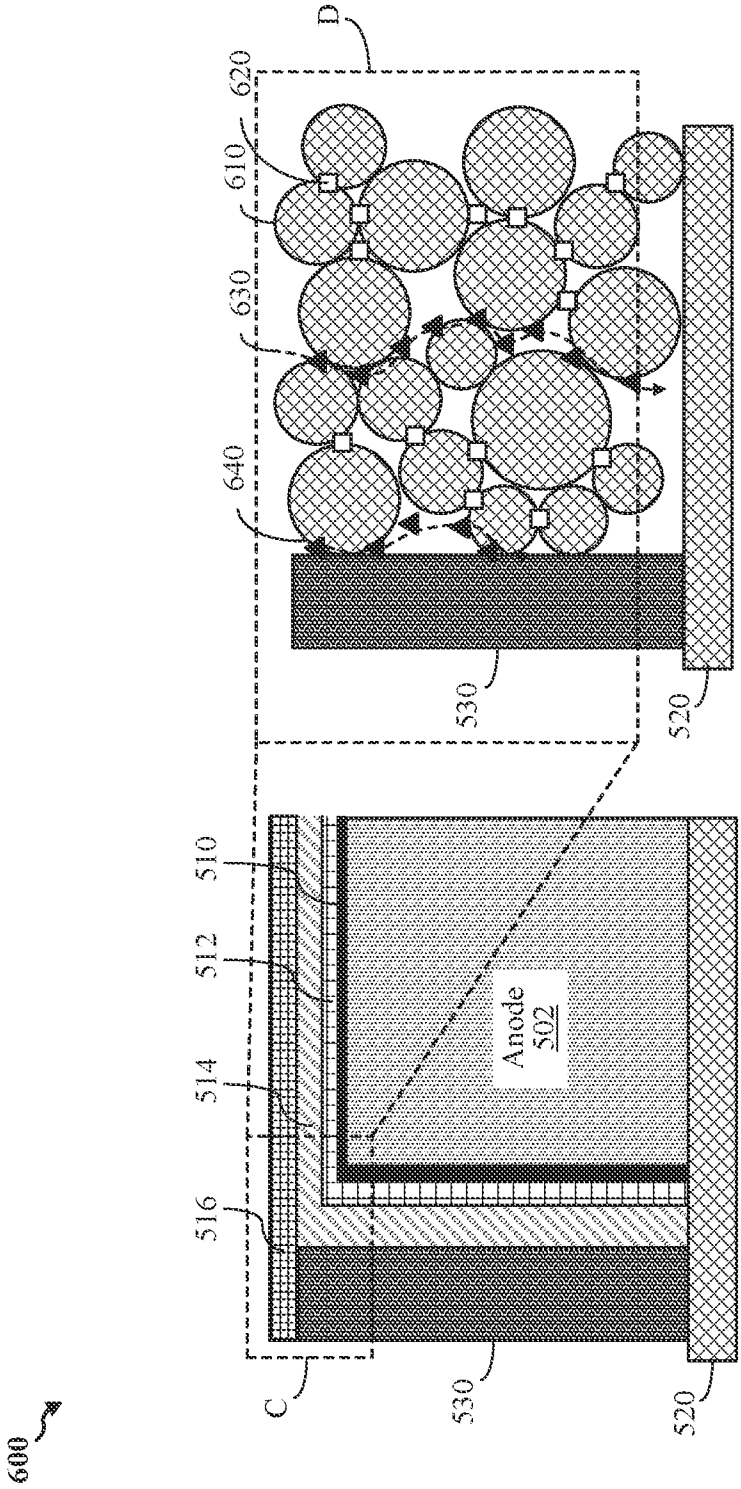


*Figure 6*

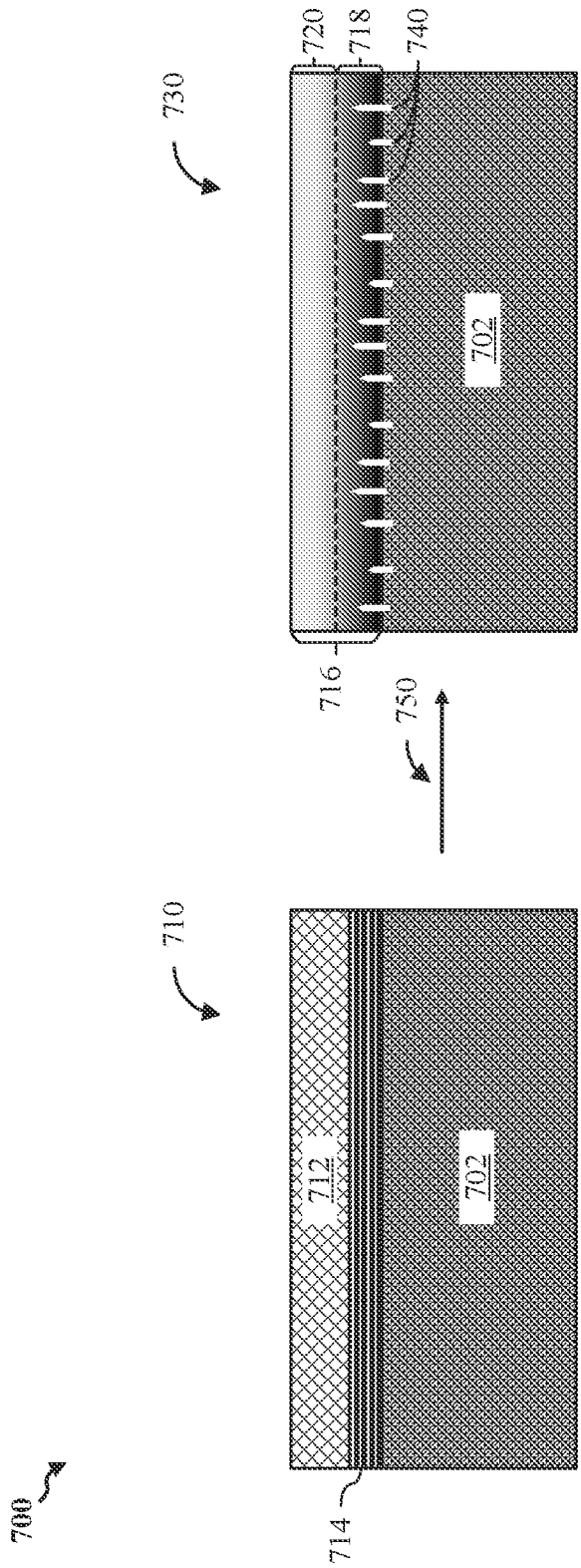


*Figure 7*

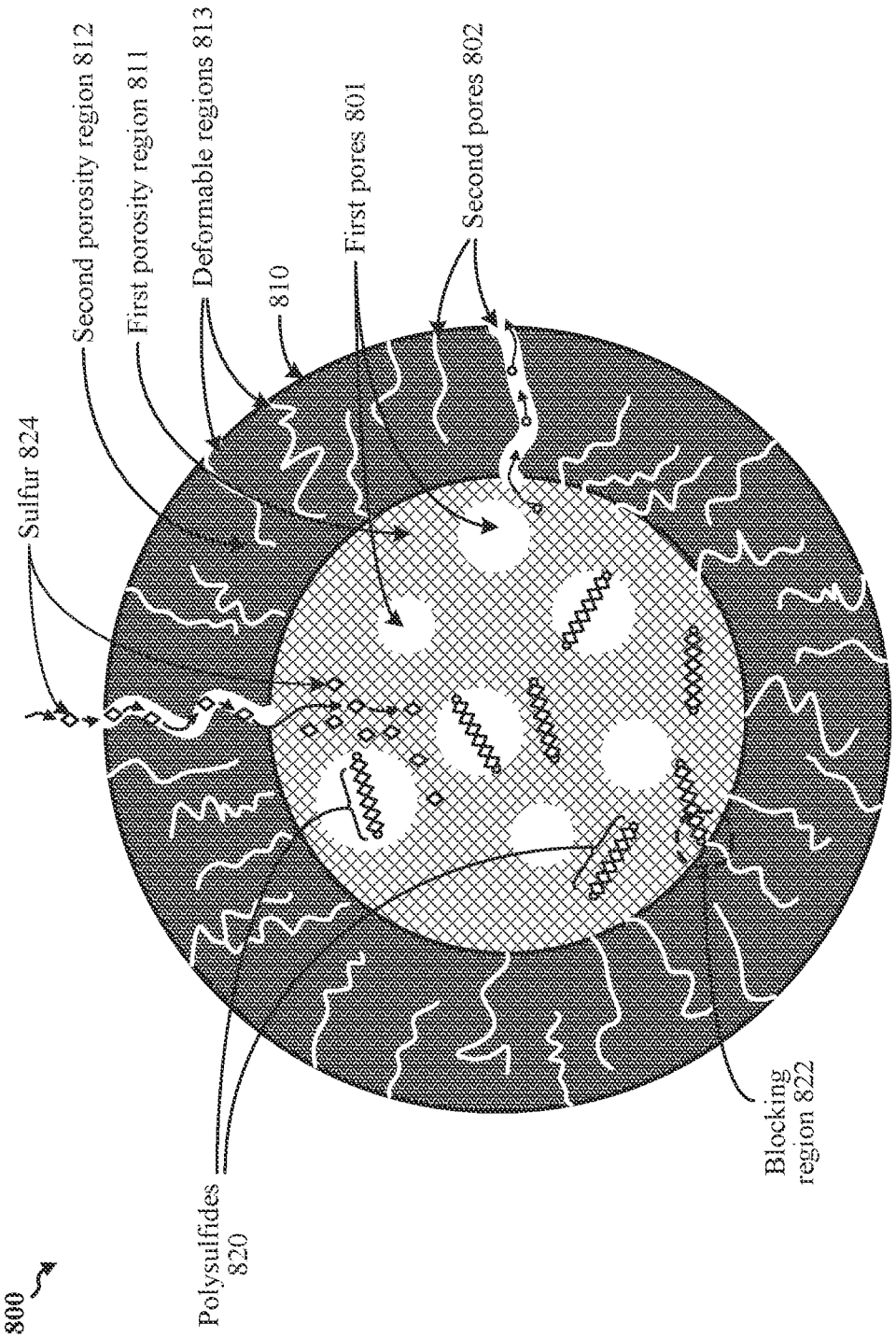
800
Polysulfides 820
Sulfur 824
Second porosity region 812
First porosity region 811
Deformable regions 813
810
First pores 801
Second pores 802
Blocking region 822
A

*Figure 8A*

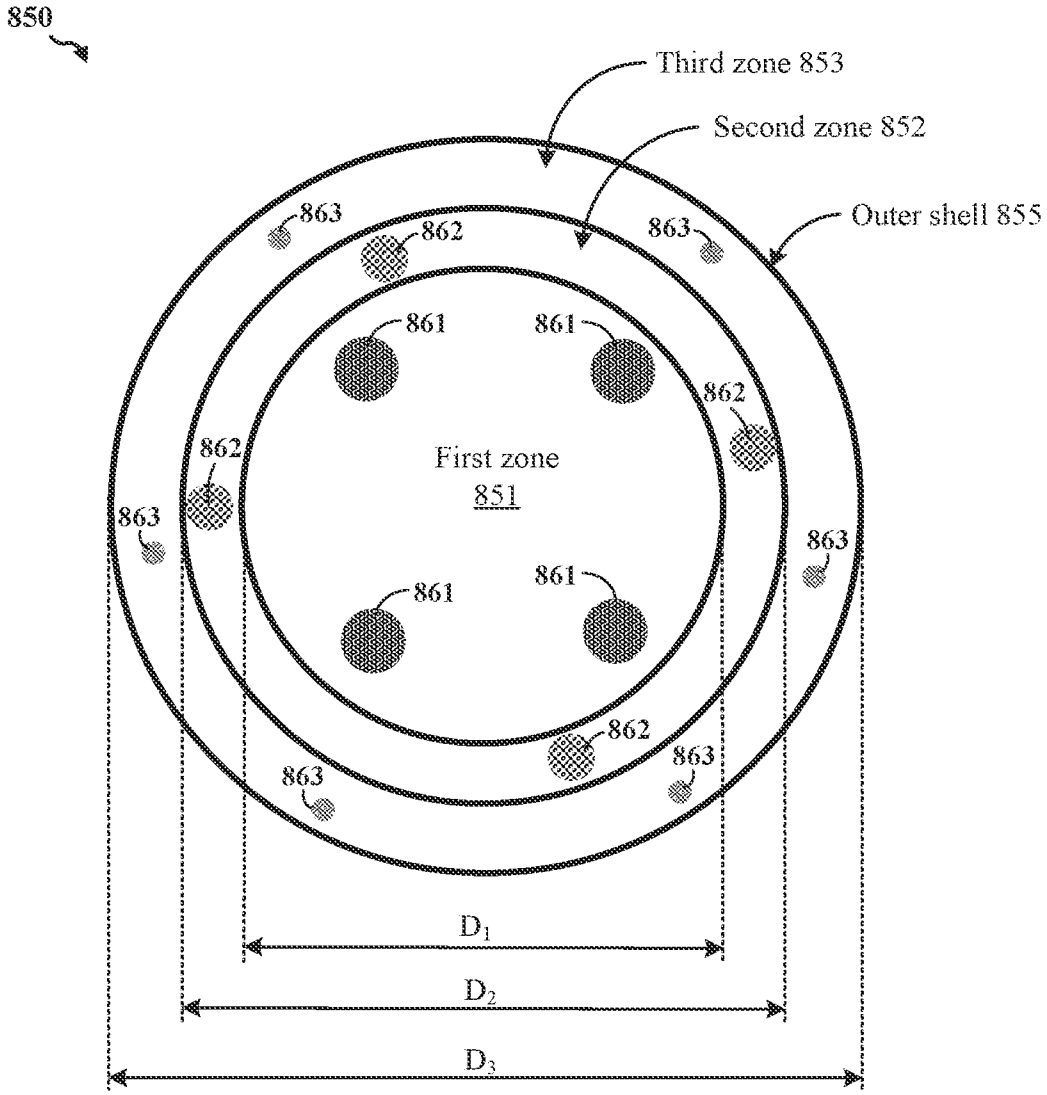
850
Third zone 853
Second zone 852
Outer shell 855
863
862
861
First zone
851
$D_1$
$D_2$
$D_3$

*Figure 8B*

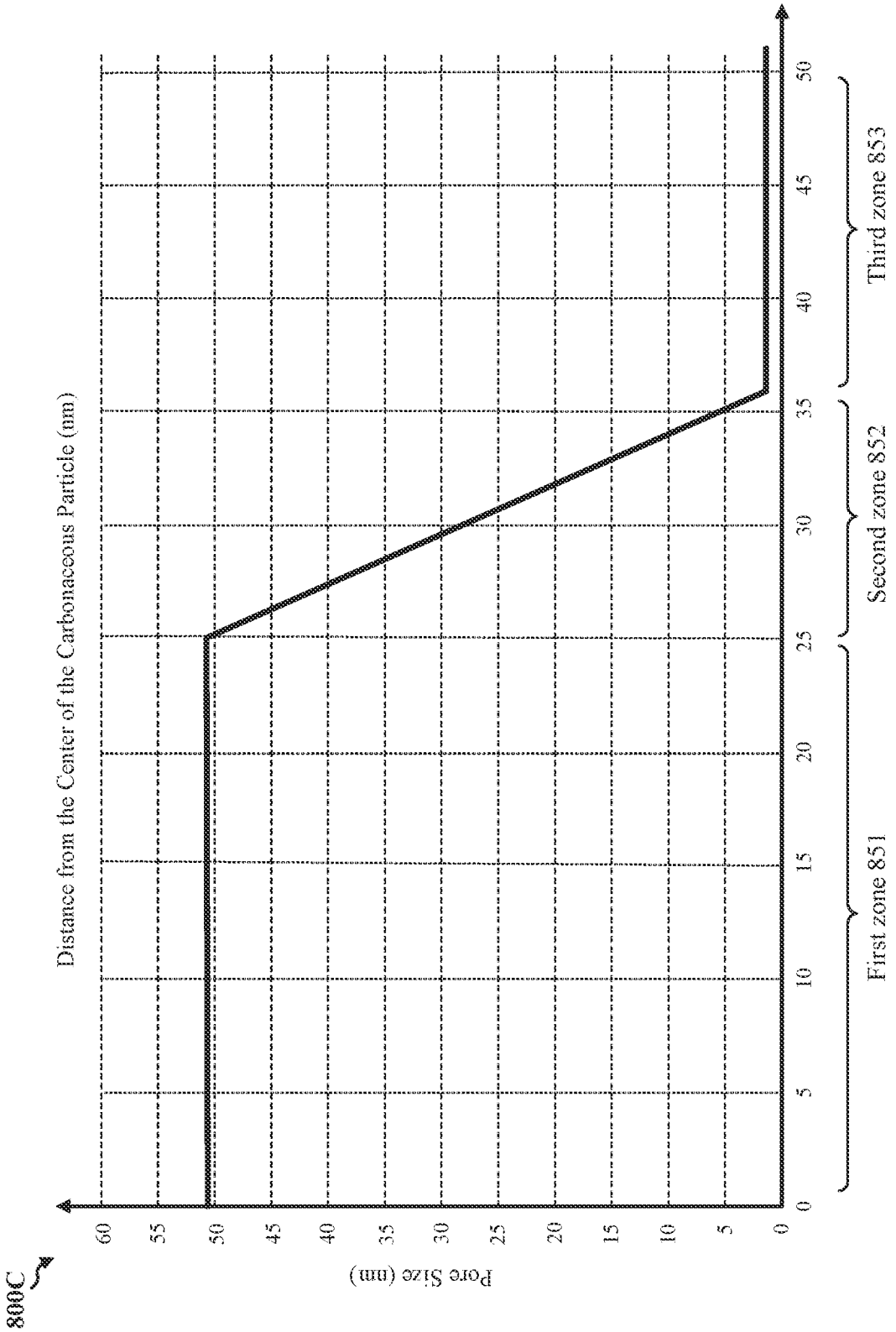
800C
Pore Size (nm)
Distance from the Center of the Carbonaceous Particle (nm)
First zone 851
Second zone 852
Third zone 853

*Figure 8C*

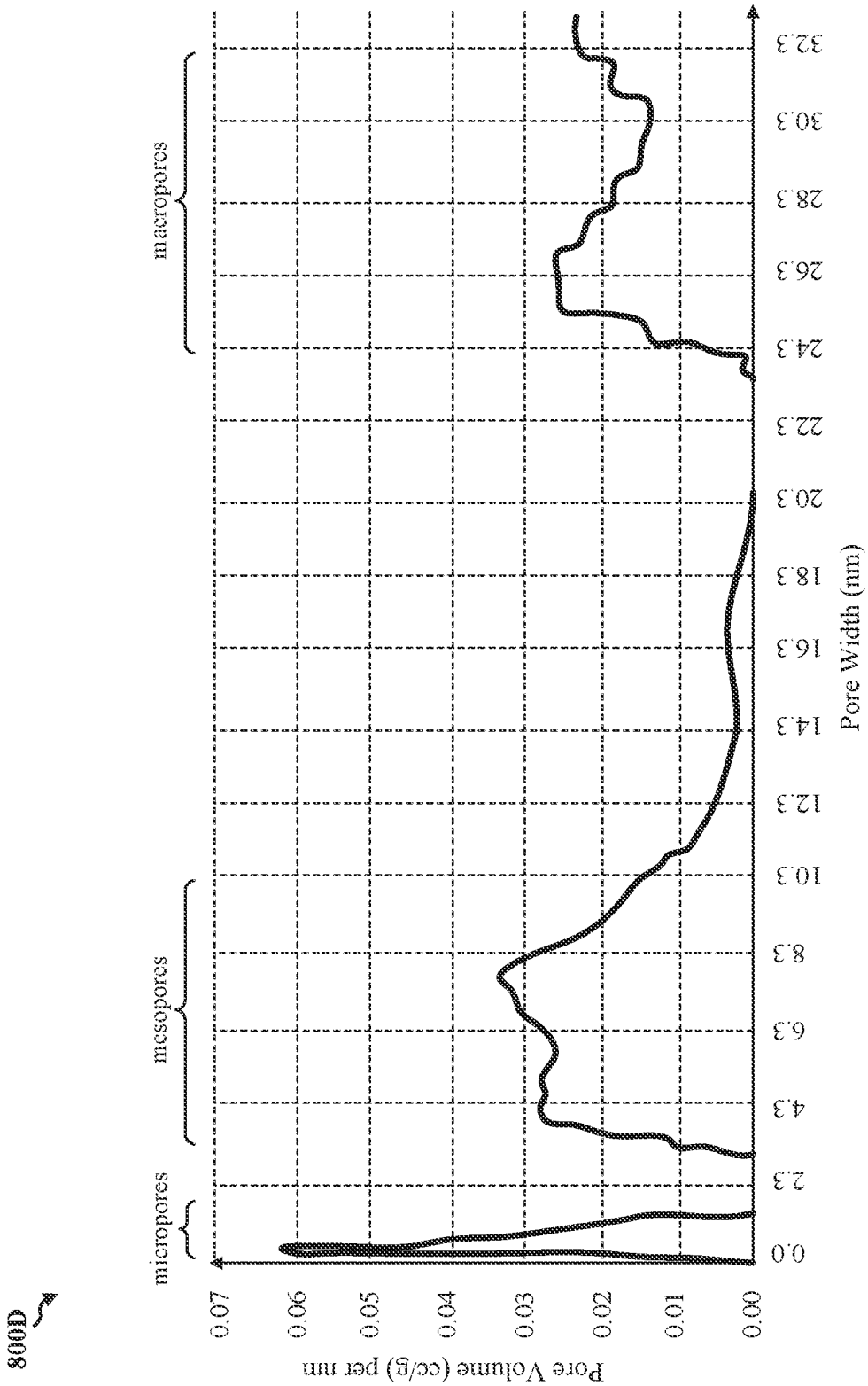
800D
micropores
mesopores
macropores
Pore Volume (cc/g) per nm
0.07
0.06
0.05
0.04
0.03
0.02
0.01
0.00
0.0
2.3
4.3
6.3
8.3
10.3
12.3
14.3
16.3
18.3
20.3
22.3
24.3
26.3
28.3
30.3
32.3
Pore Width (nm)

*Figure 8D*

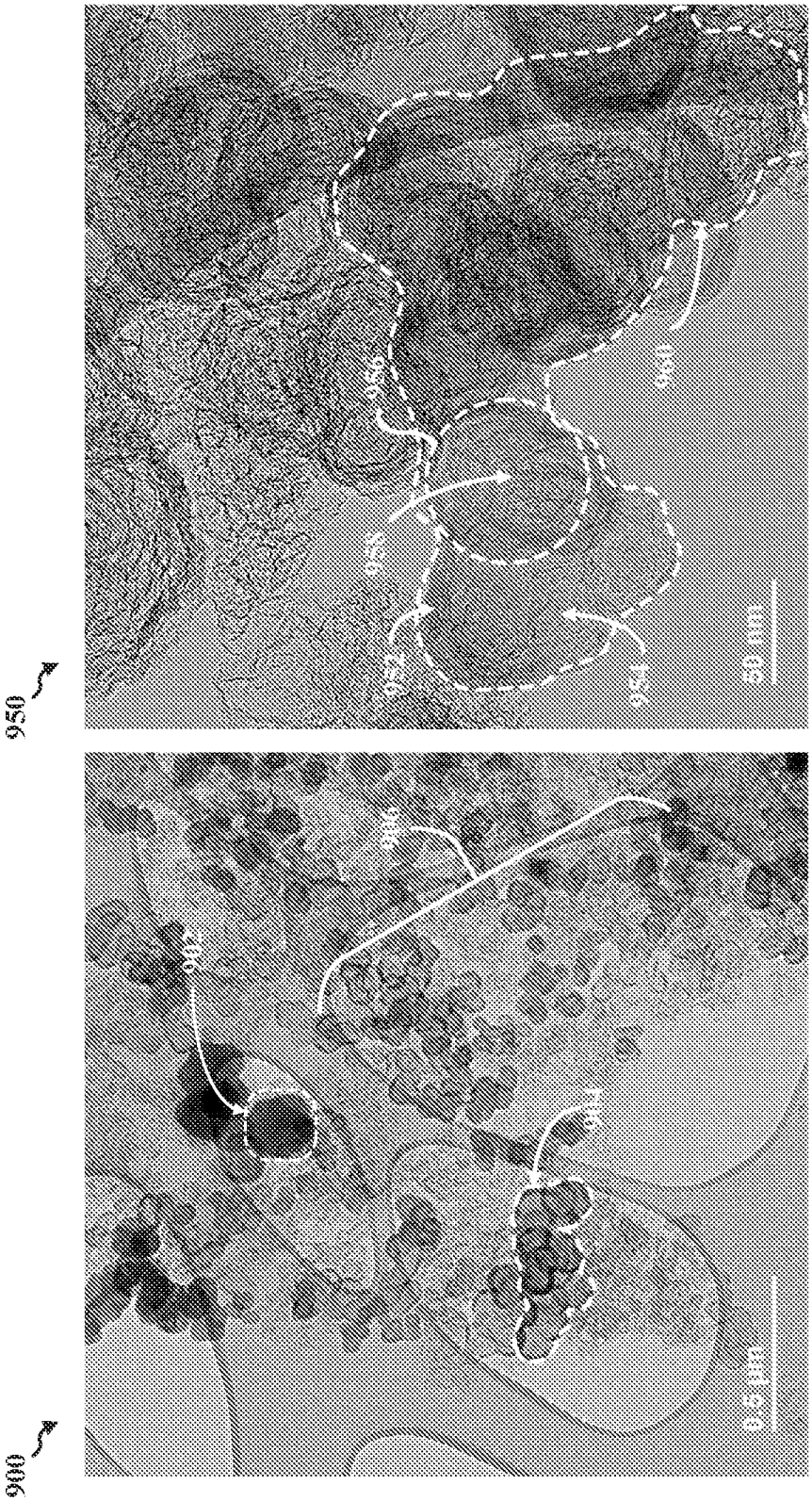


*Figure 9B*

*Figure 9A*

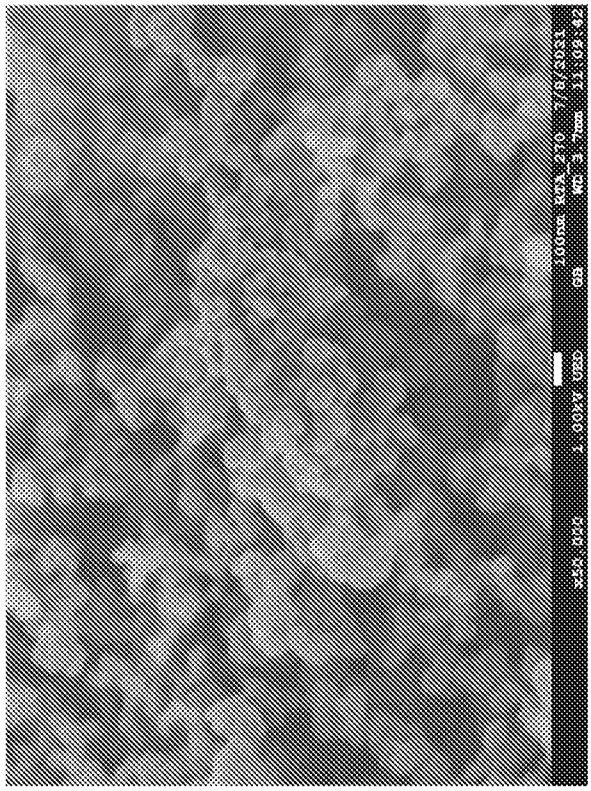

1050

*Figure 10B*

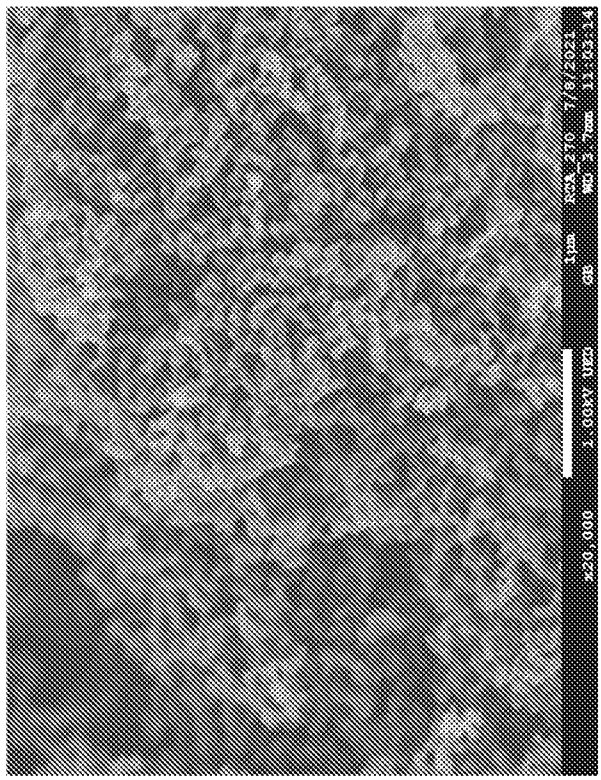

1000

*Figure 10A*

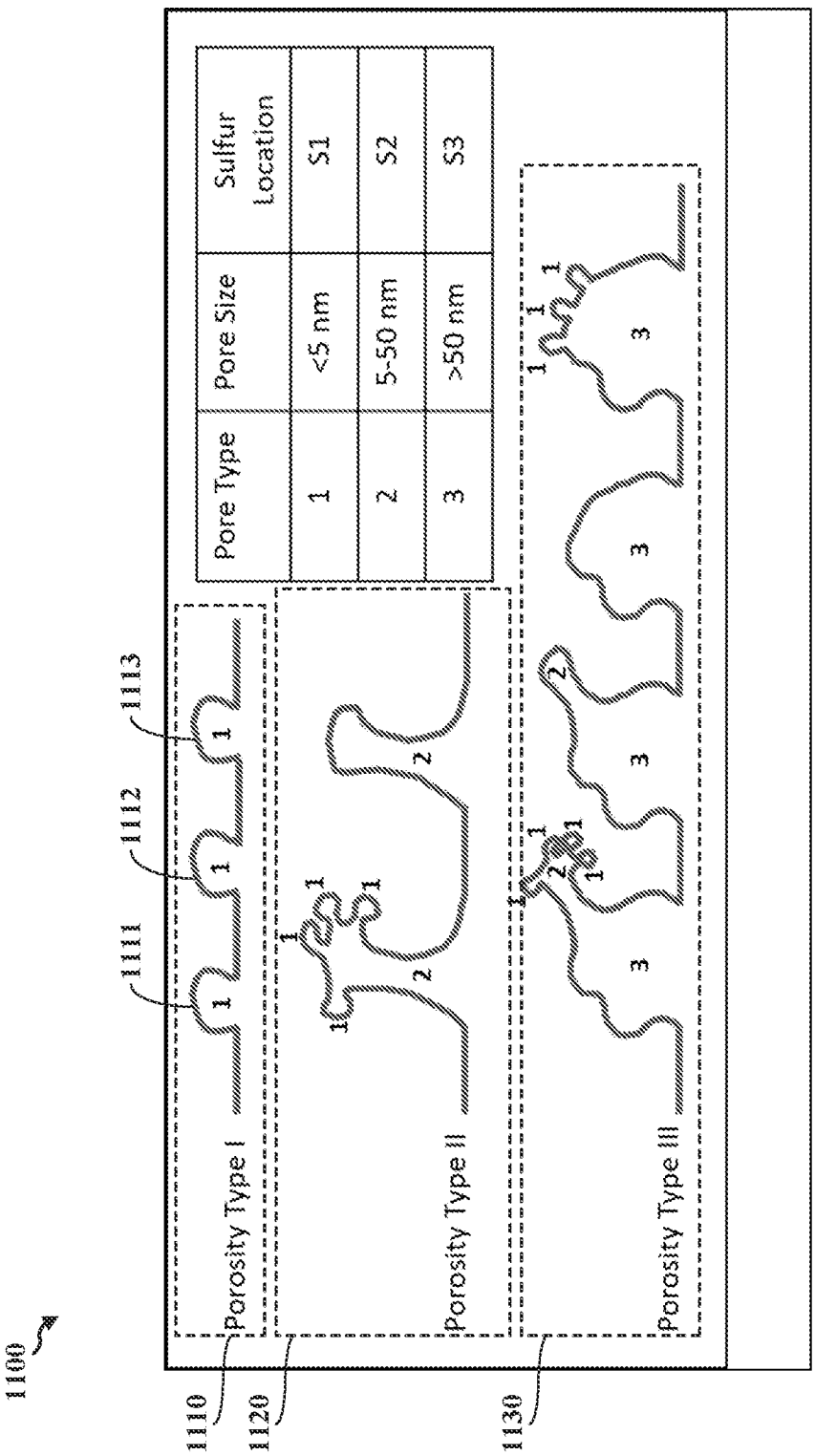
1100
1110
1120
1130
1111
1112
1113
Porosity Type I
Porosity Type II
Porosity Type III
Pore Type
Pore Size
Sulfur Location
1
<5 nm
S1
2
5-50 nm
S2
3
>50 nm
S3

*Figure 11*

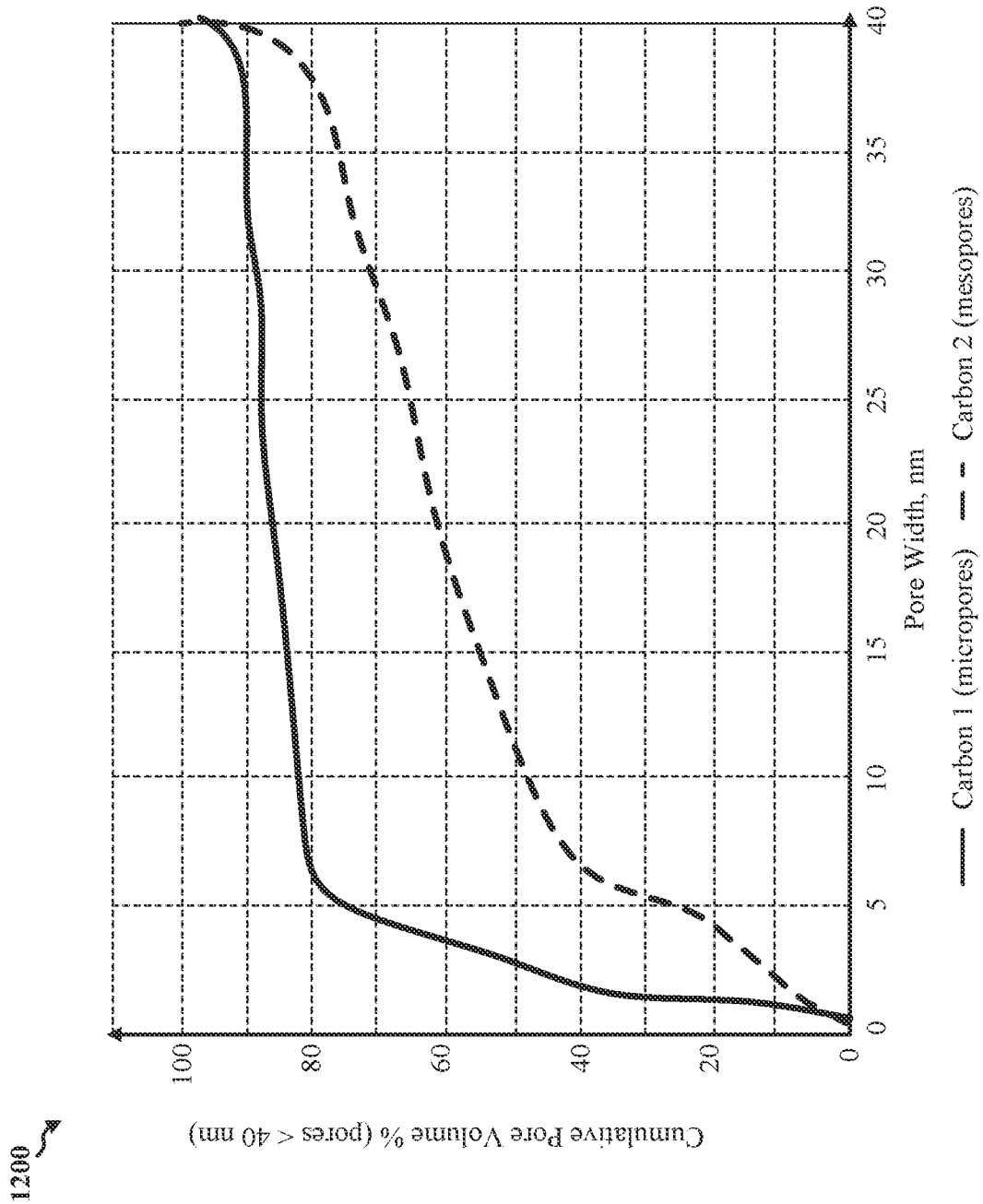
1200
Cumulative Pore Volume % (pores < 40 nm)
100
80
60
40
20
0
0
5
10
15
20
25
30
35
40
Pore Width, nm
Carbon 1 (micropores)
Carbon 2 (mesopores)

*Figure 12*

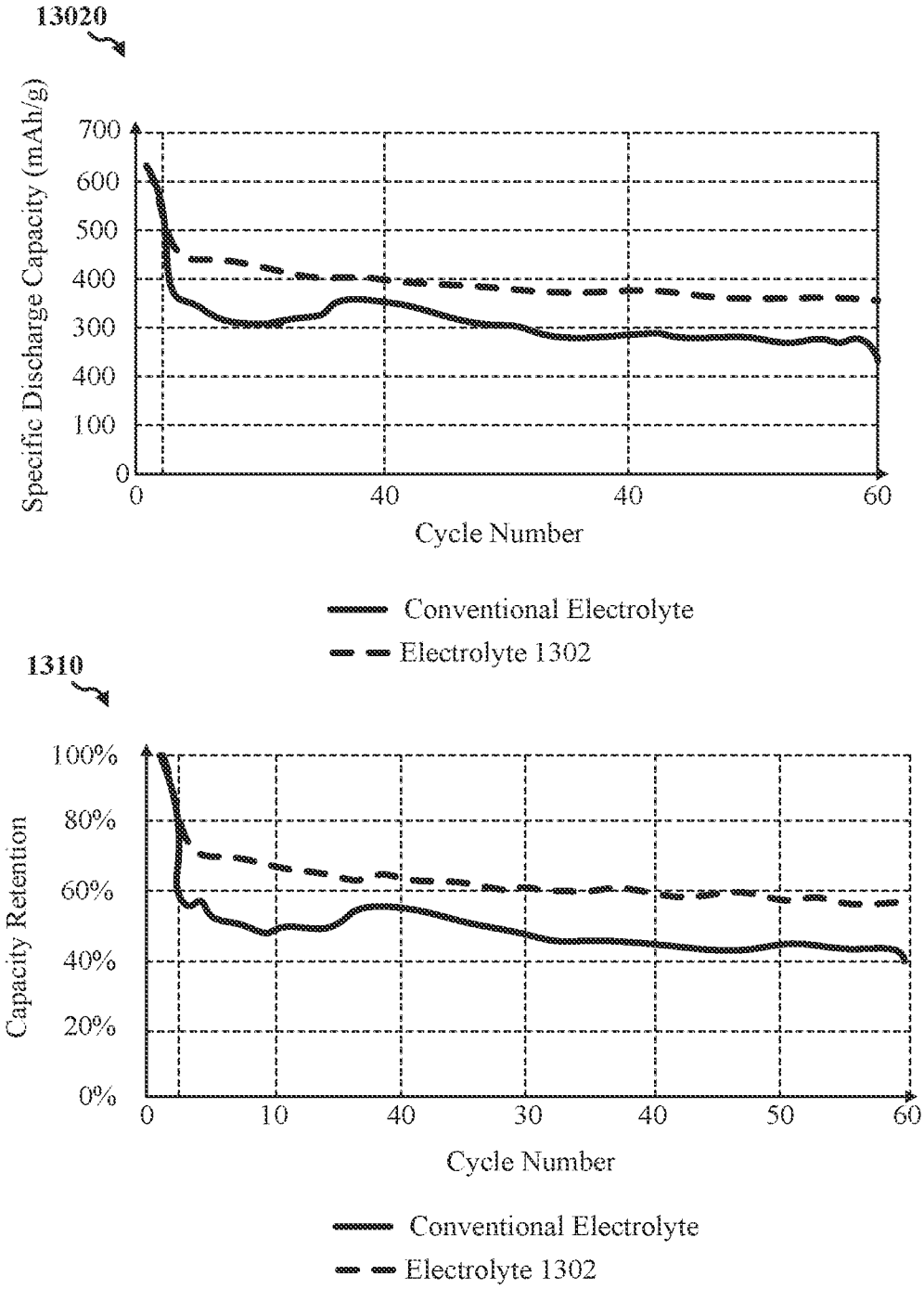
13020
Specific Discharge Capacity (mAh/g)
700
600
500
400
300
400
100
0
0
40
40
60
Cycle Number
Conventional Electrolyte
Electrolyte 1302
1310
Capacity Retention
100%
80%
60%
40%
20%
0%
0
10
40
30
40
50
60
Cycle Number
Conventional Electrolyte
Electrolyte 1302

*Figure 13*

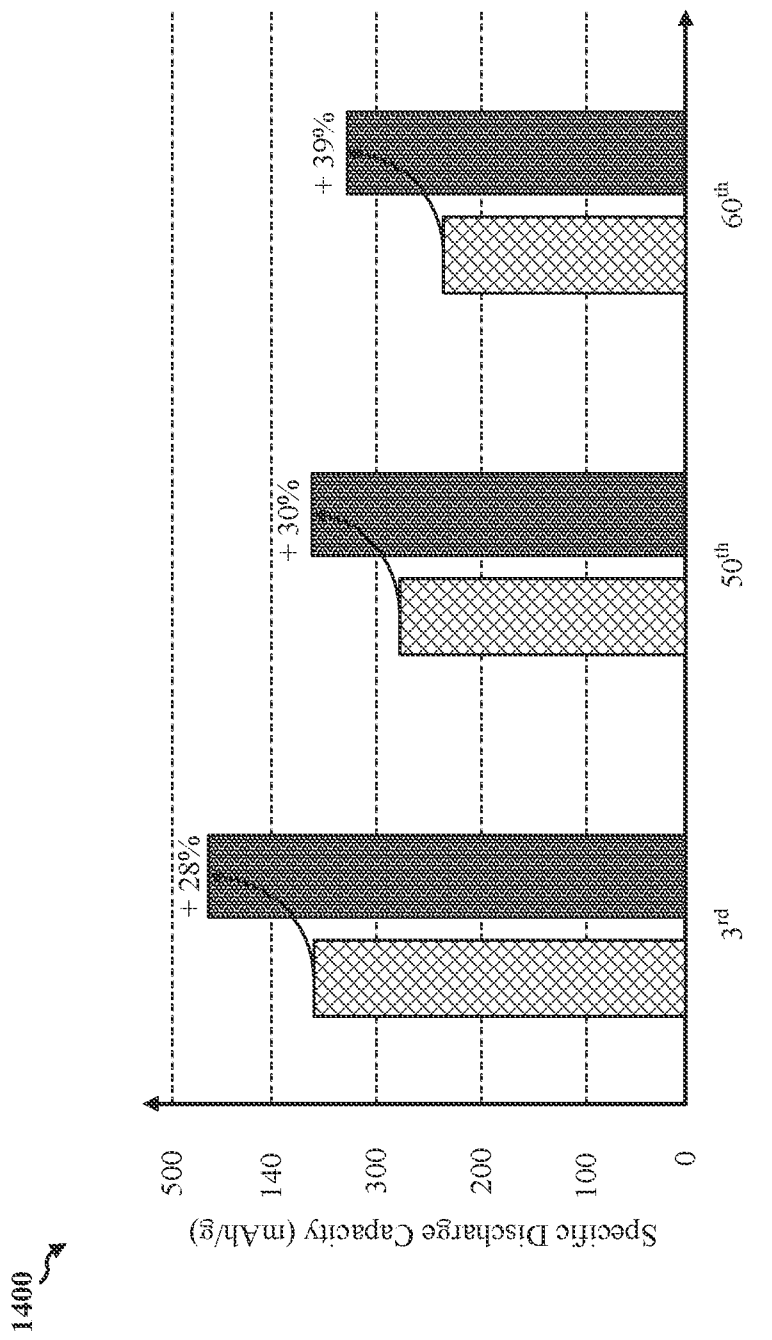
1400
Specific Discharge Capacity (mAh/g)
500
140
300
200
100
0
+ 28%
+ 30%
+ 39%
3rd
50th
60th
Cycle Number
Conventional Electrolyte
Electrolyte 1402

*Figure 14*

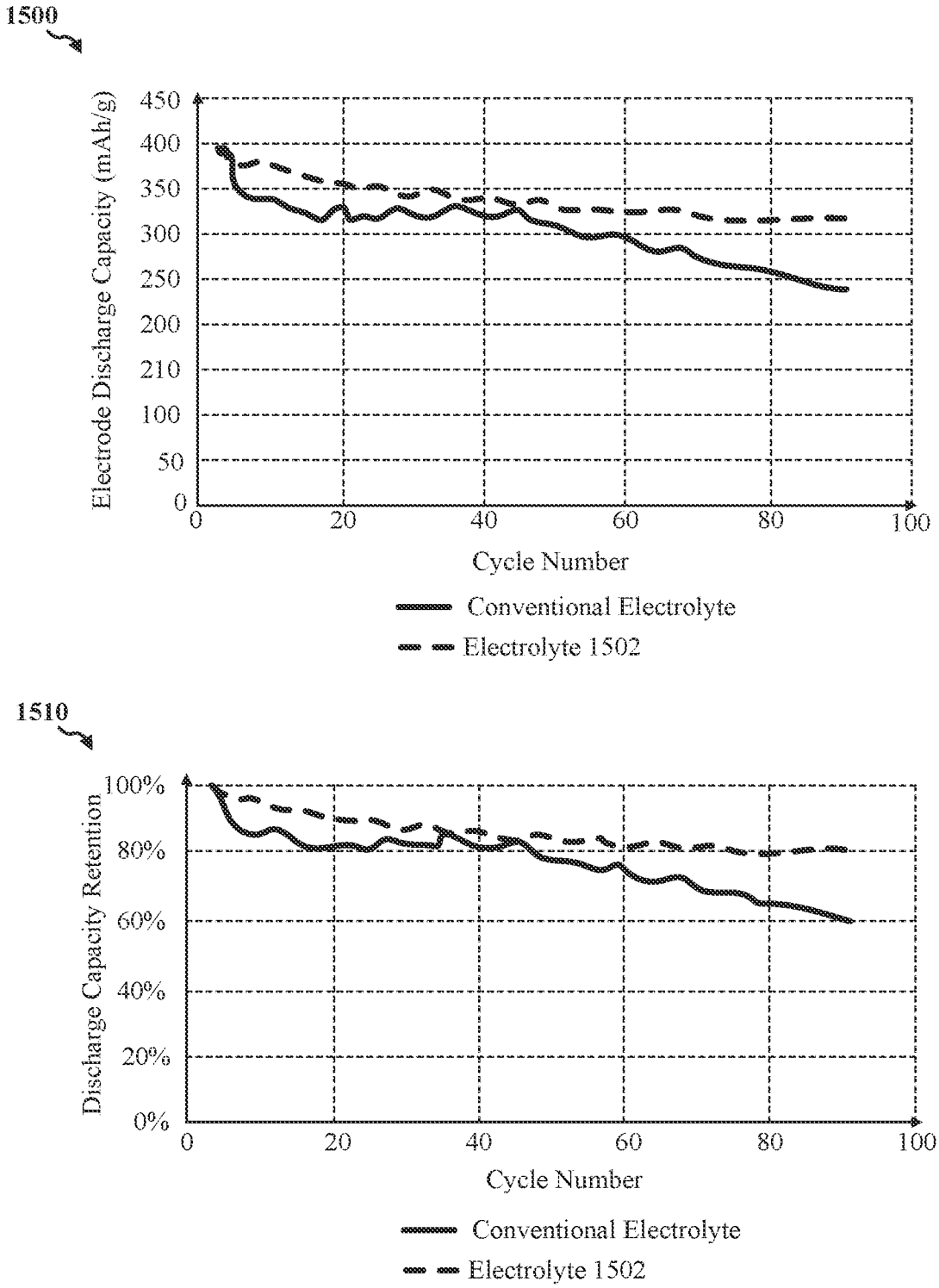
1500
Electrode Discharge Capacity (mAh/g)
450
400
350
300
250
200
210
100
50
0
0
20
40
60
80
100
Cycle Number
Conventional Electrolyte
Electrolyte 1502
1510
Discharge Capacity Retention
100%
80%
60%
40%
20%
0%
0
20
40
60
80
100
Cycle Number
Conventional Electrolyte
Electrolyte 1502

*Figure 15*

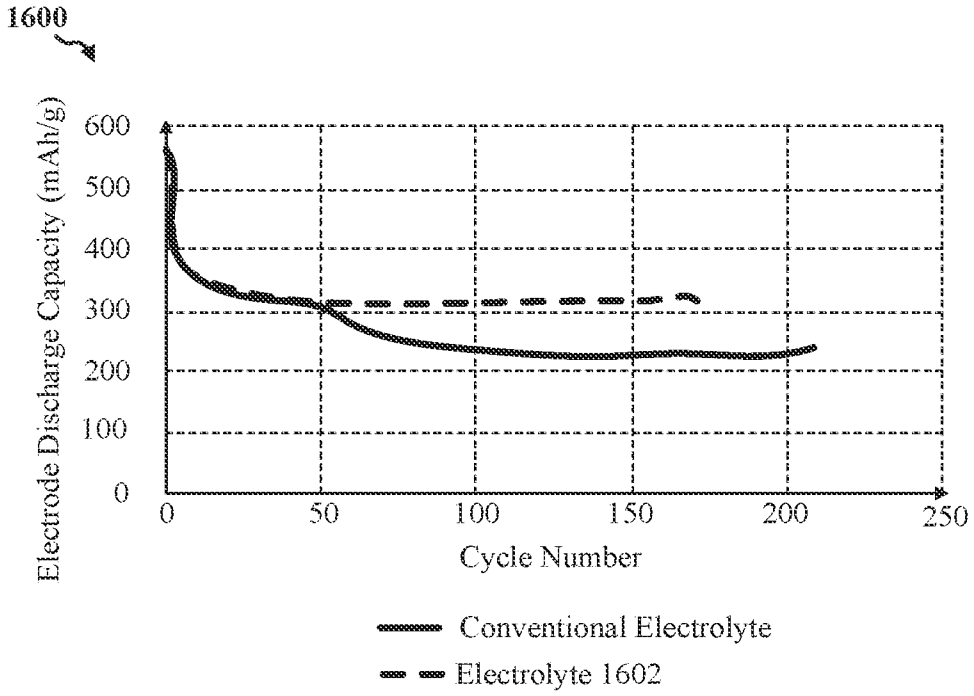


*Figure 16*

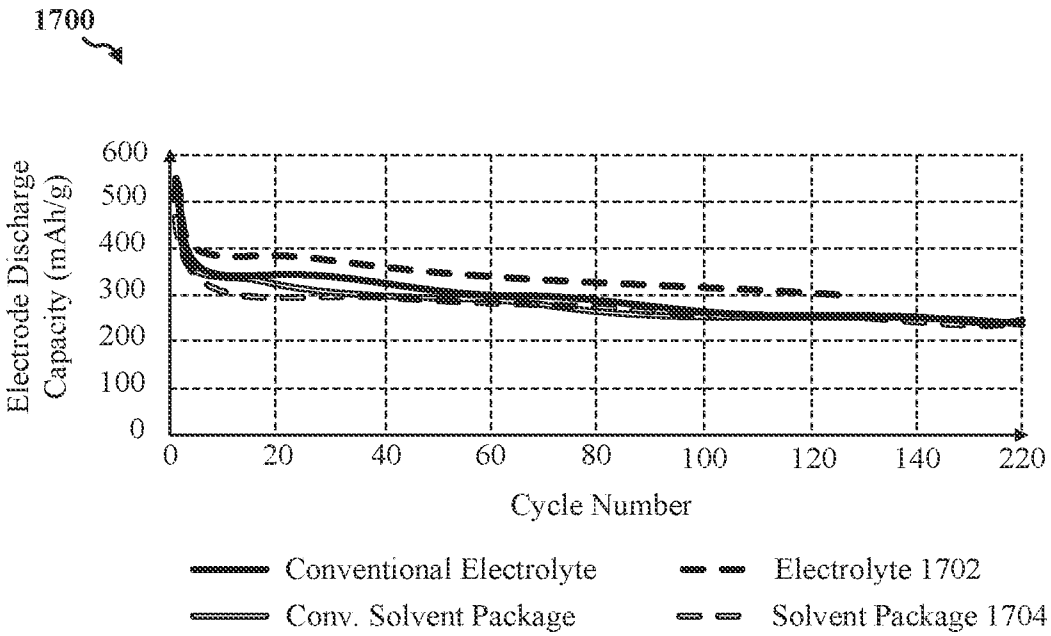


*Figure 17*

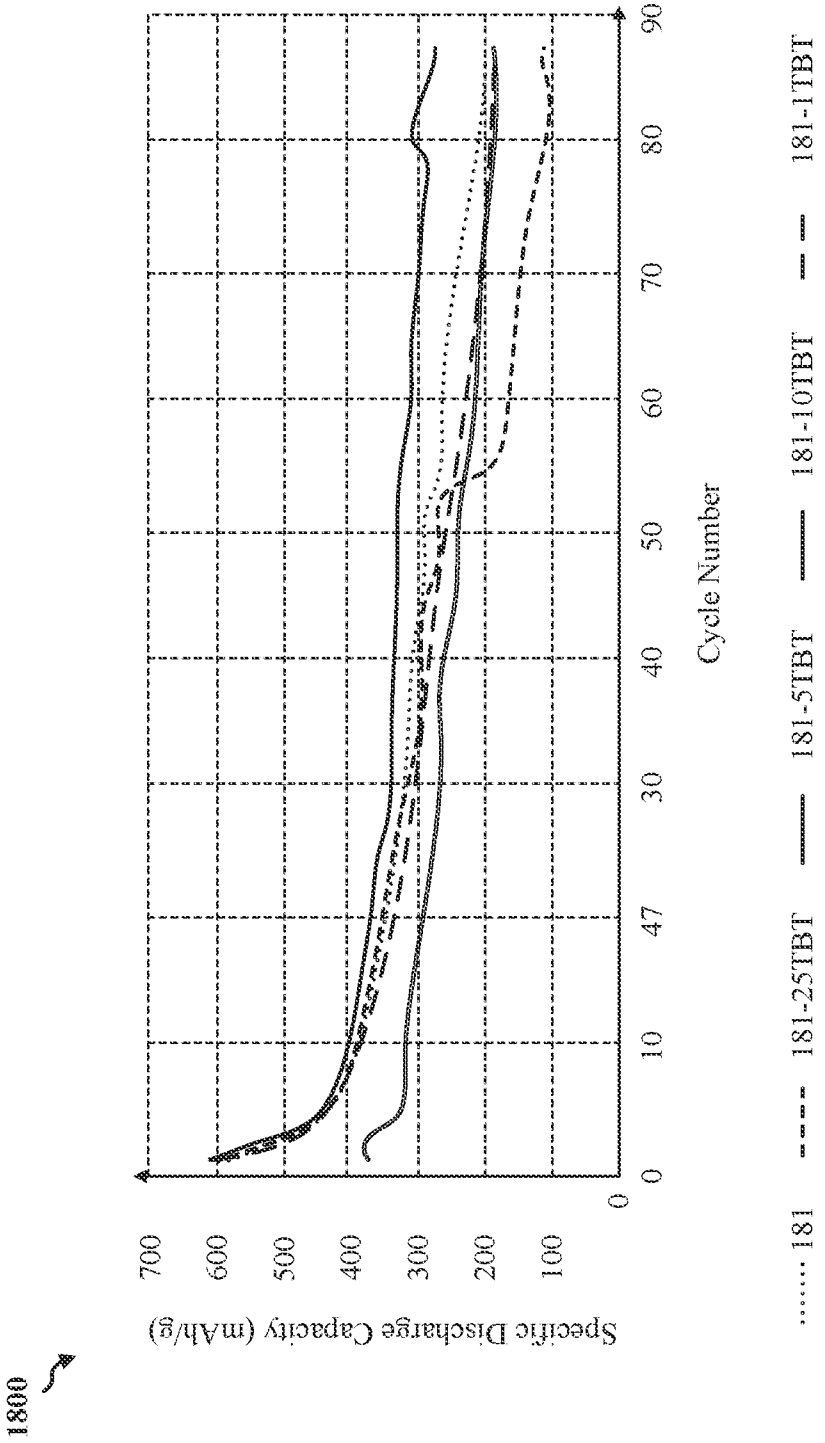
1800
Specific Discharge Capacity (mAh/g)
700
600
500
400
300
200
100
0
10
47
30
40
50
60
70
80
90
Cycle Number
181
181-25TBT
181-5TBT
181-10TBT
181-1TBT

*Figure 18*

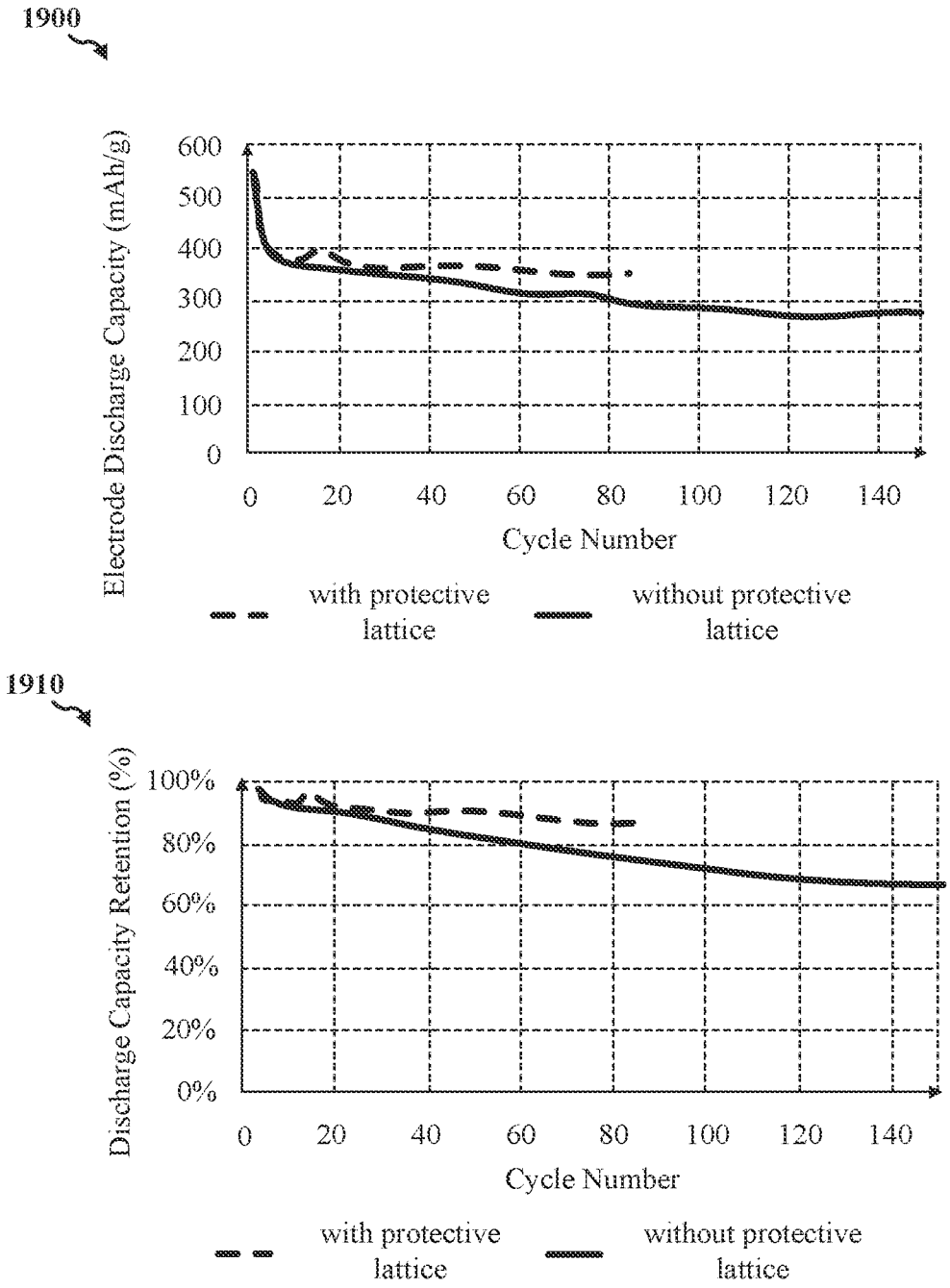
1900
Electrode Discharge Capacity (mAh/g)
600
500
400
300
200
100
0
0
20
40
60
80
100
120
140
Cycle Number
with protective lattice
without protective lattice
1910
Discharge Capacity Retention (%)
100%
80%
60%
40%
20%
0%
0
20
40
60
80
100
120
140
Cycle Number
with protective lattice
without protective lattice

*Figure 19*

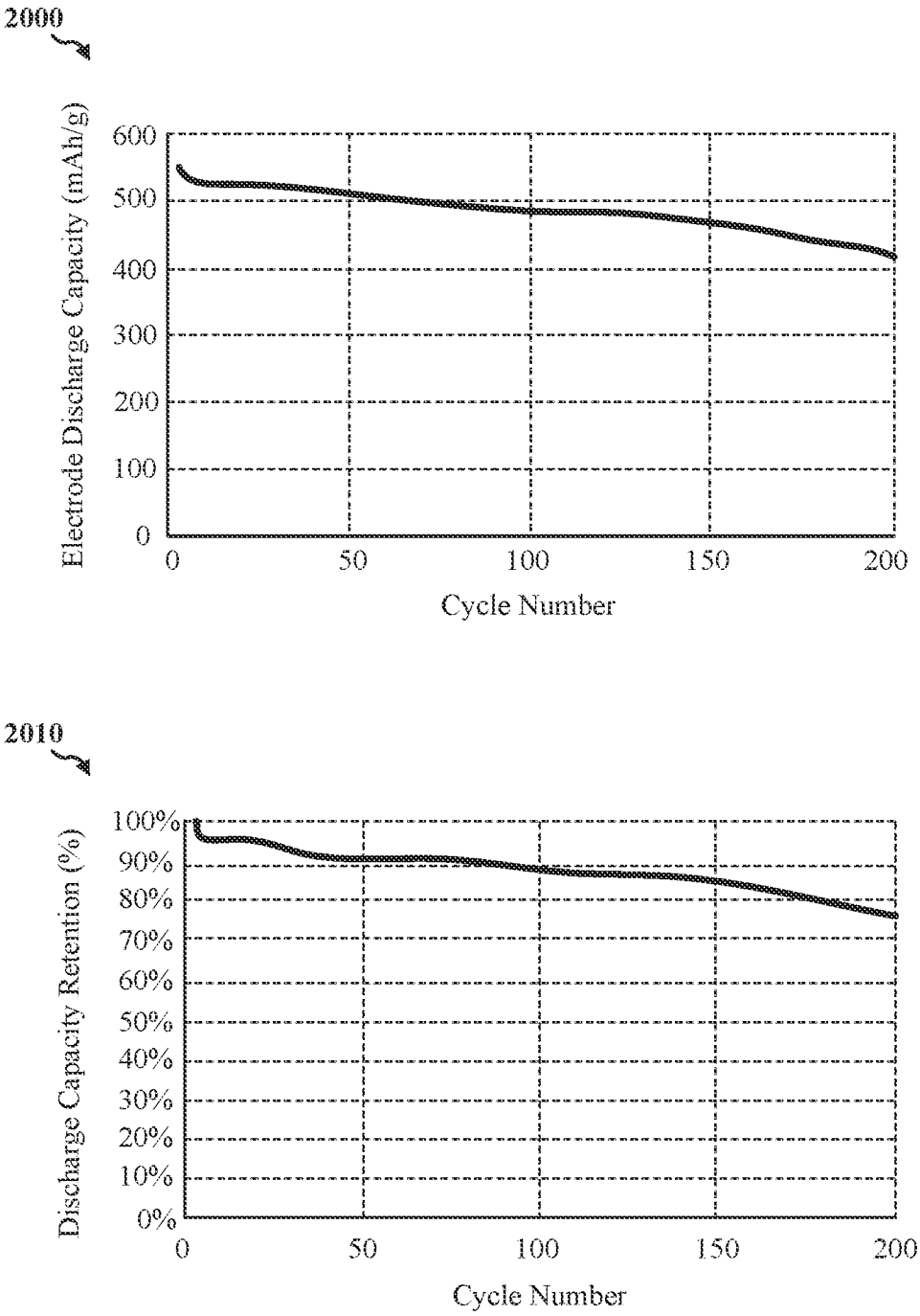
2000
Electrode Discharge Capacity (mAh/g)
600
500
400
300
200
100
0
0
50
100
150
200
Cycle Number
2010
Discharge Capacity Retention (%)
100%
90%
80%
70%
60%
50%
40%
30%
20%
10%
0%
0
50
100
150
200
Cycle Number

*Figure 20*

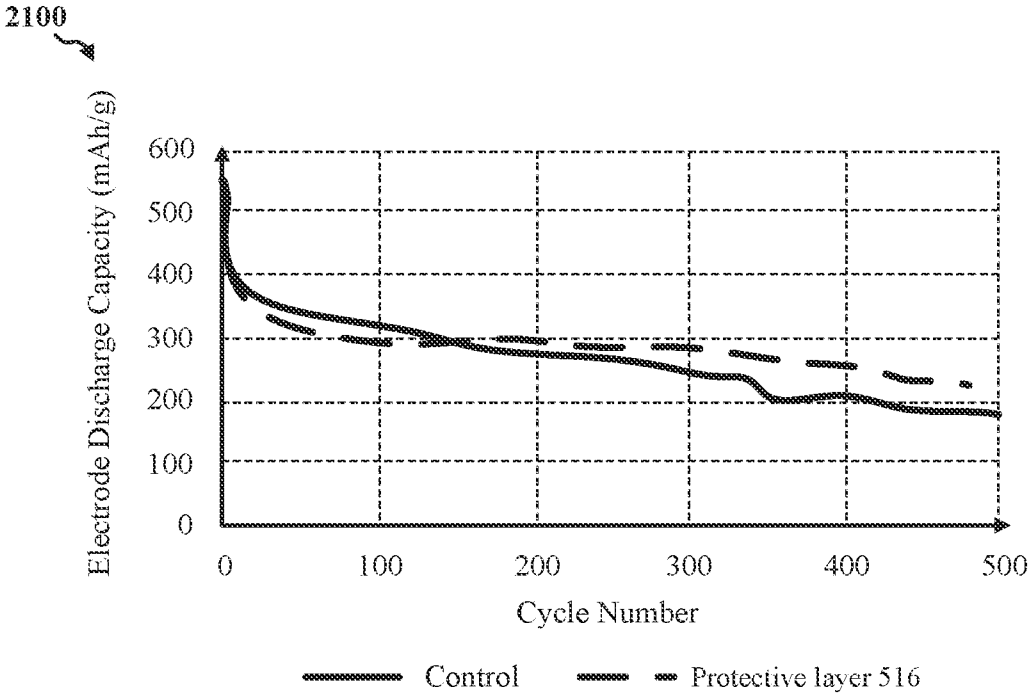
2100
Electrode Discharge Capacity (mAh/g)
600
500
400
300
200
100
0
0
100
200
300
400
500
Cycle Number
Control
Protective layer 516

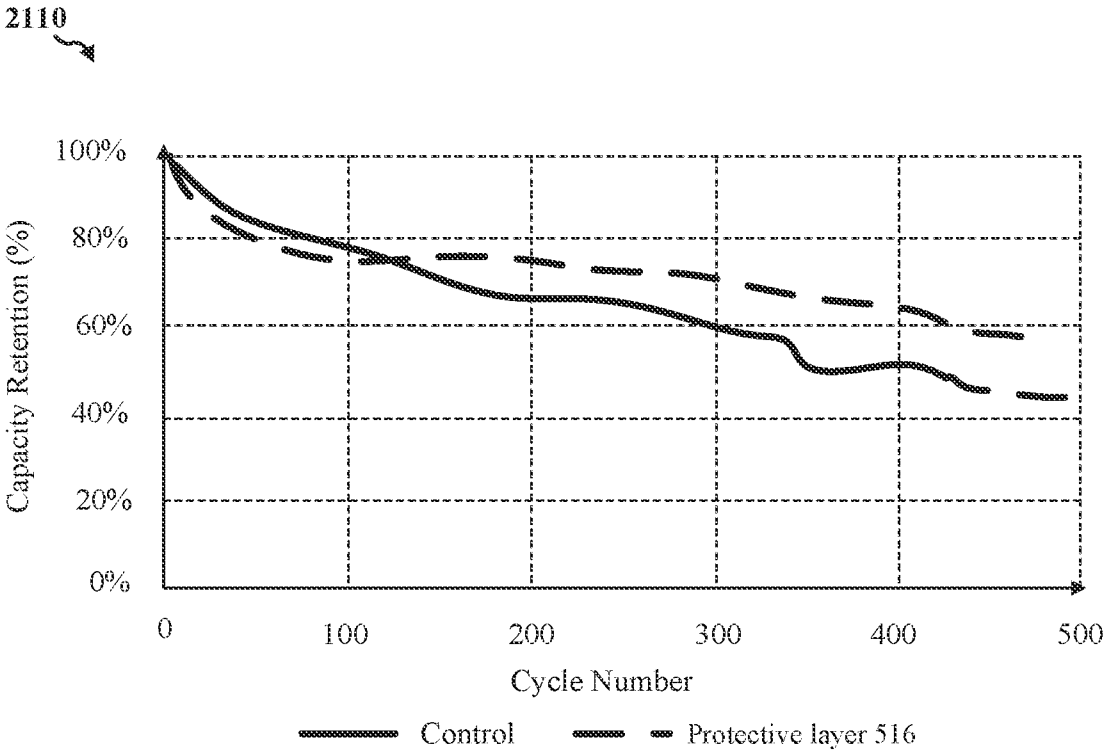
2110
Capacity Retention (%)
100%
80%
60%
40%
20%
0%
0
100
200
300
400
500
Cycle Number
Control
Protective layer 516

*Figure 21*

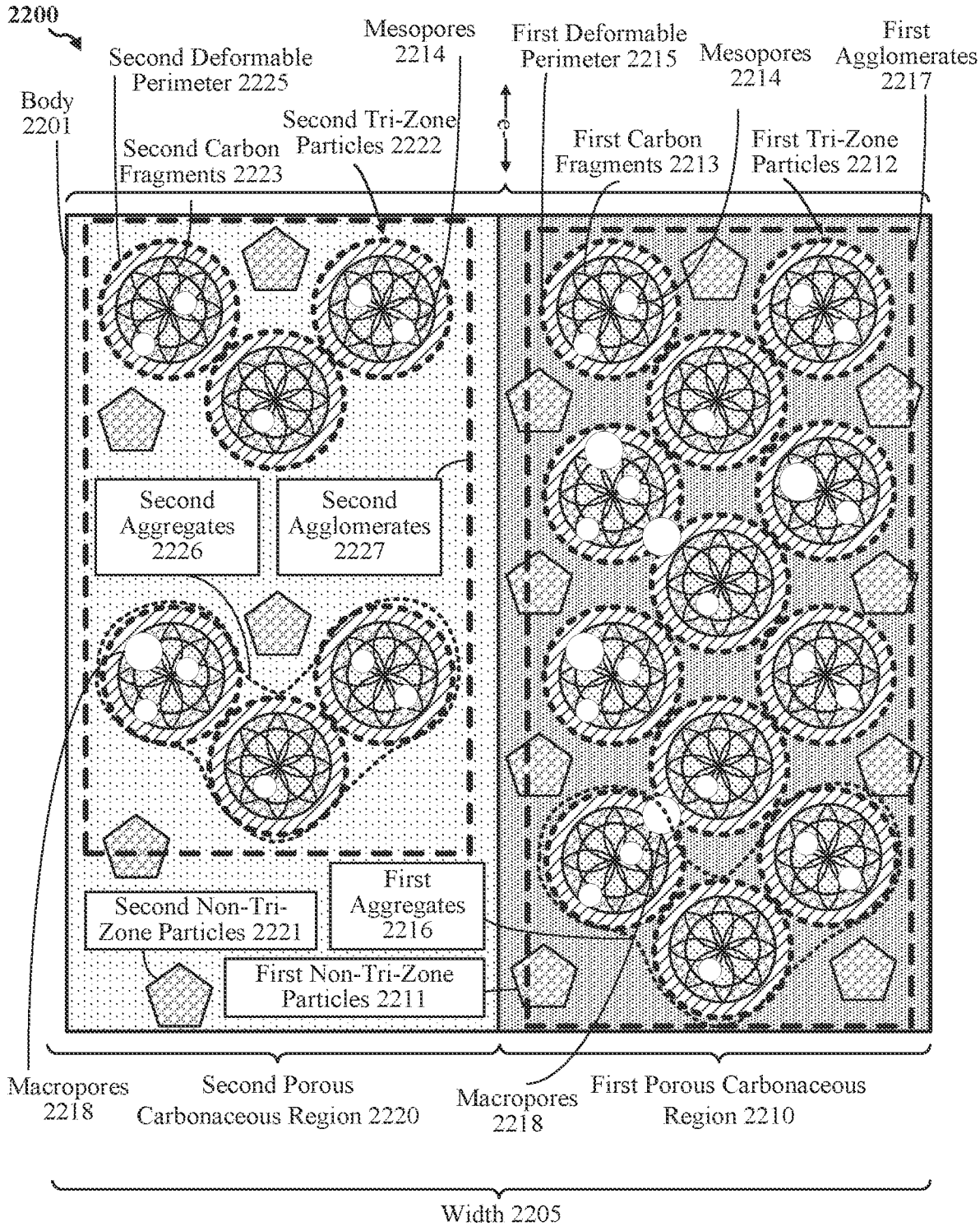
2200
Second Deformable Perimeter 2225
Mesopores 2214
First Deformable Perimeter 2215
Mesopores 2214
First Agglomerates 2217
Body 2201
Second Tri-Zone Particles 2222
Second Carbon Fragments 2223
First Carbon Fragments 2213
First Tri-Zone Particles 2212
Second Aggregates 2226
Second Agglomerates 2227
First Aggregates 2216
Second Non-Tri-Zone Particles 2221
First Non-Tri-Zone Particles 2211
Macropores 2218
Second Porous Carbonaceous Region 2220
Macropores 2218
First Porous Carbonaceous Region 2210
Width 2205

*Figure 22*